

AD/COM

PART I
APPLICATION OF ULTRA-STABLE OSCILLATORS TO
ONE-WAY RANGING SYSTEMS

PART II
FLUCTUATION SPECTRA OF ULTRA-STABLE OSCILLATORS:
MEASUREMENT AND ESTIMATION

Final Report
for
Subtask 4 under Task VI
of
Command System Study for the Operation and
Control of Unmanned Scientific Satellites

Contract NAS 5-9705

January 30, 1967

| | | |
|-------------------------------|--------------------|--------|
| FACILITY FORM 602 | N 67-27427 | _____ |
| | (ACCESSION NUMBER) | (THRU) |
| | 129 | 1 |
| | (PAGES) | (CODE) |
| CR-84444 | 07 | |
| (NASA CR OR TMX OR AD NUMBER) | (CATEGORY) | |

Prepared for
Goddard Space Flight Center
Greenbelt, Maryland

ADCOM, Inc.
808 Memorial Drive
Cambridge, Massachusetts 02139

GPO PRICE \$ _____

CFSTI PRICE(S) \$ _____

Har. copy (HC) \$ 3.00

Microfiche (MF) \$ 65

653 July 65

PART I
APPLICATION OF ULTRA-STABLE OSCILLATORS TO
ONE-WAY RANGING SYSTEMS

PART II
FLUCTUATION SPECTRA OF ULTRA-STABLE OSCILLATORS:
MEASUREMENT AND ESTIMATION

Final Report
for
Subtask 4 under Task VI
of
Command System Study for the Operation and
Control of Unmanned Scientific Satellites


Contract NAS 5-9705

January 30, 1967

Authors

Ahmad F. Ghais
John H. Miller
Howard C. Salwen

Prepared for
Goddard Space Flight Center
Greenbelt, Maryland

Approved by 
Steven M. Sussman
Director of Research

ADCOM, Inc.
808 Memorial Drive
Cambridge, Massachusetts 02139

TABLE OF CONTENTS

PART I

APPLICATION OF ULTRA-STABLE OSCILLATORS TO ONE-WAY RANGING SYSTEMS

| Section | | Page |
|---------|------------------------------------------------------------------|------|
| 1 | INTRODUCTION. | 1 |
| 2 | ONE-WAY RANGING TECHNIQUES | 3 |
| 3 | DOPPLER MEASUREMENT ERROR DUE TO OSCILLATOR INSTABILITY. | 7 |
| | 3.1 Analytical Model | 8 |
| | 3.2 Analysis of Error. | 10 |
| | 3.3 Oscillator Frequency Fluctuations | 17 |
| | 3.4 Doppler Error | 21 |
| | 3.5 Summary. | 23 |
| 4 | ONE-WAY TRACKING WITH A CARRIER ONLY | 24 |
| | 4.1 Statement of the Problem | 24 |
| | 4.2 Analysis for Two Points. | 25 |
| | 4.3 Error Analysis. | 29 |
| | 4.4 Symmetrical Arrays and Singular Paths | 30 |
| | 4.5 Analysis for m Points | 32 |
| | 4.6 The Free-Fall Case | 35 |
| | 4.7 Summary. | 36 |
| 5 | ONE-WAY RANGING WITH RANGE-TONES. | 37 |
| 6 | CONCLUSIONS | 39 |
| | REFERENCES FOR PART I. | 40 |

TABLE OF CONTENTS
PART II

FLUCTUATION SPECTRA OF ULTRA-STABLE OSCILLATORS:
MEASUREMENT AND ESTIMATION

| Section | Page |
|--------------------------------------------------------------------------------------------------------------|------|
| 1 INTRODUCTION | 41 |
| 2 EXTRACTION OF OSCILLATOR FLUCTUATIONS | 43 |
| 2.1 Available Fluctuation Extraction Techniques | 43 |
| 2.2 Spectral-Estimation Considerations | 48 |
| 2.3 Digital Filtering | 52 |
| 3 THEORETICAL FOUNDATIONS OF SPECTRAL ESTIMATION | 55 |
| 3.1 Introduction | 55 |
| 3.2 The General Structure of Time Series | 55 |
| 3.3 Important Special Cases | 60 |
| 3.4 Regression Analysis and Spectral Analysis | 61 |
| 3.5 Figures of Merit for Estimates | 62 |
| 3.6 Covariance and Spectral Averages | 64 |
| 3.7 Consistency, Bias and Variances of Estimates | 66 |
| 3.8 Window Generating Functions and Estimates of the Autocovariance and Spectral Density Functions | 67 |
| 3.9 Parzen's Kernel, Tukey's Kernel and the Periodogram | 73 |
| 3.10 Theorems on Estimates and Windows for Stationary Time Series | 75 |
| 3.11 Theorems on Estimates for Normal Time Series | 80 |
| 4 COMPUTATIONAL PROCEDURES FOR SPECTRAL ESTIMATION | 84 |
| 4.1 Computation of the Truncated Spectral Estimate | 84 |
| 4.2 Discussion of the Computation | 86 |
| 4.3 Correlation Analysis | 93 |
| 4.4 Finding the Noise and Signal Components from the Truncated Spectral Estimate | 95 |
| 4.5 Estimates of the Derivatives of the Noise Spectral Density Function | 100 |

TABLE OF CONTENTS (Cont'd)

| Section | Page |
|---------------------------------------------------|------|
| 4.6 Estimates of the Signal Frequency | 105 |
| 4.7 Narrowband Signals in Noise | 106 |
| 4.8 Stageswise Autoregressive Estimation. | 108 |
| 5 CONCLUSIONS AND RECOMMENDATIONS. | 113 |
| NOTATION FOR PART II. | 115 |
| REFERENCES FOR PART II. | 119 |

LIST OF ILLUSTRATIONS

PART I

APPLICATION OF ULTRA-STABLE OSCILLATORS TO
ONE-WAY RANGING SYSTEMS

| Figure | | Page |
|--------|-------------------------------------------------------------------------------------------------------|------|
| 1 | One-Way Ranging Utilizing a Single Event | 4 |
| 2 | One-Way Ranging Utilizing Doppler Count (two dimensional) | 5 |
| 3 | Analytical Model | 9 |
| 4a | $g(\mu)$ as a Function of μ | 13 |
| 4b | $g(t - \mu)$ as a Function of μ | 13 |
| 5 | $g(t)$ as a Function of t | 14 |
| 6 | Equivalent Model of a Stable Source. | 18 |
| 7 | Velocity Error as a Function of Round-Trip Delay Time with Averaging Time as a Parameter | 22 |

PART II

FLUCTUATION SPECTRA OF ULTRA-STABLE OSCILLATORS
MEASUREMENT AND ESTIMATION

| | | |
|---|--------------------------------------------------------------------------|-----|
| 1 | Error Multiplication and Synthesis System | 43 |
| 2 | Three Fluctuation Extraction Techniques | 45 |
| 3 | Spectrum Folding or Aliasing. | 49 |
| 4 | Procedure Covariance (from Ref. 9) | 85 |
| 5 | Procedure Transform (from Ref. 9). | 92 |
| 6 | Procedure Select for Stagewise Autoregression (from Ref. 9) | 112 |

PART I

APPLICATION OF ULTRA-STABLE OSCILLATORS TO
ONE-WAY RANGING SYSTEMS

1. INTRODUCTION

Great advances have been made in recent years in the field of ultra-stable oscillators. Attainable stabilities, both "long" and "short term," have been greatly enhanced at the same time that flexibility and reliability have been improved. Pertinent examples of such ultra-stable oscillators are some hydrogen-maser oscillators recently acquired and evaluated by GSFC, and cesium beam primary standards available as commercial products.

The availability of these oscillators naturally raises the possibility of utilizing them in the design of space-vehicle tracking systems, with the objectives of improving system accuracy and/or greatly reducing system complexity. One intriguing possibility is to turn away from coherent two-way tracking techniques (involving transponders) in favor of the simpler but heretofore less precise (noncoherent) one-way tracking techniques. This possibility is explored below.

The objective of the study documented in Part I of this report, as defined in the Task Statement, is:

Determine the feasibility of designing a one-way or passive ranging system given the fact that a spacecraft oscillator is highly stable and its frequency is well known. The analysis should take into account all possible system errors such as propagation anomalies, small drifts in system oscillators, etc., and evaluate quantitatively expected system performance.

In Sec. 2 the basic techniques of trajectory measurement in a one-way tracking system are described; then in Sec. 3 the effects of lack of coherence between transmitter and receiver on system operation and accuracy are analyzed and discussed. It is found that in many applications such as deep-space tracking, coherent doppler demodulation is not attained because of the oscillator instability incurred during the elapsed time between transmission and reception.

Thus, one-way tracking suffers no disadvantage in this respect in comparison with coherent two-way tracking. On the other hand, one-way tracking techniques are quite sensitive to geometric dilution of precision (GDOP). Sections 4 and 5 are devoted to the exploration of these geometrical problems. Conclusions as to the feasibility of precision one-way tracking systems are drawn in Sec. 6, and suggestions are offered concerning the development of such systems.

2. ONE-WAY RANGING TECHNIQUES

It is possible to determine the trajectory of a vehicle by performing measurements at ground sites on signals which originate at the vehicle. Since transmissions from the ground sites to the vehicle are not required, this ranging technique is called one-way or passive ranging.

A possible one-way ranging technique is demonstrated with the aid of Fig. 1. The vehicle is located at P at time $t = 0$, and there are receiving stations at A, B, C, and D. Assume that the vehicle radiates a single event such as an impulse at $t = 0$. This is received at A at $t_a = r_a/c$, at B at $t_b = r_b/c$, etc., where c is the speed of light. The absolute time of occurrence of the impulse transmission is not known at the ground sites so the ranges, r_a, r_b, \dots , cannot be determined directly. However, the differences in time of arrival at the ground sites can be determined exactly with the aid of a precise reference time distribution system. The timing system provides synchronized clocks at each of the ground sites. In this way the difference ranges, $r_a - r_b, r_b - r_c, \dots$, can be determined uniquely. Note that four stations produce three independent range differences. Each range difference defines a hyperboloid of revolution. For example, the range difference $r_a - r_b$ defines a hyperboloid with foci at A and B, and the difference of distances of any point on the hyperboloid from the foci is just $r_a - r_b$. Thus, three surfaces of revolution are generated from the range difference data obtained from four receiving stations, and these surfaces intersect at P, which is the target position.

It is not reasonable to assume that the vehicle will transmit just one impulse in a practical application of the one-way ranging technique. A periodic waveform, such as a periodic pulse train, is more convenient. In fact, a pure CW carrier can be used.

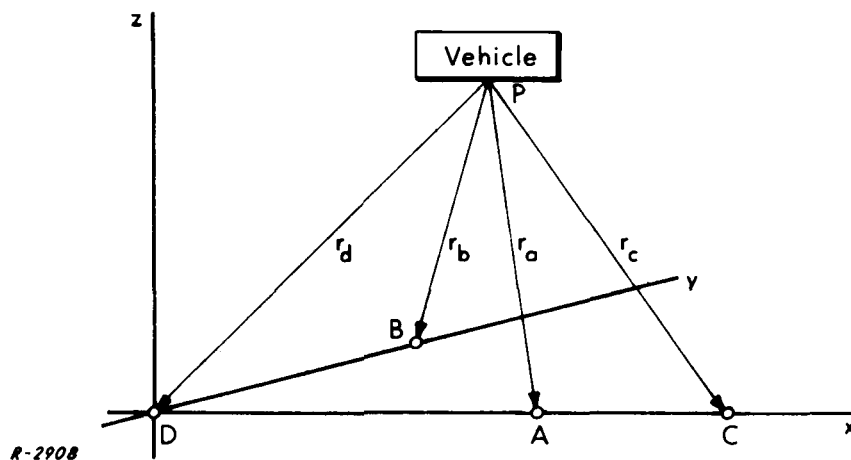


Fig. 1 One-Way Ranging Utilizing a Single Event.

When a periodic pulse train is transmitted, the range difference determinations become ambiguous. As a result, the determination of target position P , is ambiguous and some a priori knowledge of target position is necessary to resolve the ambiguity. Similarly, a CW transmission produces highly ambiguous data. For the case of pulsed signals, the ambiguity arises from the inability to distinguish one pulse from another at the ground sites. Analogously, for CW transmission, the ambiguity arises from the inability to distinguish one zero crossing of the CW sine wave from another. The ambiguity thus produced is so severe that resolution with the aid of a priori information is not practical.

A one-way ranging technique is available which employs additional stations to combat this ambiguity problem. Consider the two-dimensional configuration shown in Fig. 2. Although $r_{a_1} - r_{b_1}$ can only be determined ambiguously, note that $r_{a_1} - r_{a_2}$ can be determined unambiguously. This is the change

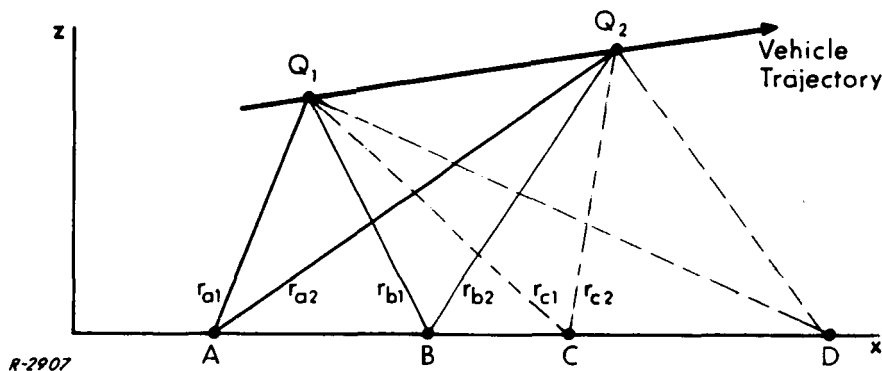


Fig. 2 One-Way Ranging Utilizing Doppler Count
(two dimensional).

in range due to target motion observed at A by counting doppler cycles of the CW sine wave. Similarly, the change in range observed at B, C, and D, can be measured. With this data four equations can be written with four unknowns. These are the coordinates of Q_1 and Q_2 . The technique is extended for application in three dimensions by utilizing six stations. Clearly, this technique only works with moving vehicles.

Other techniques are available which utilize one-way transmissions to determine target position. For example, if the vehicle is in free-fall or orbit, a great deal is then known about its trajectory. A priori advantage can be taken of this extra information to either reduce the number of observations required or to enhance the accuracy of the trajectory determination. Another example is the use of multiple-tone modulation of the CW carrier to generate widely spaced periodic events and thus greatly reduce the range ambiguity. The errors

incurred with the four techniques mentioned above will be considered in the following sections. But first, a two-way CW doppler system is considered in Sec. 3 in order to demonstrate how oscillator instability can result in loss of coherence, and thus eliminate the advantage of coherence expected in a two-way system under certain conditions.

3. DOPPLER MEASUREMENT ERROR DUE TO OSCILLATOR INSTABILITY*

In this section, the effect on doppler measurement accuracy of oscillator instability is determined. Then, as an example, the doppler error due to the instability of a cesium beam ultrastable oscillator in a monostatic system is determined.

It is found that the short-term instability contributes more significantly to the doppler error than the long-term instability. The validity of this conclusion is a function of the noise bandwidth of the receiver. In the example below, a noise bandwidth of 2 kHz is assumed. With noise bandwidths on this order, the long-term stability enhancement of the cesium resonator has little effect on the doppler error. Similar accuracy could be obtained using the quartz oscillator only. The cesium beam resonator improves the stability of the source when the averaging time is greater than 100 s. Thus its relative contribution is important only when the noise bandwidth of the receiver is extremely narrow.

The system assumed for analysis below is monostatic. That is, a stable reference is used to generate the transmitted signal. This signal is transponded (without distortion) at the vehicle and returned to a receiver which is contiguous with the transmitter. The same stable reference is used to detect the doppler data. During the round trip, the short-term instability of the stable reference causes it to shift frequency slightly. It is found that if the round-trip time is short enough, the instability component on the returning signal is correlated with the stable reference's instability component and, thus, causes little error. On the other hand, if the round-trip time is long, the instability component on the return is uncorrelated with the instability component of the reference. In that case, a separate stable oscillator of the same quality could be used to detect the doppler data at the receiver without any decrease in doppler accuracy.

* The material of this section is based on work performed under Contract DA-31-124-ARO-D-393 with the U.S. Army White Sands Missile Range.

It is concluded that a one-way doppler measurement will be as accurate as a two-way doppler measurement provided that

1. the target is at long-range for a given data rate,
2. the long-term instability of the oscillators does not contribute significant error (say, less than the error due to uncertainty in the speed of light), and
3. the receiver noise-bandwidth is greater than 100 Hz.

The error in doppler measurement due to oscillator instability is derived and discussed below. The measurement under consideration is the time required, Δt , for a given change in range, Δr ; or, alternatively, the change in range in a given time. In other words the determined parameter is the average velocity during the measurement interval not the instantaneous velocity.

3.1 Analytical Model

The system to be analyzed is shown in Fig. 3. The transmitted carrier is generated by multiplying up the output of a 5 MHz stable source. The signal received at the transponder is at the transmitting carrier frequency, f_o , plus one-way doppler, f_d . The transponder output frequency is k times its input frequency, where it is assumed that $k = 99/100$ for the sake of example. The received downlink signal is then approximately $kf_o + 2kf_d$. This is mixed down to an IF by beating the received signal with a sample of the transmitted carrier. The signal in the IF amplifier is at $(1 - k)f_o = 100$ MHz and is tracked by a PLL with noise bandwidth of approximately 2 kHz. Finally, the offset frequency is removed (or partially removed) at the output of the PLL and a filtered signal which contains the doppler data is sent to a cycle counting measurement device. There, the number of cycles in a given

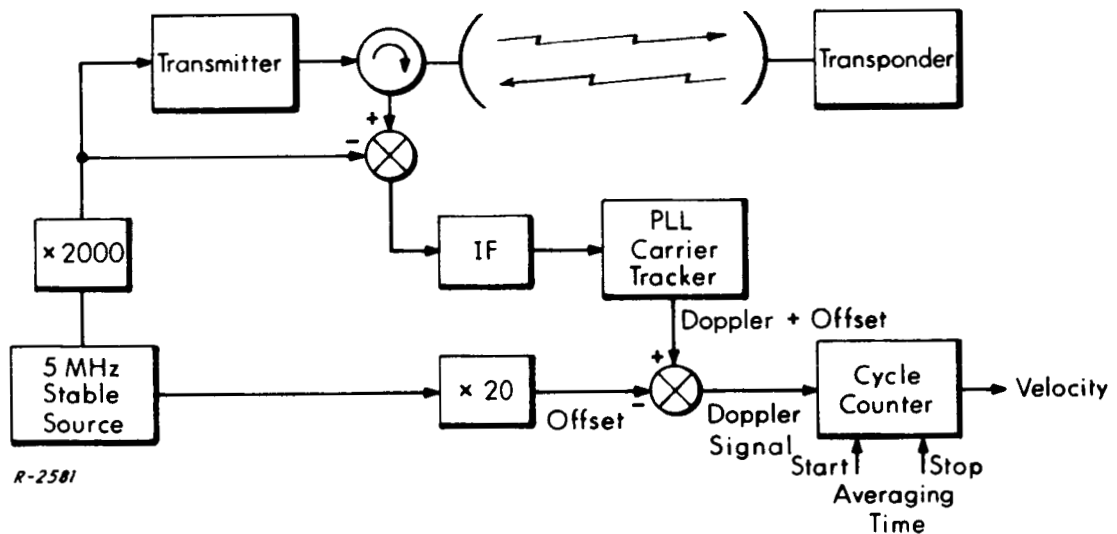


Fig. 3 Analytical Model.

number of seconds or the number of seconds for a given number of cycles is measured to determine the average velocity during the measurement interval.

There are many possible sources of error inherent to the measurement technique just described, such as receiver noise, vehicle dynamics, quantizing errors, etc. But, the only one considered here is caused by a slight change of frequency (or phase) of the stable source during the round-trip time to the transponder and back. If, for example, the stable frequency changes by Δf cycles during the transit time, the IF becomes $100 \text{ MHz} + 2kf_d + \Delta f$. Obviously, such a change in frequency contributes directly to doppler error. That is, the velocity error is given by

$$\Delta v = \frac{c\Delta f}{2f_0} \quad (1)$$

This type of error generation should not be confused with the case in which the transmitted frequency is constant but in error by Δf Hz. Then the resulting velocity error is approximately*

$$\Delta v = v \frac{\Delta f}{f_0} \quad (2)$$

Consider, for example, a Δf of 1 Hz at X-band. The resulting velocity error of the type described by Eq. (1) is 0.05 ft/sec. On the other hand, a constant offset of 1 Hz at x-band yields an error given by Eq. (2) which is on the order of $v \cdot 10^{-10}$. Assuming a maximum velocity of, say, 35,000 ft/sec, the velocity error is 3.5×10^{-6} ft/sec. It is clear, then, that random changes in the stable oscillator frequency during the round-trip time to the target are much more important than constant offsets of the oscillator frequency. For this reason, the short-term stability of the stable source must be examined carefully to determine its effect on doppler accuracy.

3.2 Analysis of Error

With reference to Fig. 3, the X-band output of the stable source has a phase given by $2\pi f_0 t + \phi(t)$ at time t , where $\phi(t)$ represents the phase fluctuations due to oscillator instability. Furthermore, the phase of the received signal at time t is given by $2\pi k f_0 (t - \tau) + k\phi(t - \tau)$. The round-trip time to the target is denoted by τ and it is a function of time, i.e., the target is moving. The input phase to the IF amplifier is

$$\begin{aligned} 2\pi f_{if} t &= 2\pi f_0 t + \phi(t) - 2\pi k f_0 (t - \tau) - k\phi(t - \tau) \\ &= 2\pi \cdot 100 \text{ MHz} \cdot t + 2\pi k f_0 \tau + \phi(t) - k\phi(t - \tau) \end{aligned} \quad (3)$$

* Uncertainty in the speed of light, Δc , causes a similar error, i.e., $\Delta v = v \Delta c / c$.

A short time, Δt , later the input phase has the form,

$$2\pi f_{if}(t + \Delta t) = 2\pi \cdot 100 \text{ MHz}(t + \Delta t) + 2\pi k f_o(\tau + \Delta\tau) + \phi(t + \Delta t) - k\phi(t + \Delta t - \tau - \Delta\tau) \quad (4)$$

where $\Delta\tau$ is the change in delay during the interval Δt caused by target motion. The inputs to the cycle counter at times t and $t + \Delta t$ are similar to the IF signals of Eqs. (3) and (4) except that the PLL narrows the noise bandwidth and the 100 MHz offset is removed. The cycle counter accumulates the phase of its input signal over the interval Δt . That is, it is started at t and stopped at $t + \Delta t$. Thus its contents at time $t + \Delta t$ is just

$$\Delta\phi = 2\pi k f_o \Delta\tau + \phi(t + \Delta t) - k\phi(t + \Delta t - \tau - \Delta\tau) - \phi(t) + k\phi(t - \tau) \quad (5)$$

If the system is the type which determines the change in range in a given time, then, the average velocity measured is

$$\begin{aligned} \bar{v}_m &= \frac{\Delta r}{\Delta t} = \frac{c\Delta\phi}{4\pi f_o \Delta t k} \\ &= \frac{c\Delta\tau}{2\Delta t} + \frac{c}{4\pi f_o \Delta t k} \left[\phi(t + \Delta t) - k\phi(t + \Delta t - \tau - \Delta\tau) - \phi(t) + k\phi(t - \tau) \right] \end{aligned} \quad (6)$$

The first term on the right of Eq. (6) is exactly the desired output. The second term on the right is the error in doppler measurement due to oscillator instability. Since $k \approx 1$, the mean-square velocity error is approximated by

$$\sigma_v^2 \approx \left[\frac{c}{4\pi f_o \Delta t} \right]^2 \times \left[\phi(t + \Delta t) - \phi(t + \Delta t - \tau - \Delta\tau) - \phi(t) + \phi(t - \tau) \right]^2 \quad (7)$$

Without any loss of generality, the time scale can be shifted in Eq. (7) to yield a more symmetric form. Replacing t by $t - \Delta t/2 + (\tau + \Delta\tau)/2$ in Eq. (7) results in

$$\sigma_v^2 = \left[\frac{c}{4\pi f_0 \Delta t} \right]^2 \times \left[\phi\left(t + \frac{\Delta t}{2} + \frac{\tau + \Delta\tau}{2}\right) - \phi\left(t + \frac{\Delta t}{2} - \frac{\tau + \Delta\tau}{2}\right) - \phi\left(t - \frac{\Delta t}{2} + \frac{\tau + \Delta\tau}{2}\right) - \phi\left(t - \frac{\Delta t}{2} - \frac{\tau - \Delta\tau}{2}\right) \right]^2 \quad (8)$$

The second term in brackets of Eq. (8) is difficult to evaluate. The procedure is as follows: First, the sum of the phase functions in Eq. (8) is interpreted as the result of a convolution of $\phi(t)$ with some function, $g(t)$. That is,

$$\left[\phi(t - t_1) - \phi(t - t_2) - \phi(t - t_3) - \phi(t - t_4) \right] = \int_{-\infty}^{\infty} \phi(\mu) g(t - \mu) d\mu \quad (9)$$

where

$$t_1 = -\frac{\Delta t}{2} - \frac{\tau + \Delta\tau}{2}, \quad t_2 = -\frac{\Delta t}{2} + \frac{\tau + \Delta\tau}{2}$$

$$t_3 = \frac{\Delta t}{2} - \frac{\tau + \Delta\tau}{2}, \quad t_4 = \frac{\Delta t}{2} + \frac{\tau - \Delta\tau}{2}$$

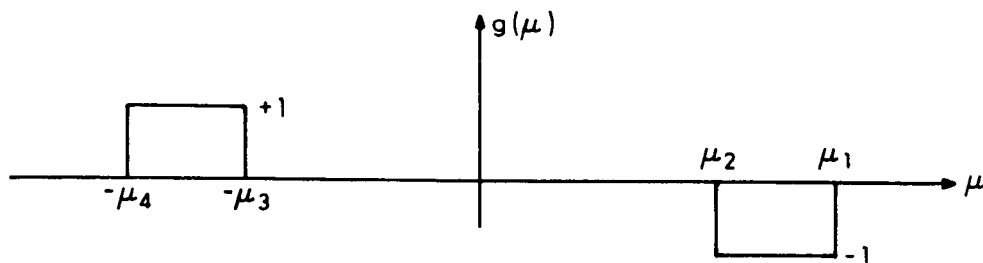
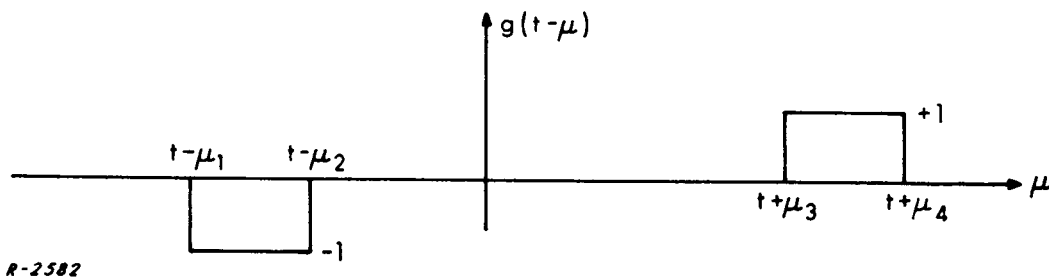
Assume, for the moment, that $g(\mu)$ has the form shown in Fig. 4a. Then, $g(t - \mu)$ has the form shown in Fig. 4b. The convolution of Eq. (9) can now be carried out

$$\int_{-\infty}^{\infty} \phi(\mu) g(t - \mu) d\mu = -\phi(t - \mu_2) + \phi(t - \mu_1) + \phi(t + \mu_4) - \phi(t + \mu_3) \quad (10)$$

Equation (9), is valid when

$$\mu_1 = t_1 = -\frac{\Delta t}{2} - \frac{\tau + \Delta\tau}{2} \quad \mu_2 = t_2 = -\frac{\Delta t}{2} + \frac{\tau + \Delta\tau}{2}$$

$$\mu_3 = -t_3 = -\frac{\Delta t}{2} + \frac{\tau + \Delta\tau}{2} \quad \mu_4 = -t_4 = -\frac{\Delta t}{2} - \frac{\tau - \Delta\tau}{2}$$

Fig. 4a $g(\mu)$ as a Function of μ .

R-2582

Fig. 4b $g(t-\mu)$ as a Function of μ .

The function, $g(t)$, is plotted in Fig. 5. Equation (8) can now be expressed in terms of $\dot{\phi}(t)$ and $g(t)$ using Eq. (9) as follows

$$\sigma_{\bar{v}}^2 = \left[\frac{c}{4\pi f_0 \Delta\tau} \right]^2 \times \left[\int_{-\infty}^{\infty} \dot{\phi}(\mu) g(t - \mu) d\mu \right]^2 \quad (11)$$

It is recognized that the right-hand term of Eq. (11) is the mean-square value of the response of some linear system with impulse response $g(t)$ to a stochastic

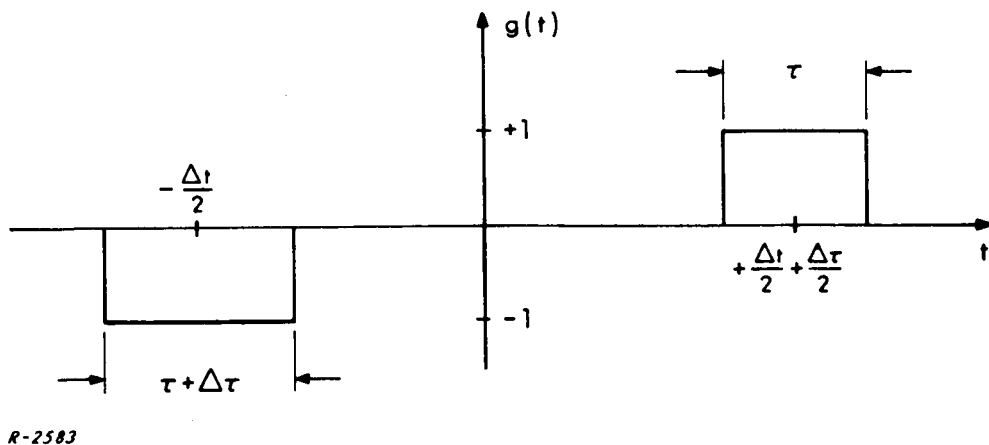


Fig. 5 $g(t)$ as a Function of t .

input $\dot{\phi}(t)$. The autocorrelation of the linear system's response is given by

$$\begin{aligned}
 R(\tau) &= \lim_{T \rightarrow \infty} \frac{1}{2T} \int_{-T}^T dt \int_{-\infty}^{\infty} d\mu \int_{-\infty}^{\infty} d\nu g(\mu) g(\nu) \dot{\phi}(t - \mu) \dot{\phi}(t + \tau - \nu) \\
 &= \int_{-\infty}^{\infty} d\mu \int_{-\infty}^{\infty} d\nu g(\mu) g(\nu) R_{\dot{\phi}}(\tau - \nu + \mu)
 \end{aligned} \tag{12}$$

Where $R_{\dot{\phi}}(\tau)$ is the autocorrelation of the frequency fluctuations, and the mean-square of the response is $R(0)$. The power spectral density of $R(\tau)$ is

$$\begin{aligned}
 S(\omega) &= \int_{-\infty}^{\infty} R(\tau) e^{-j\omega\tau} d\tau \\
 &= S_{\dot{\phi}}(\omega) |G(\omega)|^2
 \end{aligned} \tag{13}$$

where $S_{\dot{\phi}}(\omega)$ is the power spectral density of $\dot{\phi}(t)$ and $G(\omega)$ is the transform of $g(t)$. Transforming back into the time domain and remembering that $R(0)$ is the mean-square of the response,

$$R(\tau) = \frac{1}{2\pi} \int_{-\infty}^{\infty} S_{\dot{\phi}}(\omega) |G(\omega)|^2 e^{j\omega\tau} d\omega \quad (14)$$

and, finally,

$$R(0) = \frac{1}{2\pi} \int_{-\infty}^{\infty} S_{\dot{\phi}}(\omega) |G(\omega)|^2 d\omega = \left[\int_{-\infty}^{\infty} \dot{\phi}(\mu) g(t-\mu) d\mu \right]^2 \quad (15)$$

So,

$$\sigma_{\frac{2}{V}}^2 = \left[\frac{c}{4\pi f_o \Delta t} \right]^2 \left[\frac{1}{2\pi} \int_{-\infty}^{\infty} S_{\dot{\phi}}(\omega) |G(\omega)|^2 d\omega \right] \quad (16)$$

By inspection of Fig. 5, the power spectrum of $g(t)$ is

$$|G(\omega)|^2 = \left| \frac{2}{j\omega} \left[e^{+j\omega \Delta\tau/2} \cos \omega \left(\frac{\Delta t}{2} - \frac{\tau}{2} \right) - \cos \omega \left(\frac{\Delta t}{2} + \frac{\Delta\tau}{2} + \frac{\tau}{2} \right) \right] \right|^2 \quad (17)$$

At this point it is recalled that the doppler data is filtered in a PLL. The effect of the PLL is included by passing the linear system's response of Eq. (10), through an additional filter with impulse response, $h(t)$, and transfer function $H(\omega)$. Thus $G(\omega)$ is cascaded with $H(\omega)$, the transfer function of the PLL. Equation (16) becomes

$$\sigma_{\frac{2}{V}}^2 = \left[\frac{c}{4\pi f_o \Delta t} \right]^2 \left[\frac{1}{2\pi} \int_{-\infty}^{\infty} S_{\dot{\phi}}(\omega) |G(\omega)|^2 |H(\omega)|^2 d\omega \right] \quad (18)$$

For simplicity, the characteristic of the PLL is approximated by an ideal lowpass filter with cutoff at 2kHz. That is,

$$\sigma_{\frac{2}{V}}^2 = \left[\frac{c}{4\pi f_o \Delta t} \right]^2 \left[\frac{1}{\pi} \int_0^{2\pi 2000} S_{\phi}^{\cdot}(\omega) |G(\omega)|^2 d\omega \right] \quad (19)$$

The highest frequency of interest is $\omega/2\pi = 2\text{kHz}$. When the target is moving at its assumed maximum velocity, 35,000 ft/sec, the maximum change in the round-trip time during a measurement interval is given by

$$\begin{aligned} \Delta\tau_{\text{max}} &= \frac{2\Delta r}{c} = \frac{2V_{\text{max}} \Delta t}{c} = \frac{2 \times 3.5 \times 10^4 \times 10^{-1}}{10^9} \\ &= 7 \mu\text{sec} \end{aligned} \quad (20)$$

where it is assumed that the maximum duration of a measurement interval, Δt , is 0.1 sec. Then, the phase, $\omega\Delta\tau/2$, in Eq. (17), is negligibly small throughout the region of interest. Its highest value is

$$\frac{\omega\Delta\tau}{2} = \frac{2\pi \times 2 \times 10^3 \times 7 \times 10^{-6}}{2} = 44 \text{ mrad} \quad (21)$$

Thus,

$$|G(\omega)|^2 \approx \frac{16}{\omega^2} \sin^2 \frac{\omega\Delta t}{2} \sin^2 \frac{\omega\tau}{2} \quad (22)$$

This means that the doppler error due to oscillator instability is essentially independent of target velocity. Substituting Eq. (22), into Eq. (19), yields

$$\sigma_{\frac{2}{V}} \approx \frac{c}{\pi f_o \Delta t} \left[\frac{1}{\pi} \int_0^{2\pi 2000} S_{\phi}^{\cdot}(\omega) \frac{1}{\omega^2} \sin^2 \frac{\omega\Delta t}{2} \sin^2 \frac{\omega\tau}{2} d\omega \right]^{1/2} \quad (23)$$

Using Eq. (23), the velocity error as a function of Δt and τ can be found provided that the power spectral density of oscillator frequency fluctuations is known. In the next section a high quality oscillator is investigated and its associated $S_{\phi}^{\cdot}(\omega)$ is determined.

3.3 Oscillator Frequency Fluctuations

The particular oscillator to be analyzed is similar to a Hewlett-Packard 5060A Cesium Beam Frequency Standard. Table I shows those specifications of the oscillator which are necessary to determine the power density spectrum of its frequency fluctuations.

Table I
OSCILLATOR SPECIFICATIONS¹

1. Short Term Stability (Quartz Oscillator Effects)

| <u>Ave. Time</u> | <u>rms. Fractional Freq. Deviation</u> |
|------------------|----------------------------------------|
| 1 ms | 6×10^{-10} |
| 10 ms | 1.2×10^{-10} |
| 100 ms | 1.5×10^{-11} |
| 1 sec | 1.5×10^{-11} |
| 10 sec | 1.5×10^{-11} |

Note 1: All data based on at least 100 samples.

Note 2: Figures quoted by the manufacturer are worst case. Therefore, appropriate data for this analysis are somewhat reduced, e.g., max. rms. fractional frequency deviation for 1 ms averaging time is 8×10^{-10} , the value used in the analysis below is 6×10^{-10} .

2. Long Term Stability (Associated with Cesium Beam Operation)

| <u>Ave. Time</u> | <u>rms. Fractional Freq. Deviation</u> |
|------------------|----------------------------------------|
| 100 sec | 1×10^{-11} |

3. Oscillator Output Filter Bandwidth = 125 Hz.

The oscillator output power density spectrum $S_{\dot{\phi}}(\omega)_{out}$ is composed of the power density of the cesium reference, $S_{\dot{\phi}}(\omega)_{ref}$, and the quartz oscillator $S_{\dot{\phi}}(\omega)_{osc}$ with appropriate filtering^{2,3} as shown in Fig. 6. The ref-

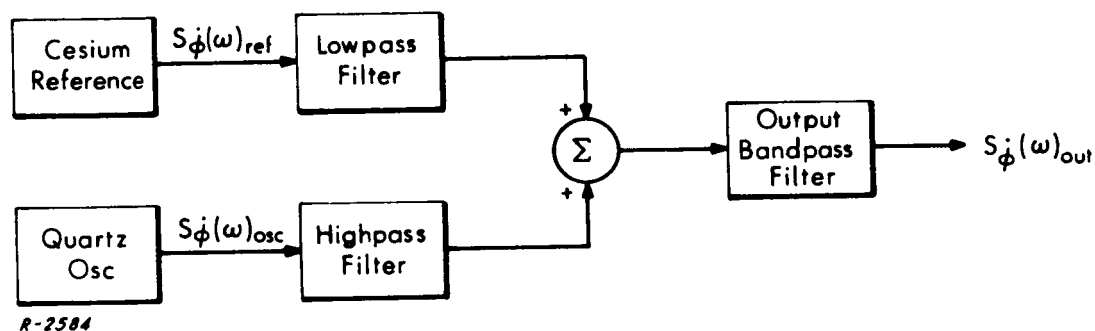


Fig. 6 Equivalent Model of a Stable Source.

erence power density is assumed to be flat³, i. e., $S_{\dot{\phi}}(\omega)_{ref} = K_r$. The mean-square fractional frequency deviation of the reference resonator is approximated by³

$$\left(\frac{\Delta f}{f}\right)^2 \approx \frac{1}{4\pi^2 f^2} \left[\frac{1}{2\pi} \int_{-\infty}^{\infty} K_r^2 \frac{\sin^2 \omega\tau/2}{(\omega\tau/2)^2} d\omega \right] \quad (24)$$

when τ is large. Substituting from Table I that $\Delta f/f = 1 \times 10^{-11}$ when $\tau=100$ sec, it is found that $K_r = 40$ (rad/sec)² per Hz when $f = 10$ GHz. This factor predominates in the expressions of $S_{\dot{\phi}}(\omega)_{out}$ below the cross-over point of the high and lowpass filters of Fig. 6, and down to dc.

Immediately above the cross-over point the factor which predominates is associated with the "flicker" noise, K_f/f , of the quartz oscillator. K_f can be found from²

$$\overline{\left(\frac{\Delta f}{f}\right)^2} \approx \frac{2K_f}{4\pi^3 f^2} \left[1.04 + \frac{1}{2} \ln\left(\frac{T}{2\tau}\right) \right] \quad (25)$$

where T = measurement interval. In particular, T/τ , for the oscillator data under examination here, is approximately 200. The appropriate value of the fractional frequency stability to be substituted into Eq. (25) is less than or equal to 1.5×10^{-11} . This is the level where the rms frequency fluctuations become independent of the averaging time, τ , and such a phenomenon can only be caused by $1/f$ noise⁴. Thus, it is found that $K_f/\omega \approx 0.4/\omega$ for the oscillator under consideration.

The $1/f$ contribution of the quartz oscillator is equal to the white noise density of the reference at

$$\omega = \frac{K_f}{K_r} = \frac{0.4}{40} = 0.01 \text{ rad/sec} \quad (26)$$

It is assumed, then, that the cross-over of the high and lowpass filters of Fig. 6 is in the vicinity of 0.01 rad/sec so that the combined $S_{\phi}^{\dot{}}(\omega)_{\text{out}}$ is constant at 40 from $\omega = 0$ to $\omega = 0.01$ then decreases with value $0.4/\omega$ above $\omega = 0.01$ until the next term becomes predominant.

Perturbation noise contributions to the frequency fluctuations of an oscillator can generate the next important term but these are sometimes masked by its $1/f$ noise². An examination of the short term stability data of Table I shows that this is the case for this oscillator⁴, so the next term of importance comes from additive noise. This term has the form $S_{\phi}^{\dot{}}(\omega)_{\text{osc}} = K_a \omega^2$, and it predominates from the point where its contribution is equal to the $1/f$ noise contribution out to $\omega = \infty$. Somewhere in this region the output

bandpass filter has a roll-off. It is assumed that the lowpass equivalent of this filter is²

$$|H(\omega)|^2 = \frac{(125\pi)^2}{(125\pi)^2 + \omega^2} \quad (27)$$

so that the output power density has the form

$$S_{\phi}(\omega)_{\text{out}} \approx K_a \omega^2 \frac{(125\pi)^2}{(125\pi)^2 + \omega^2} \quad (28)$$

in this region. The mean-square fractional frequency deviation is given by^{2,3,5}

$$\overline{\left(\frac{\Delta f}{f}\right)^2} \approx \frac{1}{4\pi^2 f^2} \left[\frac{1}{2\pi} \int_{-\infty}^{\infty} K_a \frac{4}{\tau^2} \frac{(125\pi)^2}{(125\pi)^2 + \omega^2} \sin^2 \frac{\omega\tau}{2} d\omega \right] \quad (29)$$

Equation (29) can be approximated by

$$\overline{\left(\frac{\Delta f}{f}\right)^2} \approx \frac{1}{4\pi^2 f^2} \cdot \left[\frac{1}{\pi} \int_0^{125\pi} K_a \frac{4}{\tau^2} \sin^2 \frac{\omega\tau}{2} d\omega + \frac{1}{\pi} \int_{125\pi}^{\infty} K_a (125\pi)^2 \frac{\sin^2 \omega\tau/2}{(\omega\tau/2)^2} d\omega \right] \quad (30)$$

Upon substitution into Eq.(30) of data from Table I (e. g., $\Delta f/f = 6 \times 10^{-10}$ at $\tau = 1$ ms or $\Delta f/f \leq 1.2 \times 10^{-10}$ at $\tau = 10$ ms) it is found that $K_a \approx 10^{-5}$.

The components in the power density spectrum of the frequency fluctuations of the oscillator under consideration are summarized in Table II below.

Table II

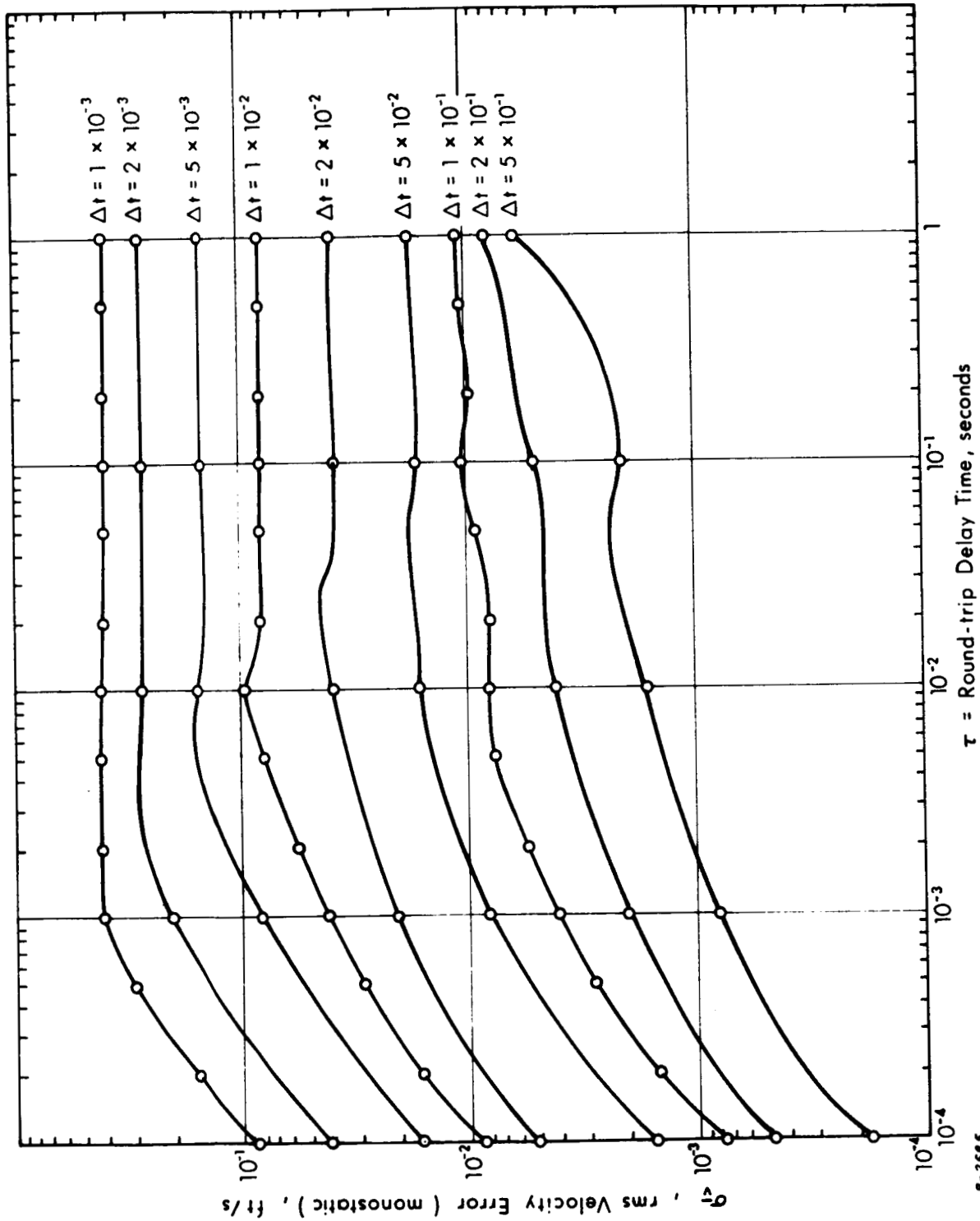
POWER DENSITY SPECTRUM OF FREQUENCY FLUCTUATIONS

| $S_{\phi}(\omega) - \left(\frac{\text{rad}}{\text{sec}}\right)^2$ per Hz | Frequency Range - $\left(\frac{\text{rad}}{\text{sec}}\right)$ | Physical Origin |
|--------------------------------------------------------------------------|----------------------------------------------------------------|-----------------------------------------------------------------------------|
| 40 | $0 \leq \omega < 0.01$ | Cesium Resonator Noise |
| $0.4/\omega$ | $0.01 \leq \omega < 34.3$ | Frequency Drift of the Quartz Oscillator |
| $10^{-5} \omega^2$ | $34.3 \leq \omega < 125\pi$ | Additive Noise in the Quartz Oscillator |
| 1.5 | $125\pi \leq \omega < \infty$ | Additive Noise in the Quartz Oscillator Outside the Output Filter Bandwidth |

Note: The values stated in the table assume an output at 10 GHz. Power density at 5 MHz is the same except that the power density scale should be divided by $(10000/5)^2$

3.4 Doppler Error

The integral of Eq. (23) was computed using the power density data of Table II. The results are plotted in Fig. 7. Consider the case when the averaging time is short, say, 1 ms. As range increases, the velocity error increases. At a range of about 50 miles the error reaches its asymptotic value, approximately 0.4 ft/sec. The round-trip time to the target is just sufficient, at this range, to cause the frequency fluctuations of the returned carrier to be uncorrelated with the transmitted carrier reference frequency fluctuations. Thus, the difference between transmitted and received frequencies is just $\sqrt{2}$ times the rms frequency deviation for that averaging time. This is



R-2585

Fig. 7 Velocity Error as a Function of Round-Trip Delay Time with Averaging Time as a Parameter.

found using Table I to be 8.5 Hz at X-band. This corresponds to a monostatic (one-way) velocity error of 0.425 ft/sec which is approximately the result obtained. The same error would have been obtained if two independent, but statistically similar, oscillators had been used. In other words, the advantages of monostatic operation, i. e., same oscillator reference for transmitter and receiver, are partially lost when the delay to the target exceeds a certain amount.

The results for averaging times, $\Delta t = 10$ ms and 100 ms, are similar except for scale changes. In particular, for $\Delta t = 10$ ms decorrelation is not evident until the target is at a range of approximately 700 miles. Note that for $\Delta t = 100$ ms decorrelation occurs with ranges on the order of 1000 miles or more. It should also be noted that the error due to instability with this particular oscillator at this averaging time is quite small regardless of round-trip delay.

3.5 Summary

In this section it was shown that coherent detection of doppler data is not necessary provided that the oscillators used in the system have adequate long- and short-term stability, and that the vehicle is at sufficiently long range. The error contours of Fig. 7 are applicable with a receiver of noise-bandwidth of 2 kHz. Narrower noise-bandwidths, such as may be appropriate for a deep space tracking mission, result in smaller errors since the doppler error due to instability is approximately proportional to the square root of the receiver noise-bandwidth.

4. ONE-WAY TRACKING WITH A CARRIER ONLY

As was mentioned briefly in Sec. 2, it is possible to determine vehicle trajectories by observing a CW carrier signal emanating from the vehicle provided there are enough observing (ground) stations in the system. This technique operates as follows: each station observes the change in range, Δr , over a time interval, Δt , by counting received doppler cycles during the interval. The measured change in range at each station can then be expressed in terms of the particular station's position and the coordinates of the trajectory at the start and end of the counting interval. For example, if the i^{th} station has coordinates (X_i, Y_i, Z_i) and the start point, Q_1 , has coordinates (x_1, y_1, z_1) and the end point, Q_2 , has coordinates (x_2, y_2, z_2) the change in range is given by

$$\Delta r_i = \sqrt{(x_2 - X_i)^2 + (y_2 - Y_i)^2 + (z_2 - Z_i)^2} - \sqrt{(x_1 - X_i)^2 + (y_1 - Y_i)^2 + (z_1 - Z_i)^2}$$

Six or more such equations can be written; one for each observing station. These are then solved for the six unknown coordinates of the start and end points.

In this section, this technique and variations of it are investigated. An error analysis is performed and some general comments on errors are included.

4.1 Statement of the Problem

We are concerned with the problem of tracking a vehicle which carries a highly stable oscillator capable of emitting a tone of known frequency.

Our ground equipment consists only of several listening stations which record the change in the phase of the tone from time t to time $t + \Delta t$. We assume that we are given nominal positions of the vehicles at times t and $t + \Delta t$, and also that the actual positions do not deviate far from the nominal ones. We wish to use our measurements at each station to determine to a first-order approximation the deviation of the actual positions from the nominal ones. Clearly a basic parameter of the system is the time change Δt over which we record the change in phase. We shall assume that Δt is fixed.

4.2 Analysis for Two Points

With the given parameter Δt fixed we cannot hope to find out anything about the motion of the vehicle at an instant of time, and we must talk always in terms of averages over a time interval of length Δt . Within this limitation we can say that the motion of the vehicle at time t is completely described by the state vector

$$s_1(t) = (x(t), y(t), z(t), v_x(t), v_y(t), v_z(t)) \quad (31)$$

where $(x(t), y(t), z(t))$ is the position of the vehicle at time t and $(v_x(t), v_y(t), v_z(t))$ is its average velocity over the time interval t to $t + \Delta t$. In the case where we are making measurements of the phase change between just two points on the vehicle's path a different state vector is convenient, namely

$$s_2(t) = (x(t), y(t), z(t), x(t + \Delta t), y(t + \Delta t), z(t + \Delta t)) \quad (32)$$

where of course $(x(t + \Delta t), y(t + \Delta t), z(t + \Delta t))$ is the vehicle's position at time $t + \Delta t$. That knowledge of one of these vectors is equivalent to knowledge of the other is seen at once from the equations

$$\left. \begin{aligned} x(t+\Delta t) &= x(t) + v_x(t) \Delta t \\ y(t+\Delta t) &= y(t) + v_y(t) \Delta t \\ z(t+\Delta t) &= z(t) + v_z(t) \Delta t \end{aligned} \right\} \quad (33)$$

and

$$\left. \begin{aligned} v_x(t) &= \frac{x(t+\Delta t) - x(t)}{\Delta t} \\ v_y(t) &= \frac{y(t+\Delta t) - y(t)}{\Delta t} \\ v_z(t) &= \frac{z(t+\Delta t) - z(t)}{\Delta t} \end{aligned} \right\} \quad (34)$$

Suppose now that we have n listening stations located at the points $P_i = (X_i, Y_i, Z_i)$ $i = 1, 2, \dots, n$ and m points $Q_j = (x_j, y_j, z_j)$ $j = 1, 2, \dots, m$ on the vehicle's path through which the vehicle passes at times $t, t+\Delta t, \dots, t+(m-1)\Delta t$ respectively. Denote the corresponding points on the nominal path by $Q_j^0 = (x_j^0, y_j^0, z_j^0)$, $j = 1, 2, \dots, m$. In this section we deal in a special way with the particular case of $m = 2$ and $n = 6$. In a later section we shall develop a theory for general m and n .

Let the change in the number of cycles on the counter at station P_i be μ_i as the vehicle moves from Q_1 to Q_2 , then the corresponding change f_i in the distance of the vehicle from P_i is given by

$$f_i = \lambda \mu_i = \frac{c \mu_i}{f} \quad (35)$$

where c, λ, f are the velocity, wavelength and frequency respectively of the tone. We can also express this distance in terms of the coordinates of the

points involved

$$f_i = \sqrt{(x_2 - X_i)^2 + (y_2 - Y_i)^2 + (z_2 - Z_i)^2} - \sqrt{(x_1 - X_i)^2 + (y_1 - Y_i)^2 + (z_1 - Z_i)^2} \quad (36)$$

But since Q_1 and Q_2 are close to Q_1^0 and Q_2^0 we have a first-order approximation

$$\delta f_i = -l_{i1} \delta x_1 - m_{i1} \delta y_1 - n_{i1} \delta z_1 + l_{i2} \delta x_2 + m_{i2} \delta y_2 + n_{i2} \delta z_2 \quad (37)$$

where δf_i is the deviation in f_i from the value it would have if the actual path passed through Q_1 and Q_2 , $(\delta x_1, \delta y_1, \delta z_1)$ and $(\delta x_2, \delta y_2, \delta z_2)$ are the differences in coordinates between the points Q_1, Q_1^0 and Q_2, Q_2^0 respectively and (l_{ij}, m_{ij}, n_{ij}) are the direction cosines of the line joining P_i to Q_j^0 . Equation (37) holds for $i = 1, 2, \dots, n$, so using (36) to determine δf_i we get a system of n equations in six unknowns which may be written in the form

$$AU = V \quad (38)$$

where

$$V = \begin{pmatrix} \delta f_i \\ ' \\ ' \\ ' \\ ' \\ \delta f_n \end{pmatrix}, \quad U = \begin{pmatrix} \delta x_1 \\ \delta y_1 \\ \delta z_1 \\ \delta x_2 \\ \delta y_2 \\ \delta z_2 \end{pmatrix} \quad (39)$$

and

$$A = \begin{pmatrix} -l_{11}, & -m_{11}, & -n_{11}, & l_{12}, & m_{12}, & n_{12} \\ & & & & & \\ & & & & & \\ & & & & & \\ & & & & & \\ & & & & & \\ & & & & & \\ & & & & & \\ & & & & & \\ -l_{n1}, & -m_{n1}, & -n_{n1}, & l_{n2}, & m_{n2}, & n_{n2} \end{pmatrix} \quad (40)$$

The least squares solution of (38) is given by

$$U = (A'A)^{-1} A'V \quad (41)$$

where A' is the transpose of the matrix A . This is a standard result and it may be found in Scheffe⁶. If $n=6$ and A is nonsingular, (41) reduces to the simpler form

$$U = A^{-1}V \quad (42)$$

If instead of the state vector $s_2(t)$ we used the state vector $s_1(t)$ we would again obtain a system of Eq. (38) where V is the same as before but U , instead of being the deviation in the state vector $s_2(t)$, is the deviation in $s_1(t)$ from its nominal value, that is

$$U = \begin{pmatrix} \delta x_1 \\ \delta y_1 \\ \delta z_1 \\ \delta v_x \\ \delta v_y \\ \delta v_z \end{pmatrix} \quad (43)$$

and

$$A = \begin{pmatrix} -l_{11} + l_{12}, & -m_{11} + m_{12}, & -n_{11} + n_{12}, & l_{12}\Delta t, & m_{12}\Delta t, & n_{12}\Delta t \\ \vdots & \vdots & \vdots & \vdots & \vdots & \vdots \\ -l_{n1} + l_{n2}, & -m_{n1} + m_{n2}, & -n_{n1} + n_{n2}, & l_{n2}\Delta t, & m_{n2}\Delta t, & n_{n2}\Delta t \end{pmatrix} \quad (44)$$

4.3 Error Analysis

In this section we shall calculate the variance of the least squares solution (41) in terms of the variances of the known quantities δf_i , which we assume are uncorrelated normally distributed random variables with equal variances σ^2 . Again from Scheffe⁶ it is a standard result that the covariance matrix C of the solution (41) defined by

$$(C)_{ij} = \text{cov} [u_i, u_j] \quad (45)$$

is given by

$$C = (A'A)^{-1} \sigma^2 \quad (46)$$

Thus, for example, the variance for the deviation δx_1 and therefore also for the coordinate x_1 is just C_{11} . More generally the variance of the solution for the point Q_1 is $C_{11} + C_{22} + C_{33}$ and for Q_2 it is $C_{44} + C_{55} + C_{66}$. Thus

the variance for finding the complete state vector s_2 is simply

$$\text{var} [s_n] = \text{Tr } C \quad (47)$$

where the right-hand side is the trace of the matrix C .

If $\{\kappa_i\}$ $i = 1, 2, \dots, 6$ denote the eigenvalues of $A'A$ we can rewrite (47) as

$$\text{var} [s_2] = \sigma^2 \left(\frac{1}{\kappa_1} + \frac{1}{\kappa_2} + \dots + \frac{1}{\kappa_6} \right) \quad (48)$$

In the case $n=6$ we may express (48) in terms of the eigenvalues of A rather than of $A'A$. Thus if $\{\lambda_i\}$ $i = 1, 2, \dots, 6$ are these eigenvalues we have

$$\text{var} [s_2] = \sigma^2 \left(\frac{1}{|\lambda_1|^2} + \frac{1}{|\lambda_2|^2} + \dots + \frac{1}{|\lambda_6|^2} \right) \quad (49)$$

We should note carefully that the above error analysis takes no account whatsoever of errors in the numerical computation of the solution (41), but only of the effect of errors with a given distribution in the determination of the deviations δf_i . Thus it is important to recall the gross errors which usually arise in the numerical inversion of a nearly singular matrix.

4.4 Symmetrical Arrays and Singular Paths

Equations (41) and (46) above show that the core of the computation is the inversion of the matrix $A'A$, and that in the special case $n=6$ we need to invert only A . Thus it is vital to recognize situations in which $A'A$ or A , as the case may be, is singular or nearly so. This is due entirely to the geometry of the station array and the relation of the vehicle's path to this array. Many interesting results remain to be discovered in this area. We give here one remarkable result mentioned in Holberg, Voss and Kampmeyer⁷.

Suppose we have six stations in a plane, that is, $n = 6$, and that the projection of the line connecting Q_1 and Q_2 onto the plane happens to pass through the array in such a way that three of the stations are reflections in the path's projection of the other three stations. We assume that none of the stations lie on the path's projection. Then the result is that the matrix A is singular. This means that we have a whole plane of possible paths which give rise to singular matrices, so that an array with such a property is very poor indeed. The result is proved by noticing that the matrix A must have the form

$$A = \begin{pmatrix} \begin{array}{ccc|ccc} \ell_{11}' & -m_{11}' & -n_{11}' & -\ell_{12}' & m_{12}' & n_{12}' \\ -\ell_{11}' & -m_{11}' & -n_{11}' & \ell_{12}' & m_{12}' & n_{12}' \\ \hline \ell_{13}' & -m_{13}' & -n_{13}' & -\ell_{23}' & m_{23}' & n_{23}' \\ -\ell_{13}' & -m_{13}' & -n_{13}' & \ell_{23}' & m_{23}' & n_{23}' \\ \hline \ell_{15}' & -m_{15}' & -n_{15}' & -\ell_{25}' & m_{25}' & n_{25}' \\ -\ell_{15}' & -m_{15}' & -n_{15}' & \ell_{25}' & m_{25}' & n_{25}' \end{array} \end{pmatrix} \quad (50)$$

the determinant of which is the same as the determinant of

$$\begin{pmatrix} \begin{array}{ccc|ccc} 0 & -m_{11}' & -n_{11}' & 0 & m_{21}' & n_{21}' \\ \ell_{11}' & 0 & 0 & \ell_{21}' & 0 & 0 \\ \hline 0 & -m_{13}' & -n_{13}' & 0 & m_{23}' & n_{23}' \\ \ell_{13}' & 0 & 0 & \ell_{23}' & 0 & 0 \\ \hline 0 & -m_{15}' & -n_{15}' & 0 & m_{25}' & n_{25}' \\ \ell_{15}' & 0 & 0 & \ell_{25}' & 0 & 0 \end{array} \end{pmatrix} \quad (51)$$

The determinant of (51) is zero, which shows that A is singular.

It is also apparent that as the points Q_1 and Q_2 get closer together the direction cosines of the lines to them from the points P_i become more nearly equal, so that in general $A'A$ has its first three columns nearly equal to its second three columns and therefore it is nearly singular. Therefore the errors in the numerical computation become predominant for sufficiently small Δt .

We conjecture the following rule of thumb for relating the vehicle's path and the geometry of the array. For a given path and a given number of stations in a plane, a good array to determine this path is one which has all the stations on a single line parallel to the path's projection, a bad array is one which has the stations on a line perpendicular to this projection.

4.5 Analysis for m Points

Suppose we have n stations P_i and m points Q_j on the vehicle's path. Our analysis here will differ from the two point case, since we do not want to single out any point Q_j for special treatment in estimating the change of range of the vehicle from the various stations P_i . We therefore introduce the bias b_i of station P_i for $i = 1, 2, \dots, n$. By this we mean $(-b_i)$ is the range of P_i from some agreed upon initial point on the path. Then if the counter reading at P_i is μ_{ij} when the vehicle is at Q_j we have

$$g_{ij} = \lambda \mu_{ij} = \frac{C \mu_{ij}}{f} \quad (52)$$

where g_{ij} is the change in range when the vehicle moves from the unspecified initial point to Q_j . Expressing this now in terms of the bias and the coordinates of P_i and Q_j we have

$$g_{ij} = \sqrt{(x_j - X_i)^2 + (y_j - Y_i)^2 + (z_j - Z_i)^2} + b_i \tag{53}$$

Assuming we are given a nominal path of the vehicle and that the deviations from it are not large we have a first-order approximation to (53) namely

$$\delta g_{ij} = \delta b_i + l_{ij} \delta x_j + m_{ij} \delta y_j + n_{ij} \delta z_j \tag{54}$$

which holds for $i = 1, \dots, n, j = 1, \dots, m$. Thus using (53) to determine δg_{ij} we may write (54) as a system of nm equations

$$AU = V \tag{55}$$

in the $n + 3m$ unknowns $\{\delta b_1, \dots, \delta b_n\}$ and $\{\delta x_j, \delta y_j, \delta z_j\} j = 1, \dots, m$.

In (55) we have

$$U = \begin{pmatrix} \delta b_1 \\ \vdots \\ \delta b_n \\ \hline \delta x_1 \\ \delta y_1 \\ \delta z_1 \\ \vdots \\ \vdots \\ \vdots \\ \hline \delta x_m \\ \delta y_m \\ \delta z_m \end{pmatrix}, \quad V = \begin{pmatrix} \delta g_{11} \\ \vdots \\ \delta g_{n1} \\ \hline \delta g_{12} \\ \vdots \\ \delta g_{n2} \\ \vdots \\ \vdots \\ \vdots \\ \hline \delta g_m \\ \vdots \\ \delta g_{mn} \end{pmatrix} \tag{56}$$

and

$$A = \begin{pmatrix} I & A_1 & 0 & \dots & 0 \\ I & 0 & A_2 & \dots & 0 \\ \vdots & \vdots & \vdots & \ddots & \vdots \\ \vdots & \vdots & \vdots & \ddots & \vdots \\ \vdots & \vdots & \vdots & \ddots & \vdots \\ \vdots & \vdots & \vdots & \ddots & \vdots \\ I & 0 & 0 & \dots & A_m \end{pmatrix} \quad (57)$$

where

$$A_j = \begin{pmatrix} l_{1j} & m_{1j} & n_{1j} \\ - & - & - \\ l_{nj} & m_{nj} & n_{nj} \end{pmatrix} \quad (58)$$

is a $n \times 3$ matrix and I is the $n \times n$ identity matrix. The least squares solution of (55) has the same form as (41) and in the special case that A is a square matrix it has the form (42). The error analysis also yields a result of the form (46). Because of the special form of A in (57), it is easy to show that the inversion of $A'A$ and of A itself involves the inversion of matrices of order n at most.

The numerical experiments of Holberg, Voss and Kampmeyer⁷ indicate that the variance of the solution for a given point is reduced if this point is one of several being determined rather than one of a pair. We stress that this is of course for fixed Δt . We have not determined in the above how the error changes if we subdivide the intervals determined by Δt and take readings at the additional points.

It is of interest to note that the only two cases where the system (57) has the same number of equations as unknowns are $m = 2, n = 6$ and $m = 4, n = 4$. The system is underdetermined in the cases $m = 1, n \geq 1$; $m = 2, 1 \leq n \leq 5$; $m = 3, 1 \leq n \leq 4$ and $m \geq 4, 1 \leq n \leq 3$. In all other cases the system is overdetermined.

4.6 The Free-Fall Case

If the vehicle is moving in the gravitational field and there is no other force influencing its motion, then it is possible in some cases to find the solutions (41), (42) and (46) rather easily. To do this we must make use of the observation by Potter in Battin⁸ that if the matrix $A'A$ is of even order, it is essentially a symplectic matrix and therefore its inverse can be found by a simple rearrangement of its elements. We say that a matrix Q of even order is symplectic if

$$Q' J Q = J \quad (59)$$

where

$$J = \begin{pmatrix} 0 & I \\ -I & 0 \end{pmatrix} \quad (60)$$

and I is an identity matrix. It is easily verified that

$$J^2 = -I \quad (61)$$

and hence that

$$Q^{-1} = -J Q' J \quad (62)$$

The importance of this result lies in its applicability to vehicles in orbit, and therefore it is useful for problems of guidance of vehicles and for terrestrial navigation systems of the Transit type.

4.7 Summary

The quality of the trajectory determination obtained with the carrier-only technique is highly dependent on the geometric relationship between the vehicle trajectory and the ground-station locations. In some cases, the error in start or end point determination can be as low of 2 or 3 times the measurement error of the changes in range observed at each site. On the other hand, it is possible for the trajectory determination equations to "blow up" yielding infinite errors. One way to avoid this difficulty is to add more stations at suitable locations. Another way is to use some inherent properties of the trajectory, if any, to provide additional information. Such a technique can be applied with free-fall vehicles. It was also found that the trajectory determination computation is considerably simplified in the free-fall case.

5. ONE-WAY RANGING WITH RANGE-TONES

The one-way ranging method described in Sec. 4 offers several advantages; namely, the hardware required for implementation of this technique is not complex and target position can be determined unambiguously. On the other hand, it cannot produce accurate tracking data in real-time (unless initialization data is supplied by other means). Accurate tracking data is available only after the vehicle moves such that the target-station configuration changes substantially. In fact, it can be generalized that the accuracy of tracking data obtained using doppler-only data is highly sensitive to the tracking geometry.

It is possible to augment the tracking characteristics of the doppler-only one-way ranging system by adding ranging tones to the vehicle-borne transmitter output. The range-tones are phase modulated onto the transmitted carrier and can be used to provide range-difference data. As described in Sec. 2, this data is ambiguous. But, note that sufficiently accurate target position data can be derived from the doppler-only measurement to resolve the ambiguities. Similarly, the data derived from the range-tones can be used to improve the doppler-only measurement because the range-tone data is available in real-time. Thus, the data obtained with these two techniques, doppler-only and range-tone, are complementary to each other.

The range-tones can be modulated onto the CW carrier without significant reduction of carrier power if the deviation of the modulation is small. Thus, there is no important deterioration of the doppler-only portion of the system due to the addition of range-tones. The addition of range-tones does, however, increase system complexity.

The advantages gained by adding range-tones must be weighed against the cost of the system required to process the range-tones to extract data. The vehicle-borne transmitter must be modified to include a range-tone generator

and modulator. This modification is not difficult technically, but any increase in complexity of the vehicle-borne part of the system is serious enough to warrant complete justification. In addition, the ground-based receiving stations must be equipped with range-tone demodulators and phasemeters. Finally, each ground station must be supplied with a synchronous timing signal. The precision required of the timing signal depends on the specified ranging accuracy of the system. For example, if the system is required to measure position to within 1000 ft., a timing reference with accuracy of at least 1 μ s is necessary. This can be obtained by synchronizing a stable local reference to a standard timing signal such as WWV or LORAN-C. On the other hand, if position data is to be obtained with accuracy of 10 ft., a special stabilized baseline timing system must be used. This latter system is costly, especially if the baseline lengths are long.

6. CONCLUSIONS

The long-term stability of presently available ultrastable oscillators is such that frequency uncertainty (long-term) can now contribute less to doppler error than the uncertainty in the speed of light. This is the basis for justifying the use of these devices in one-way tracking systems. The effect of short-term instability has been examined in detail. It is found that the doppler error due to short-term instability can be reduced by coherent demodulation using the reference for transmission and reception. However, this reduction is obtainable only for vehicles with sufficiently small range. For most long-range targets, coherent detection is unnecessary. Furthermore, the error due to short-term instability of the ultrastable source is small.

A method for determining vehicle trajectories from doppler data observed at several ground sites is presented. This technique can yield high quality trajectory data provided the geometric relationship between trajectory and ground sites is suitable. A method for augmenting the capability of this technique is described which requires the addition of sinusoidal PM ranging tones to the carrier transmitted from the vehicle. This modification also requires a considerable increase in overall system and data processing complexity. However, this modification allows for one-way tracking with geometries which preclude the use of carrier-only operation.

The detailed design of a suitable one-way tracking system is strongly dependent on the particular tracking requirements and vehicle dynamics. But, in general, it can be seen that one-way tracking can be implemented successfully for deep-space tracking missions, especially with free-fall vehicles. Furthermore, the usefulness of this technique in a global navigation system has already been demonstrated. This application has a great deal of potential, considering the present state-of-the-art.

REFERENCES FOR PART I

1. Hewlett-Packard Catalog No. 25, April 1965, except as noted.
2. Cutler, L. S. , and Searle, C. L. , "Some Aspects of the Theory and Measurement of Frequency Fluctuations in Frequency Standards," Proc. IEEE, Vol. 54, No. 2, pp.136-154, February 1966.
3. Lacey, R. F. , et al, "Short Term Stability of Atomic Frequency Standards," Proc. IEEE, Vol. 54, No. 2, pp. 170-175 February 1966.
4. Cutler and Searle, loc. cit. Fig. 13.
5. Baghdady, E. J. , Lincoln, R. N. and Nelin, B. D. , "Short Term Frequency Stability," Proc. IEEE, Vol. 53, No. 7, pp. 704-722, July 1965.
6. Scheffe, Henry, The Analysis of Variance, Wiley, 1961.
7. Holberg, Dieter E. , Voss, Robert A. , and Kampmeyer, Preston M. , "Statistical Error Analysis of Trajectory Determination from Non-Initialized Doppler-Cycle Counts," Instrumentation Development Directorate, White Sands Missile Range, New Mexico, June 1966.
8. Battin, Richard H. , Astronautical Guidance, McGraw-Hill, 1966.

PART II

FLUCTUATION SPECTRA OF ULTRASTABLE OSCILLATORS:
MEASUREMENT AND ESTIMATION

1. INTRODUCTION

The increased accuracies and precisions demanded of space and ground-support systems have led to the need for ultrastable signal sources. The characterization of the stability of such sources has been the subject of much recent research.

A characterization in terms of the power spectrum of phase or frequency fluctuations has been found highly useful and meaningful¹⁻⁵. This offers a direct link between oscillator behavior and the performance of the system incorporating the oscillator. Further, it enables the identification and evaluation of the instability mechanisms within an oscillator.

This report is principally concerned with the measurement of the fluctuation spectra of ultrastable oscillators. The objective of the study documented in Part II of this report, as defined in the Task Statement, is:

Development of a measurement technique for determining in the frequency domain the phase fluctuation spectrum of highly stable oscillators. The major area of interest is that part of the spectrum from 10^{-5} Hz to 10^3 Hz. This task will not include hardware development but will consider the best way to use available equipment to produce the desired results.

The measurement of oscillator fluctuation spectra involves two distinct steps. First, there is the extraction of the phase or frequency fluctuations from the oscillation signal; and then there is the measurement or estimation of the corresponding power spectra from the extracted fluctuations.

While these two steps are indeed distinct both logically and experimentally, nevertheless the spectral-estimation techniques to be utilized dictate the

manner of extraction and presentation of the fluctuations. Consequently, we begin in Sec. 2 by considering the general spectral-estimation techniques capable of achieving the task requirements in order to determine the methods of extraction and presentation of the oscillator fluctuations that must be used.

Several fluctuation-extraction techniques are currently available, some (described in Sec. 2.1) are utilized in the laboratories of GSFC, and another⁶ was developed by ADCOM, Inc. Section 2 includes specific recommendations on the use of some of these techniques to extract the fluctuations of ultrastable oscillators. We find it necessary to obtain sequences of samples of the fluctuations, utilizing several observation periods and sampling rates. The samples must be suitably recorded for presentation to a digital computer programmed to estimate the spectra.

Mathematical techniques for spectral estimation are presented in detail in Secs. 3 and 4. The estimation of spectra of random processes from finite observations is a very young science. The earliest exposition of the subject⁷ is less than eight years old. We have drawn in Secs. 3 and 4 on the results of very recent research⁸⁻¹¹, some of which is not widely available. Consequently, we have found it necessary to compile, in Sec. 3, an exposition of the theoretical foundations of spectral estimation.

The foundations compiled in Sec. 3 lead to the practical computational procedures detailed in Sec. 4. The most useful procedure for our purposes is presented and discussed in Secs. 4.1 - 4.3. Sections 4.4 - 4.7 are concerned with the estimation of discrete (i. e., periodic) components which may be embedded in the spectra. Section 4.8 outlines a useful procedure applicable to a special class of fluctuations (autoregressive time series). Conclusions and recommendations on the use of these procedures are drawn in Sec. 5.

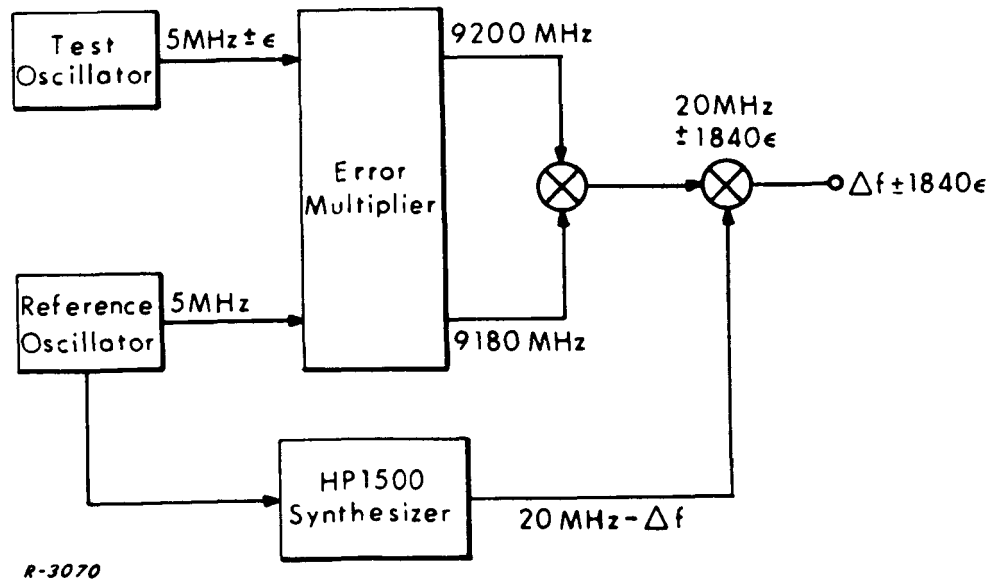
2. EXTRACTION OF OSCILLATOR FLUCTUATIONS

2.1 Available Fluctuation Extraction Techniques

Several techniques are currently utilized in the laboratories of GSFC to extract oscillator fluctuations. We begin by reviewing these techniques in order to determine their usefulness for the task at hand.

Since all oscillator fluctuations are only relative with respect to another oscillation, any extraction system must utilize two oscillators, one of which acting as reference. Providing that the statistical independence of all oscillator fluctuations are assured, two-at-a-time measurements upon three oscillators are sufficient to determine the fluctuation spectrum of each. Of course, if it is known beforehand that the spectral density of the reference oscillator fluctuations are negligible in comparison with that of the oscillator under test, at least in the spectral region of interest, then the desired spectrum can be obtained from one measurement.

Figure 1 depicts the configuration of the error-multiplication system common to the available GSFC extraction techniques. (The frequencies



R-3070

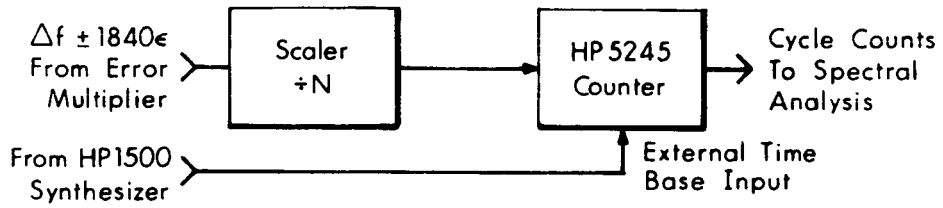
Fig. 1 Error Multiplication and Synthesis System.

in Fig. 1 are offered only as examples.) The frequency fluctuation, denoted by ϵ , is magnified by a large factor (1840) and emerges on a low frequency output oscillation Δf (typically 100 kHz). This error multiplication enhances the sensitivity to small fluctuations of the fluctuation extraction techniques.

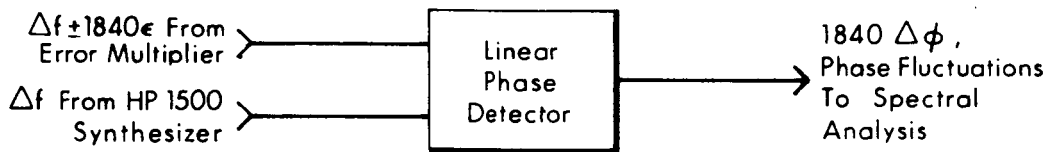
Figure 2 illustrates three different fluctuation-extraction instrumentations that can follow the error multiplier. Each technique has inherent advantages and limitations that determine its usefulness for the present purposes.

The cycle-counting technique (also called period-counting) shown in Fig. 2(a) was utilized primarily to determine "fractional frequency instability." The output of the error multiplier is first divided for convenience then introduced as a triggering signal to a gate in the counter. The gate opens at one zero-crossing, passing the high-frequency external clock signal (obtained from the reference oscillator via the synthesizer) which is "accumulated" or counted in the counter register. After an integral number of periods of the error-multiplier output, the gate is closed and the total count read. As the period of the external clock signal is chosen a simple decimal fraction of a second, say $0.1 \mu s$, the counter will display the total number of $0.1 \mu s$ that equals the integral number of the input periods. We denote the length of time the gate is open by τ . Usually several consecutive measurements of length τ are made, and the resulting data reduced to yield the average value and the mean-square deviation of the accumulated periods. The rms value of the deviation divided by the average of the period accumulated in a time τ is denoted by $I(\tau)$. It can readily be shown that this normalized rms deviation of period is essentially equal to the normalized rms deviation of frequency for highly stable oscillators.

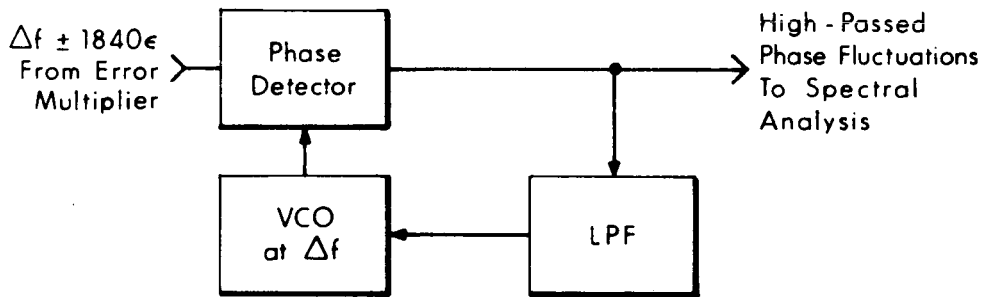
For the present purposes, the cycle-counting technique may be utilized to yield directly a measure of frequency fluctuations. The least significant



(a) Cycle - Counting Technique



(b) Phase - Detector Technique



(c) Phase-Locked Loop Technique

R-3071

Fig. 2 Three Fluctuation Extraction Techniques.

digits of the counter readout are directly proportional to frequency fluctuation $\Delta\dot{\phi}$, the proportionality factor being readily determined by initial calibration.

The conditions for the validity of this statement are:

- a. the oscillator is highly stable, and
- b. the reciprocal of the counting duration τ is much greater than the extent of the region of interest in the spectrum of the frequency fluctuations.

The cycle counter should be operated without averaging, i. e., each count should appear separately at the output. The output is then a sequence of samples of the frequency deviations $\Delta\dot{\phi}$, which must be digitally recorded (e. g., on punched-paper tape) for subsequent processing. A question arises as to the uniformity of the sampling intervals. Since the gate time τ varies (slightly) according to the oscillator fluctuations, and since most counters have a fixed dead time between gate closing after one count and gate opening for the next count (typical dead time is 100 ms) it follows that the sampling intervals are not uniform. However, as long as the oscillator is highly stable, the sampling intervals are almost exactly uniform, and should introduce negligible inaccuracy in the measured spectrum.

A simple way exists for avoiding this slight sampling nonuniformity, namely to utilize the counter in the frequency (vs period) count mode. In this case the $\div N$ scaler shown in Fig. 2(a) is removed and Δf is chosen high enough for good resolution. The counter gate is controlled by the external clock input thereby ensuring uniform sampling, and the number of cycles of the error multiplier output are counted. Again, the least significant digits of the counter are directly proportional to the frequency fluctuation $\Delta\dot{\phi}$, and may be digitally recorded for subsequent processing. The only limitation for the validity of this measurement is that $1/\tau$ must be much greater than the extent of the region of interest in the spectrum of the frequency fluctuations. Furthermore, the sampling intervals are now exactly uniform.

A limitation of the cycle-counting technique is imposed by the counter dead time which places a lower limit on sampling period. For example, a counter with dead time of 100 ms cannot sample as fast as 10 samples per second. Such a sampling rate would not be suitable for fluctuations containing significant spectral components above 5 Hz, otherwise spectral folding (or aliasing) will occur. We shall return to this aliasing problem a little further on. We simply point out here that a long dead time can readily be reduced by appropriate circuit modifications in the counter, since the counter speed is fundamentally restricted only by the counter recovery time which is much shorter than the dead time.

The phase-detector technique shown in Fig. 2(b) is direct and simple. It yields an analog waveform proportional to the phase fluctuation $\Delta\phi$ provided it does not exceed $\pm\pi$ radians. This waveform may be recorded directly or it may be sampled and digitally recorded for subsequent processing. The limitations of this technique are:

- a. The output waveform suffers large discontinuities as $\Delta\phi$ goes through $\pm\pi$ radians. This can be remedied in subsequent processing, however, by identifying the direction of the discontinuities and accumulating multiples of π radians.
- b. The phase detector is sensitive to incidental AM at its input, especially when $\Delta\phi$ approaches $\pm\pi$ radians. This AM-to-PM susceptibility may be reduced by introducing an amplitude limiter before the phase detector.

The phase-locked loop technique shown in Fig. 2(c) utilizes the VCO essentially as another phase reference. It is well known that the output of such a loop is a high-passed version of the phase fluctuations $\Delta\phi$ plus the phase fluctuations of the VCO itself. The high-pass cutoff frequency is essentially the loop bandwidth. Since loop bandwidths narrower than 1 Hz are difficult to implement, this technique is not suitable for extraction of slow phase fluctuations.

Satisfactory results have been obtained with this technique in conjunction with an automatic spectrum analyzer, down to about 15 Hz. The internal VCO fluctuations in this spectral region are apparently small compared with the measured maser fluctuations. A simple way to check this is to use an identical VCO, with its control terminals shorted, as the input to the loop. The measured spectral density is then simply twice that of each VCO, and should be found to be negligible compared to the fluctuation spectra measured with the oscillator. By utilizing narrow loop bandwidths and low-frequency automatic spectrum analyzers, it should be possible to obtain spectral measurements down to about 3 Hz.

Finally, it is important to recognize that any fluctuation extraction technique introduces some internal fluctuations of its own. These are best characterized by the residual fluctuation spectra measured with the extraction system operating in common mode, i. e., with a single stable oscillator used both as reference and as input to be measured. No satisfactory measurements of the residual spectra of the three techniques are presently available, so that it is impossible to tell the relative merits of the techniques beyond the limitations discussed above.

2.2 Spectral-Estimation Considerations

In this section we consider some general properties of the spectral-estimation techniques capable of achieving the present task requirements in order to determine the methods of extraction and presentation of the oscillator fluctuations that must be used.

Automatic spectrum analyzers can accommodate the high two or three orders of magnitude of the desired spectrum (10^0 or 10^1 to 10^3 Hz). Below this range (below 10^1 Hz, say) we must resort to computational techniques utilizing suitable records of the fluctuations. These computations would have

to be performed on the only available and practical tool, namely the digital computer. Thus the fluctuations must be suitably sampled and quantized before presentation to the computer. This raises several questions:

- a. How long must the sampled record be?
- b. How rapidly must the fluctuations be sampled?
- c. Which fluctuation-extraction technique is suitable for the purpose?

The first question is related to the spectral resolution obtainable from a finite record. A well-established result is (see Ref. 7, p. 147) that it is impossible to resolve two spectral components closer than $1/T$ Hz apart from a record of duration T . Since it is desired to extract the spectrum down to 10^{-5} Hz, we must resolve any component at that frequency from one at zero frequency. We find that the corresponding duration of the record must be greater than 28 hours!

Question (b) is related to the spectrum folding (or aliasing) phenomenon mentioned earlier. When an analog waveform is uniformly sampled every Δt seconds, the spectrum of the samples can be shown to be related to that of the analog waveform in the manner illustrated in Fig. 3 (see Ref. 7, p. 31 and p. 117 for a proof and full discussion). The "Nyquist frequency" around whose

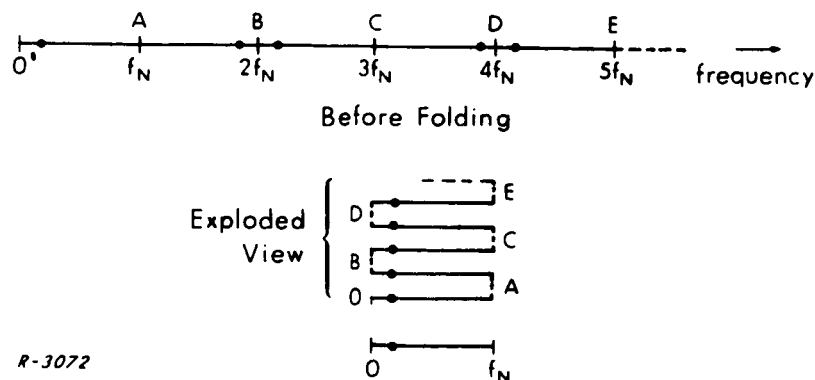


Fig. 3 Spectrum Folding or Aliasing.

multiples folding occurs is $f_N = \frac{1}{2\Delta t}$, and the value of the spectrum of the sampled waveform is the sum of the values of the spectrum of the original waveform at the dotted frequencies. Clearly, if the original analog waveform contained significant components at frequencies above the Nyquist frequency, then the spectrum estimated from the sampled replica of the waveform will not be a good estimate of the spectrum of the original waveform. Stated in a different way, the sampling must be rapid enough so that the significant part of the spectrum lies below the Nyquist frequency.

Now, if the original spectrum contains significant components up to 1 kHz, the sampling period must be 1/2 ms. Combining this figure with the 28-hour required duration, we have a staggering amount of input data that must be processed by the computer. To avoid this problem, we recommend breaking the spectrum into three overlapping regions, and then recording data and performing computations for each region individually. The proposed regions are listed below, along with the corresponding minimum record lengths and maximum sampling intervals.

| <u>Region</u> | <u>From</u> | <u>To</u> | <u>Min T</u> | <u>Max Δt</u> |
|---------------|--------------|-----------|--------------|----------------------------------|
| High | 10^{-1} Hz | 10^2 Hz | 10 sec | 5 ms |
| Medium | 10^{-3} | 10^0 | 1000 sec | 0.5 sec |
| Low | 10^{-5} | 10^{-2} | 28 hours | 50 secs |

In taking data for each region, it is intended that the fluctuations be lowpass filtered prior to sampling in order to avoid aliasing problems, with the filter cutoff frequency placed below the upper end of the region. We shall return to the matter of filtering a little further on.

regions. Furthermore, since the long dead time (100 ms) causes aliasing about a Nyquist frequency of 5 Hz, we must ensure beforehand that the spectral content above this frequency is small compared with that below it. Otherwise, the dead time must be reduced. To obtain data for lower regions, the digital-filtering technique presented in the following section must be used.

A word about recording of the samples is in order here. For accuracy reasons, it is best to use digital recording, i. e., after quantization. Punched-paper tape is very suitable for this purpose, at least for the low and medium regions. The high region requires 200 recorded samples per second, which may be too fast for punched tape. Magnetic tape can be used in this case. Analog recording (magnetic or strip chart) should be used only as a last resort, because of the quantization and synchronization problems upon replay, as well as the possible inaccuracies.

2.3 Digital Filtering

Powerful techniques for lowpass filtering of sampled waveforms by digital means are available¹². They have the advantages of arbitrary cutoff frequency unrestricted by component size as in analog filters, almost flat amplitude and perfectly flat phase responses in the passband, and extremely sharp cutoff rate in the hundreds of dBs per octave. We shall not attempt here an exposition of the theory behind these techniques, but simply indicate the computational procedures involved.

Basically, a discrete version of the convolution integral is implemented on the computer, according to the formula

$$y(n\Delta t) = \sum_{i=-m}^m \frac{\sin \omega_{co} i\Delta t}{\omega_{co} i\Delta t} x((n+i)\Delta t) \quad (2.1)$$

The input data $x(n\Delta t)$ are the samples obtained with a short enough Δt that no significant aliasing occurs. The filtering function $\sin \omega_{co} i \Delta t / \omega_{co} i \Delta t$ corresponds to the impulse response of the ideal lowpass filter with cutoff frequency ω_{co} . The summation in Eq.(2.1) is over $(2m)$ terms rather than an infinite number, so that the resulting filtering will be only an approximation to the ideal, the quality of the approximation being determined by the number of terms $(2m)$. Generally, a good approximation of ideal filtering is obtained if several "lobes" of the $\sin \omega_{co} i \Delta t / \omega_{co} i \Delta t$ are included in the summation. If we include three lobes, the corresponding m can be found to be $3\pi / \omega_{co} \Delta t$. Other filtering functions are available⁷, e. g. using Chebyshev polynomials, and some of these reduce the amount of computations required. The lowpass-filtered samples $y(n\Delta t)$ obtained by digital filtering need not, of course, be as finely sampled as the original samples $x(n\Delta t)$. In fact, since the cutoff frequency is ω_{co} , the samples need only be spaced by $1/4\pi\omega_{co}$ seconds. Thus, it is necessary to compute $y(n\Delta t)$ at widely spaced values on n , the increments of n being given by $\pi/\omega_{co} \Delta t$.

Let us illustrate the above discussion by a typical example. Suppose that the fluctuations were filtered by an analog filter cutting off at 1 Hz. Samples were obtained at $\Delta t = 0.5$ secs for use in estimating the medium spectral region. It is desired to digitally filter these samples to accommodate the low region, so that $\omega_{co} = 2\pi \times 10^{-2}$ rad/sec. To include three lobes of the filtering function we must use $m = 3\pi/\omega_{co} \Delta t \approx 300$, i. e., 600 input samples are fed into the computer to compute each value of $y(n\Delta t)$. The increments of n should be $\pi/\omega_{co} \Delta t \approx 100$, i. e., $y(n\Delta t)$ need be computed only for $n = 0, 100, 200$, etc. The computational procedure would then be to apply Eq. (2.1) to the first 600 samples to obtain $y(0)$, then shift 100 samples by dropping the first 100 and inserting a new 100 samples to compute $y(100 \Delta t)$, and so on. Inner product programs, such as the

one presented in Sec. 4.1 below, may be used to facilitate the implementation of Eq.(2.1). Data must be taken for a period of at least 28 hours in order to obtain spectral resolution down to 10^{-5} Hz. Thus, the input data consists of at least 2×10^5 samples obtained at 0.5 sec intervals. If a small digital computer is available, it is possible to avoid recording this long string of data by using the computer in an on-line configuration, and only recording the output consisting of at least 2×10^3 samples.

3. THEORETICAL FOUNDATIONS OF SPECTRAL ESTIMATION

3.1 Introduction

In Sec. 2 of this report samples $\{X(t), t = \Delta t, 2\Delta t, \dots, N'\Delta t\}$ of the time series $\{X(t), t \text{ in } T\}$ were obtained where $X(t)$ is any one of a number of observables of significance in the study of highly stable oscillators. For example $X(t)$ may be the phase or frequency of the oscillator at time t , or the fluctuations of the frequency about the nominal frequency or of the phase about the nominal ramp, or more probably some multiple of the phase or frequency difference between two oscillators. Questions concerning the choice of observables to be measured, the appropriate instrumentation for these measurements, the length of the samples and the sampling rate were considered there. In Sec. 3 we shall be concerned principally with the extraction, from a sample $\{X(t), t = \Delta t, 2\Delta t, \dots, N'\Delta t\}$, of an estimate of the spectral density function if the process has a continuous spectrum, or of the spectral density function and the signal power and frequency if the process has a mixed spectrum. Sections 3.1 - 3.11 provide a general theoretical introduction to the problem. Section 4 is more practical. The reader who simply wants to know how to process the sample time series should concentrate on Secs. 4.1, 4.3, and 4.8. The choice of various parameters in the computations is discussed in Sec. 4.2 and the additional procedures needed for the case of mixed spectra may be found in Secs. 4.4- 4.7. We make liberal use of Refs. 8-11 in Secs. 3 and 4.

3.2 The General Structure of Time Series

A time series is a family $\{X(t), t \text{ in } T\}$ of random variables $X(t)$ where the parameter t is interpreted as real time. If the set T is the real line then $X(\cdot)$ is called a random function, if $T = \{0, \pm\Delta t, \pm 2\Delta t, \dots\}$ or $T = \{\Delta t, 2\Delta t, \dots\}$ then $X(\cdot)$ is called a random sequence. Continuous (discrete) parameter

processes are those for which the random variables are functions (sequences). In practice we have a continuous or discrete sample of length N' of the time series $X(t)$. The general problem is to infer the statistical characteristics of $X(t)$ from this sample. In order to do this we assume one or other model for $X(t)$ and we use our observations to fit the model in the best possible way. We shall treat both the continuous and discrete parameter cases simultaneously, and whenever the equations for the cases differ we write the equation for the continuous case above and its discrete analogue below.

A common model for $X(t)$ is

$$X(t) = m(t) + Y(t) \quad (3.1)$$

where $m(t)$ represents a mean function, signal or trend which is assumed to be nonrandom and $Y(t)$ is a fluctuation or noise function which is stochastic. Furthermore it is assumed that there is a fixed number q of known functions $g_1(t), \dots, g_q(t)$ such that $m(t)$ may be written as a linear combination

$$m(t) = C_1 g_1(t) + \dots + C_q g_q(t) \quad (3.2)$$

For example, we may have

$$g_k(t) = \sin(\omega_k t + \phi_k) \quad \text{or} \quad g_k(t) = t^k \quad (3.3)$$

The constants C_k , ω_k and ϕ_k ($k = 1, 2, \dots, q$) have to be estimated from the sample. Also it is assumed that

$$E[Y(t)] = 0 \quad (3.4)$$

for all t , and that $Y(t)$ has finite second moments, i. e.,

$$E|Y(t)|^2 < \infty \quad (3.5)$$

for all t . Some notion of stationarity is required for the validity of our analysis

so we assume $Y(t)$ is covariance (i. e., weakly or wide sense) stationary, that is $E[Y(t)Y(t+v)]$ is independent of t and depends only on v . The autocovariance function $R(v)$ can then be defined by

$$R(v) = \begin{cases} \text{cov} [Y(t), Y(t + v)] & \text{for } v \geq 0 \\ R(-v) & \text{for } v < 0 \end{cases} \quad (3.6)$$

The domain of definition of $R(v)$ which we shall denote by V is given by

$$V = \{ v, -\infty < v < \infty \} \quad (3.7)$$

in the continuous parameter case, and by

$$V = \{ v, v=0, \pm\Delta t, \pm 2\Delta t, \dots \} \quad (3.8)$$

in the discrete parameter case. From (3.4) it is clear that

$$m(t) = E[X(t)] \quad (3.9)$$

and that

$$\text{cov} [Y(t), Y(t + v)] = E [Y(t) Y(t + v)] - m(t)m(t+v) = \text{cov} [X(t), X(t+v)] \quad (3.10)$$

It should be noted that the process $X(t)$ may have a trend $m(t)$ which depends on t and still be covariance stationary according to our definition.

Assuming $R(\cdot)$ is continuous at $v = 0$, in the continuous (discrete) parameter case Khintchine (Wold) showed that

$$R(v) = \int_{\Omega} e^{iv\omega} dF(\omega) \quad (3.11)$$

where

$$\Omega = \{ \omega, -\infty < \omega < \infty \} \quad (3.12)$$

in the continuous parameter case, and

$$\Omega = \{\omega, -\pi/\Delta t \leq \omega \leq \pi/\Delta t\} \quad (3.13)$$

in the discrete parameter case. In both cases the spectral distribution function $F(\omega)$ is a nondecreasing bounded function defined for all ω in Ω . Now in general $F(\omega)$ has the following form

$$F(\omega) = F_d(\omega) + F_{sc}(\omega) + F_{ac}(\omega) \quad (3.14)$$

The function $F_{ac}(\omega)$ is absolutely continuous and is the integral of a nonnegative function $f(\omega)$ called the spectral density function of the time series

$$dF_{ac}(\omega) = f(\omega) d\omega \quad (3.15)$$

The function $F_d(\omega)$ is a step function

$$F_d(\omega) = \sum_{\omega_j \leq \omega} J(\omega_j) \quad (3.16)$$

where $J(\omega)$, the spectral jump function, is given by

$$J(\omega) = F(\omega + 0) - F(\omega - 0) \quad (3.17)$$

Finally $F_{sc}(\omega)$ is a singular continuous function which we shall assume is always zero. We therefore have

$$F(\omega) = \sum_{\omega_j \leq \omega} J(\omega_j) + \int_{-\infty}^{\omega} f(\omega') d\omega' \quad (3.18)$$

where the summation is over all frequencies ω_j such that $\omega_j \leq \omega$ and $J(\omega_j) > 0$ and it is assumed that in any finite interval of the real line there are only a finite number of points ω for which $J(\omega) > 0$. Also $f(\omega)$ is assumed to be continuous everywhere except for a finite number of points where it has finite left- and right-hand limits. If (3.18) holds with these conditions we say that the time series has

a mixed spectrum; if the spectral jump function vanishes for all ω we say it has a continuous spectrum; if the spectral density function vanishes everywhere it has a discrete spectrum.

$J(\omega)$ accounts for all lines in the spectrum, that is the components in the spectrum due to signals $m(t)$ of given frequency and power, $f(\omega)$ represents the background noise $Y(t)$. At zero frequency both $J(0)$ and $f(0)$ may be nonzero. If $J(0) \neq 0$ there is a signal of zero frequency, that is a dc component, present. One of the reasons for separating the signal and noise components is because (3.5) implies that

$$R_Y(v) \rightarrow 0 \text{ as } v \rightarrow \infty \quad (3.19)$$

which cannot be fulfilled for a single sinewave since the autocovariance function of $C_k \cos(\omega_k t + \phi_k)$, where ϕ_k is distributed uniformly over the interval $0 \leq \phi_k \leq 2\pi$, is given by

$$\frac{1}{2} C_k^2 \cos v \omega_k \quad (3.20)$$

which does not satisfy (3.19).

Before concluding this section we must point out a very important property of $R(v)$ and $f(\omega)$. These functions form a Fourier transform pair, and since it can be proved from (3.6) that $R(v)$ is a positive definite function, that is

$$\sum_{i=1}^k \sum_{j=1}^k c_i \overline{c_j} R(v_i - v_j) \geq 0 \quad (3.21)$$

for any complex vectors $\{c_1, \dots, c_k\}$ of arbitrary length k and any points v_1, \dots, v_k in the set $\{0, \pm \Delta t, \pm 2\Delta t, \dots\}$ with the equality sign holding only for zero vectors, it follows from a theorem of Bochner that the spectral density function $f(\omega)$ is nonnegative

$$f(\omega) \geq 0 \quad (3.22)$$

for all ω in Ω .

3.3 Important Special Cases

For discrete-parameter time series with a mixed spectrum whose spectral density function satisfies

$$\int_{\Omega} \log f(\omega) d\omega > -\infty \quad (3.23)$$

it may be shown that the process can be written in the form

$$X(t) = \sum_k A_k e^{it\omega_k} + \sum_{s'=0}^{\infty} C_{s'} \eta(t-s) \quad (3.24)$$

for suitable sequences of frequencies $\{\omega_k\}$, constants $\{C_{s'}\}$ and uncorrelated random variables $\{A_k\}$ and $\{\eta(\cdot)\}$. This structure includes as special cases the scheme of moving averages and the scheme of hidden periodicities corresponding to the vanishing of the first and second summations respectively.

Another important structure for a time series arises if it satisfies an autoregressive scheme of order p

$$\sum_{s'=0}^p a_{s'} X(t-s) = \epsilon(t) \quad (3.25)$$

where the a 's are constants and $\epsilon(t)$ is a white noise process. It may be shown that the spectral density function of such a process is

$$f(\omega) = \frac{\sigma_{\epsilon}^2}{2\pi \left| \sum_{s'=0}^p a_{s'} e^{is'\omega} \right|^2} \quad (3.26)$$

where σ_{ϵ} is the variance of the $\epsilon(t)$. An example of such a process is the random walk which satisfies

$$X(t) - X(t-1) = \epsilon(t) \quad (3.27)$$

with

$$f(\omega) = \frac{\sigma^2 \epsilon}{2\pi \left[(1 - \cos \omega)^2 + \sin^2 \omega \right]} \quad (3.28)$$

Autoregressive schemes always correspond to processes with an absolutely continuous spectrum.

3.4 Regression Analysis and Spectral Analysis

We wish to describe two possible approaches to estimating the signal component $m(t)$ and the noise component $Y(t)$ of (3.1).

First: we determine the trend $m(t)$ directly from the sample series by choosing the unknown constants in the linear combination (3.2) to give a least squares fit to the sample series. The linear combination arrived at in this way is taken to be an estimate $m_N(t)$ of the true trend $m(t)$. The determination of $m_N(t)$ in this manner is known as regression analysis and it is a well-known procedure. To complete the analysis we approximately detrend the sample series $X(t)$ by subtracting out the estimated trend $m_N(t)$ and we are ready to carry out a spectral analysis of the residual series which we assume is now free of trends, in other words, its spectrum is continuous. This analysis produces then an estimate of the true spectral density function $f(\omega)$.

The other approach referred to above is to carry out a spectral analysis of the sample series as if it were free of trends. Doing this produces what we call the truncated spectral estimate. We then use methods, which are developed below, for separating the signal and noise components in the

truncated spectral estimate. Of course, if the time series has a continuous spectrum the truncated spectral estimate will itself be an estimate of the true spectral density function. This is the approach we shall adopt for our analysis. It has the great advantage that it requires less a priori knowledge about the signal than is required for the preliminary regression analysis in the first approach.

Before we make any estimate we must define what we mean by a good estimate, and this is done in the next section.

3.5 Figures of Merit for Estimates

We shall consider only figures of merit based on the mean-square error of the estimate from the true value. Suppose $f(\omega)$ is the function we are interested in estimating by means of an estimate $f_N(\omega)$ formed from a sample $\{X(t), t = \Delta t, 2\Delta t, \dots, N'\Delta t\}$ of the time series. (The same considerations will hold for functions other than the spectral density function.) The mean-square error of $f_N(\omega)$ is defined to be

$$E | f(\omega) - f_N(\omega) |^2 \quad (3.29)$$

This expression clearly depends on the point ω . It is easily shown that it may be written as the sum of two terms

$$E | f(\omega) - f_N(\omega) |^2 = \text{var} [f_N(\omega)] + | \text{bias} [f_N(\omega)] |^2 \quad (3.30)$$

where the variance and bias are defined by

$$\text{var} [f_N(\omega)] = E | f_N(\omega) - E f_N(\omega) |^2 \quad (3.31)$$

$$\text{bias} [f_N(\omega)] = E [f_N(\omega)] - f(\omega) \quad (3.32)$$

Thus a good estimate in the mean-square sense will minimize the effects of variance and bias on the error at all points ω . It will be found that unbiased estimates (where the bias is zero at all points) are not always the best and that it is better to divide the error up into the two types. The difficulty of having the error depend on the point of evaluation ω may be removed by taking other criteria such as the mean-square integrated error

$$\int_{\Omega} E |f_N(\omega) - f(\omega)|^2 d\omega \quad (3.33)$$

or the mean-square maximum error

$$E \sup_{\omega} |f_N(\omega) - f(\omega)|^2 \quad (3.34)$$

both of which are independent of ω . Of course

$$\int_{\Omega} E |f_N(\omega) - f(\omega)|^2 d\omega = \int_{\Omega} \text{var} [f_N(\omega)] d\omega + \int_{\Omega} |\text{bias} [f_N(\omega)]|^2 d\omega \quad (3.35)$$

and an upperbound for (3.34) is given by

$$\sqrt{E \sup_{\omega} |f_N(\omega) - f(\omega)|^2} \leq \sqrt{E \sup_{\omega} |f_N(\omega) - E f_N(\omega)|^2} + \sup_{\omega} |\text{bias} [f_N(\omega)]| \quad (3.36)$$

The mean-square and mean-square integrated errors are the most easily handled mathematically; however the most useful criterion for our purposes is the mean-square maximum error since this automatically gives us satisfactory confidence bands for good spectral density estimates. This follows from the Chebyshev-type inequality

$$P \left[\sup_{\omega} |f_N(\omega) - f(\omega)| > \epsilon \right] \leq \frac{1}{\epsilon^2} E \sup_{\omega} |f_N(\omega) - f(\omega)|^2 \quad (3.37)$$

since a good estimate in the mean-square maximum error sense means that the right-hand side is a small multiple of $1/\epsilon^2$.

3.6 Covariance and Spectral Averages

The dual concepts of covariance and spectral averages are important because the finite length of our sample makes it unrealistic to attempt to estimate the true autocovariance or spectral density function at a point. Rather, we shall obtain estimates of these quantities which are averages of the true quantities over a domain which depends on the length of the sample.

To form a spectral average we start with a well behaved function $A(\omega)$ (for example an infinitely differentiable function of compact support or a simple function) defined on Ω the domain of definition of $f(\omega)$. Then instead of the function $f(\omega)$, which we have agreed it is unreasonable to expect to estimate, we consider T_f the generalized function or distribution (in the sense of Laurent Schwarz) corresponding to the function f . The spectral average generated by the function $A(\omega)$ is then defined to be the effect of T_f on $A(\cdot)$. Thus we have

$$T_f(A) = \int_{\Omega} A(\omega) f(\omega) d\omega \quad (3.38)$$

For example if we take

$$A(\omega) = \begin{cases} 1 & \text{for } \omega < \omega_0 \\ 0 & \text{for } \omega \geq \omega_0 \end{cases} \quad (3.39)$$

then $T_f(A) = F_{ac}(\omega_0)$ the spectral distribution function evaluated at ω_0 . On the other hand we may take $A(\omega)$ to be sharply peaked at ω_0 and small elsewhere in which case $T_f(A)$ is looked on as the nearest we can get to assigning a value at ω_0 to the generalized function T_f , or in other words to finding $f(\omega_0)$.

Since $f(\omega)$ and $R(v)$ form a Fourier transform pair we have

$$f(\omega) = \frac{1}{2\pi} \int_V e^{-iv\omega} R(v) dv \quad (3.40)$$

Using this in (3.38) we obtain

$$\int_{\Omega} A(\omega) f(\omega) d\omega = \int_V a(v) R(v) dv \quad (3.41)$$

where $a(v)$ is the Fourier transform of $A(\omega)$

$$a(v) = \frac{1}{2\pi} \int_{\Omega} e^{-iv\omega} A(\omega) d\omega \quad (3.42)$$

which we shall call a covariance window. But the right-hand side of (3.41) is the distribution T_R applied to the function $a(v)$, so that every spectral average may also be regarded as a covariance average

$$T_f(A) = T_R(a) \quad (3.43)$$

having their corresponding windows related through (3.42). From (3.43) it is seen at once that there will be inherent limitations on our ability to obtain simultaneously satisfactory estimates of $f(\cdot)$ and $R(\cdot)$ at a point in their respective domains. For example in the extreme case where $A(\omega) = \delta(\omega - \omega_0)$ we have $a(v) = e^{-iv\omega_0}$ so that while $T_f(A) = f(\omega_0)$, the value of f at ω_0 , we have $T_R(a) = \int_V e^{-iv\omega_0} R(v) dv$ which in no way approximates the value of R at a point. In fact $T_R(a)$ is not an observable since $e^{-iv\omega_0}$ is not a function of compact support, so that we can never obtain $f(\cdot)$ at a point in practice using covariance averages. However, we do hope to approximate the value of $f(\cdot)$ at a point ω_0 by means of covariance averages with $a(\cdot)$ chosen in such a way that $A(\cdot)$ is sharply spiked at ω_0 . This produces then a spectral average of $f(\cdot)$ over a narrowband of frequencies centered about ω_0 .

An important measure of the shape of a spectral window $A(\cdot)$ (the same considerations hold for covariance windows) is its bandwidth $\beta(A)$ defined by

$$\beta(A) = \frac{\int_{\Omega} A(\omega) d\omega}{\sup_{\omega} |A(\omega)|} \quad (3.44)$$

The bandwidth is thus simply the width of a window of height equal to the maximum height of the window $A(\cdot)$ and of equal area.

3.7 Consistency, Bias and Variance of Estimates

For simplicity we confine ourselves to estimates $f_N(\omega)$ of the spectral density function $f(\omega)$ formed from the sample $\{X(t), t = \Delta t, \dots, N\Delta t\}$ of the process $\{X(t), t \text{ in } T\}$. Except in simple cases no expressions have been found for the bias and variance of estimates of the type we are interested in. However, simple expressions are known for the asymptotic form of these quantities which will now be defined. By asymptotic we mean in the limit as $N \rightarrow \infty$, where $N = N'\Delta t$.

An estimate $f_N(\omega)$ of $f(\omega)$ is said to be consistent in quadratic mean if

$$\lim_{N \rightarrow \infty} E |f_N(\omega) - f(\omega)|^2 = 0 \quad (3.45)$$

It is asymptotically unbiased if

$$\lim_{N \rightarrow \infty} (E f_N(\omega) - f(\omega)) = 0 \quad (3.46)$$

It is easily shown that a consistent estimate is asymptotically unbiased.

We may be interested in the rate of convergence in (3.45) and (3.46), and this leads us to the following definitions. We say an estimate is consistent

of order $N^{2\alpha}$ with asymptotic variance σ^2 if

$$\lim_{N \rightarrow \infty} N^{2\alpha} E |f_N - E f_N|^2 = \sigma^2 \quad (3.47)$$

and asymptotically unbiased of order N^α with asymptotic bias β if

$$\lim_{N \rightarrow \infty} N^\alpha (E f_N(\omega) - f(\omega)) = \beta \quad (3.48)$$

3.8 Window Generating Functions and Estimates of the Autocovariance and Spectral Density Functions

A window generating function is a function $k(x)$ satisfying the following conditions:

- (i) $k(x)$ is bounded
- (ii) $k(0) = 1$
- (iii) $k(x) = k(-x)$
- (iv) $k(x) = 0$ for $|x| > 1$ (3.49)

Such functions will be useful in forming our estimates of the spectral density function. However, first of all we form our estimate of the autocovariance function.

As our estimate of the autocovariance function we shall always take the sample autocovariance function defined by

$$R_N(v) = \begin{cases} \frac{1}{N'} \sum_{t'=1}^{N'-v'} X(t) X(t+v) & \text{for } v \text{ in } \{0, \Delta t, \dots, (N'-1)\Delta t\} \\ R_N(-v) & \text{for } v \text{ in } \{-\Delta t, \dots, -(N'-1)\Delta t\} \\ 0 & \text{otherwise.} \end{cases} \quad (3.50)$$

A possible estimate of the spectral density function is the sample spectral density function or periodogram defined by

$$f_N(\omega, P, N) = \frac{\Delta t}{2\pi} \sum_{v'=-N'+1}^{N'-1} R_N(v) e^{-i v \omega} \quad (3.51)$$

Inverting (3.51) we obtain

$$R_N(v) = \int_{\omega} e^{i v \omega} f_N(\omega, P, N) d\omega \quad (3.52)$$

and it is easily shown that (3.51) may be written in the more familiar form

$$f_N(\omega, P, N) = \frac{\Delta t}{2\pi N'} \left| \sum_{t'=1}^{N'} X(t) e^{-i t \omega} \right|^2 \quad (3.53)$$

where t runs over $\{\Delta t, \dots, N' \Delta t\}$. However it is well known that (3.51) is not a consistent estimate of the spectral density function.

By means of window generating functions we shall generate estimates of the spectral density function which are consistent. We first choose a truncation point $M \leq V$, which is of course a multiple of Δt , and we define the truncated spectral estimate by

$$f_N(\omega, V, M) = \frac{\Delta t}{2\pi} \sum_{v'=-M'}^{M'} k\left(\frac{v}{M}\right) R_N(v) e^{-i v \omega} \quad (3.54)$$

in which the summation is chopped off for all $|v| > M$ because of the properties of $k(\cdot)$. We shall now show that this is a spectral average of the periodogram.

We define the central spectral window as

$$K(\lambda, 0, M) = \frac{\Delta t}{2\pi} \sum_{v'=-M'}^{M'} k\left(\frac{v}{M}\right) e^{-i v \lambda} \quad (3.55)$$

which of course we can invert to obtain a formula for $k\left(\frac{v}{M}\right)$ as follows:

$$k\left(\frac{v}{M}\right) = \int_{\Lambda} K(\lambda, 0, M) e^{i v \lambda} d\lambda \quad (3.56)$$

where Λ is the same set as Ω , that is

$$\Lambda = \{\lambda, \quad -\pi/\Delta t \leq \lambda \leq \pi/\Delta t\} \quad (3.57)$$

in the case we are especially interested in. We note that $K(\lambda, 0, M)$ has a single peak at $\lambda = 0$ while $K(\lambda, \omega, M)$ defined as

$$K(\lambda, \omega, M) = 1/2 [K(\lambda + \omega, 0, M) + K(\lambda - \omega, 0, M)] \quad (3.58)$$

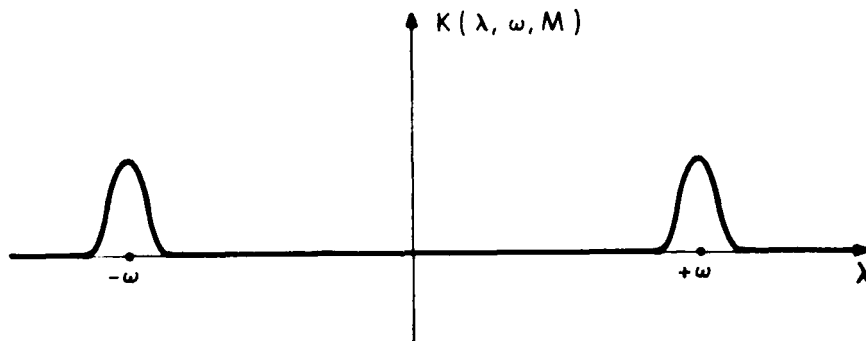
has peaks at $\lambda = \pm \omega$. Condition (ii) of (3.49) guarantees that

$$\int_{\Lambda} K(\lambda, \omega, M) d\lambda = 1 \quad (3.59)$$

It is now easily verified that

$$f_N(\omega, K, M) = \int_{\Lambda} K(\lambda, \omega, M) f_N(\lambda, P, N) d\lambda \quad (3.60)$$

so that our truncated spectral estimate is a spectral average of the periodogram viewed through the spectral window $K(\lambda, \omega, M)$ which satisfies (3.59) and looks like



We next investigate various quantities associated with windows. For a central spectral window we define the peak height to be $K(0, 0, M)$ which is given from (3.55) by

$$K(0, 0, M) = \frac{\Delta t}{2\pi} \sum_{v'=-M'}^{M'} k\left(\frac{v}{M}\right) \quad (3.61)$$

which we shall show later is approximately proportional to M . We call the constant of proportionality K the peak height factor so that

$$K(0, 0, M) \approx KM \quad (3.62)$$

In fact a theorem below shows that

$$K(0, 0, M) = KM + O(M^{-(p+1)}) \quad (3.63)$$

where p is a non-negative integer depending on the smoothness of the covariance window generator $k(\cdot)$ and

$$K = \frac{1}{2\pi} \int_{-1}^1 k(x) dx \quad (3.64)$$

The bandwidth β of a central spectral window is defined to be

$$\beta = \frac{\int_{-\Lambda}^{\Lambda} K(\lambda, 0, M) d\lambda}{K(0, 0, M)} \quad (3.65)$$

and from (3.59) and (3.62) this is given by

$$\beta \approx \frac{1}{KM} \quad (3.66)$$

so that for a fixed window with varying truncation point the bandwidths of the estimates are approximately inversely proportional to their truncation points. We now look at an asymptotic formula for the variance of our estimate if it is used to obtain an estimate of the spectral density function of a normal noise

process with zero spectral jump function. The result (3.67) which we now quote follows from Theorem 5, and (3.68) follows from Theorem 3 below. For $0 < \omega < \pi/\Delta t$ we have, for large N

$$\text{var} \left[f_N(\omega, K, M) \right] \approx \frac{1}{N} \int_{\Lambda} f^2(\lambda) K^2(\lambda, \omega, M) d\lambda \quad (3.67)$$

$$\approx \frac{M}{N} f^2(\omega) \int_{-\infty}^{\infty} k^2(x) dx \quad (3.68)$$

and the same holds true for $\omega = 0$ or $\omega = \pi/\Delta t$ if we multiply the right-hand sides by a factor of 2. Thus for a normal noise process with fixed window and varying truncation point we see from (3.68) that the variance of our estimate is approximately proportional to the truncation point M . From this we can take the product of the variance and the bandwidth of the estimate and obtain approximately

$$\frac{f^2(\omega)}{N} \cdot \frac{\int_{-\infty}^{\infty} k^2(x) dx}{K} \quad (3.69)$$

This expression is independent of the truncation point M and we define the part of it which depends on the window to be the variance-bandwidth factor $\text{VBW}(\cdot)$ thus

$$\text{VBW}(k) = \frac{2\pi \int_{-\infty}^{\infty} k^2(x) dx}{\int_{-\infty}^{\infty} k(x) dx} \quad (3.70)$$

For some time series, such as those with a mixed spectrum, we cannot find a true spectral density function $f(\omega)$. However, we may always obtain an expected spectral estimate defined as

$$f(\omega, K, M) = \lim_{N \rightarrow \infty} E \left[f_N(\omega, K, M) \right] \quad (3.71)$$

If $X(\cdot)$ is a stationary process we then have from (3.71) and Theorem 5

$$f(\omega, K, M) = \int_{\Lambda} f(\lambda) K(\lambda, \omega, M) d\lambda \quad (3.72)$$

which is a spectral average of the true spectral density function through the window $K(\lambda, \omega, M)$. For completeness we define the spectral window generator to be the Fourier transform of the covariance window generator

$$K(\lambda) = \frac{1}{2\pi} \int_{-\infty}^{\infty} k(x) e^{-i\lambda x} dx \quad (3.73)$$

so of course we also have

$$k(x) = \int_{-\infty}^{\infty} K(\lambda) e^{i\lambda x} d\lambda \quad (3.74)$$

We wish to find out how $K(\lambda)$ and $K(\lambda, \omega, M)$ are related. This follows from a formula due to Poisson. The result is

$$K(\lambda, 0, M) \approx M K(M\lambda) \quad (3.75)$$

or more precisely, provided $K(\omega) = O(\omega^{-(1+\alpha)})$ for some positive α , we have

$$K(\lambda, 0, M) = \sum_{j=-\infty}^{\infty} M K\left(M\left(\omega + \frac{2\pi j}{\Delta t}\right)\right) \quad (3.76)$$

3.9 Parzen's Kernel, Tukey's Kernel and the Periodogram

We now define two frequently used $k(\cdot)$ due to Parzen and Tukey, and we explain what is meant by the periodogram. We list also the values of several quantities associated with these kernels and the periodogram.

First, Parzen's kernel is defined by

$$k(x) = \begin{cases} 2(1 - |x|)^3 - (1 - 2|x|)^3 & \text{for } |x| \leq 1/2 \\ 2(1 - |x|)^3 & \text{for } 1/2 \leq |x| \leq 1 \\ 0 & \text{for } |x| > 1 \end{cases} \quad (3.77)$$

Its spectral window generator is

$$K(\lambda) = \frac{3}{8\pi} \left(\frac{\sin \lambda/4}{\lambda/4} \right)^4 \quad (3.78)$$

Its peak height factor is

$$K = 3/8\pi \quad (3.79)$$

and its central spectral window is

$$K(\lambda, 0, M) = \frac{3 \Delta t}{8\pi M^3} \left(\frac{\sin M' \lambda \Delta t/4}{\lambda \Delta t/4} \right)^4 \quad (3.80)$$

The integral

$$\int_{-\infty}^{\infty} k^2(x) dx = \frac{151}{280} = 0.539 \quad (3.81)$$

and the variance-bandwidth factor is given by

$$\text{VBW}(k) = \frac{151\pi}{105} = 4.52 \quad (3.82)$$

Parzen's kernel has two advantages over Tukey's, namely it always gives rise to nonnegative estimates of the spectral density function of the process, and its variance bandwidth factor is almost 5% smaller. To see this we write down Tukey's kernel which is given by

$$k(x) = \begin{cases} \frac{1}{2} (1 + \cos \pi x) & \text{for } |x| \leq 1 \\ 0 & \text{for } |x| > 1 \end{cases} \quad (3.83)$$

for which

$$K(\lambda) = \frac{1}{2\pi} \cdot \frac{\pi^2}{\pi^2 - \lambda^2} \cdot \frac{\sin \lambda}{\lambda} \quad (3.84)$$

$$K = \frac{\Delta t}{2\pi} \quad (3.85)$$

$$K(\lambda, 0, M) = \frac{\Delta t}{8\pi} \left[\frac{2 \sin (M' + \frac{1}{2}) \lambda \Delta t}{\sin \frac{\lambda}{2} \Delta t} + \frac{\sin (M' + \frac{1}{2})(\lambda + \frac{\pi}{M}) \Delta t}{\sin \frac{1}{2}(\lambda + \pi/M) \Delta t} + \frac{\sin (M' + \frac{1}{2})(\lambda - \frac{\pi}{M}) \Delta t}{\sin \frac{1}{2}(\lambda - \pi/M) \Delta t} \right] \quad (3.86)$$

$$\int_{-\infty}^{\infty} k^2(x) dx = 3/4 \quad (3.87)$$

and

$$VBW(k) = 4\pi \quad (3.88)$$

Finally we must define the periodogram which is the estimate which arises from the particularly simple kernel

$$k(x) = \begin{cases} 1 & \text{for } |x| \leq 1 \\ 0 & \text{otherwise} \end{cases} \quad (3.89)$$

Corresponding to this, which is sometimes known as Bartlett's or Dirichlet's kernel, we have

$$K(\lambda) = \frac{1}{\pi} \frac{\sin \lambda}{\lambda} \quad (3.90)$$

$$K = \frac{1}{\pi} = 0.318 \quad (3.91)$$

$$K(\lambda, 0, M) = \frac{\Delta t}{2\pi M'} \frac{\sin (M' + \frac{1}{2}) \lambda \Delta t}{\sin \frac{1}{2} \lambda \Delta t} \quad (3.92)$$

$$\int_{-\infty}^{\infty} k^2(x) dx = 2 \quad (3.93)$$

and

$$VBW(k) = 2\pi = 6.28 \quad (3.94)$$

3.10 Theorems on Estimates and Windows for Stationary Time Series

We pause to define what we mean by a smooth covariance window generator $k(\cdot)$. We say $k(\cdot)$ is p-derivable on $[a, b]$ if

- (1) at each point of $[a, b]$ the first p derivatives exist, and the first $p+3$ one-sided derivatives $k(x+)$ and $k(x-)$ exist and are bounded;
- (2) there is at least one point of (a, b) at which $g^{(p+1)}(x)$ does not exist;
- (3) at all but a finite set of points Z in (a, b) the first $p+3$ derivatives of $k(\cdot)$ exist and are bounded and integrable.

The set Z is called the break point set. $k(\cdot)$ is said to be truncated p-derivable on $[a, b]$ if, when we extend $k(\cdot)$ by making it zero outside this interval, for every positive ϵ $k(\cdot)$ is p-derivable on $[a-\epsilon, b+\epsilon]$ and Z is the break point set in $(a-\epsilon, b+\epsilon)$. For Parzen's kernel $p=2$, $Z = \{-1, -\frac{1}{2}, 0, \frac{1}{2}, 1\}$ and it

is truncated 2-derivable. Tukey's kernel has $p = 1$, $Z = \{-1, 1\}$ and it is truncated 1-derivable.

We have the following theorem about spectral averages of a smooth spectral density function $f(\omega)$ for any stationary time series.

Theorem 1. Given any spectral density function $f(\omega)$ with bounded derivatives up to the n^{th} , and given any truncated p -derivable covariance window generator $k(\cdot)$, then

$$\int_{\Lambda} f(\lambda) K(\lambda, \omega, M) d\lambda = k(0) f(\omega) - \frac{1}{2! M^2} k''(0) f''(\omega) + \frac{1}{4! M^4} k^{(4)}(0) f^{(4)}(\omega) + \dots + R_M \quad (3.95)$$

where the remainder

$$R_M = \begin{cases} O(M^{-n}) & \text{if } n < p+1 \\ O(M^{-(p+1)} \log_e M) & \text{if } n \geq p+1 \end{cases} \quad (3.96)$$

Before stating the next theorem we need two more definitions. The characteristic exponent r of a covariance window generator is defined to be the largest number r such that

$$k^{[r]} = \lim_{x \rightarrow 0} \frac{1 - k(x)}{|x|^r} \quad (3.97)$$

exists, and is finite and nonzero. $k^{[r]}$ is called the characteristic coefficient. Another way of stating (3.97) is that in a neighborhood of the origin

$$k(x) = 1 - k^{[r]} |x|^r + o(x^r) \quad (3.98)$$

For Parzen's and Tukey's kernel $r = 2$, and $k^{[r]} = 6$ and $\frac{\pi^2}{4}$ ($= 2.46$) respectively.

We are now in a position to state another theorem of a similar kind to Theorem 1. It is

Theorem 2. Given (1) a covariance window generator $k(\cdot)$, bounded on $[-1, 1]$ and zero elsewhere; (2) a discrete-time stationary time series with spectral density function $f(\omega)$ on Ω and autocovariance function $R(v)$ satisfying

$$\sum_{v'=-\infty}^{\infty} |v|^{r'} |R(v)| < \infty \tag{3.99}$$

then

$$\int_{\Lambda} f(\lambda) K(\lambda, \omega, M) d\lambda = f(\omega) - \frac{k^{[r]} f^{[r]}(\omega)}{M^r} + o\left(\frac{1}{M^r}\right) \tag{3.100}$$

where the q^{th} generalized spectral derivative is defined as

$$f^{[q]}(\omega) = \frac{\Delta t}{2\pi} \sum_{v'=-\infty}^{\infty} |v|^q R(v) e^{-i v \omega} \tag{3.101}$$

We now turn to a theorem about a more complicated expression than the spectral average of (3.95) and (3.100). We first define for two truncation points $M_i \leq M_j$ the mean truncation point as

$$M_{ij} = \sqrt{M_i M_j} \tag{3.102}$$

and the truncation ratio as

$$\mu_{ij} = \sqrt{\frac{M_i}{M_j}} \leq 1 \tag{3.103}$$

In the statement of the theorem we drop the subscripts and write simply M and μ .

Theorem 3. Given (1) positive integers M_i and M_j with μ held constant; (2) a truncated p -derivable covariance window generator $k(\cdot)$; (3) a spectral density function $f(\lambda)$ with derivatives through the fourth existing and continuous on Λ ; then if $p \geq 1$ we have for the integral

$$I = 4\pi \int_{\Lambda} f^2(\lambda) K(\lambda, \omega, M_i) K(\lambda, \omega, M_j) d\lambda \quad (3.104)$$

the approximations

$$(a) \quad \text{for } \frac{1}{M} \ll \omega \ll \frac{\pi}{\Delta t} - \frac{1}{M}$$

$$I = Mf^2(\omega) \int_{-\mu}^{\mu} k(\mu^{-1}z) k(\mu z) dz + M^{-1} [f(\omega)f''(\omega) + f'(\omega)f'(\omega)] \int_{-\mu}^{\mu} k'(\mu^{-1}z) k'(\mu z) dz \\ + 0(M^{-3}) + 0(M^{-(p+1)}) \quad (3.105)$$

$$(b) \quad \text{for } 0 \leq \omega \leq 0\left(\frac{1}{M}\right) \quad (\text{in fact for } 0 \leq \omega \ll \frac{\pi}{\Delta t} - \frac{1}{M})$$

$$I = Mf^2(\omega) \int_{-\mu}^{\mu} k(\mu^{-1}z) k(\mu z) (1 + \cos 2M\omega z) dz \\ + M^{-1} [f(\omega)f''(\omega) + f'(\omega)f'(\omega)] \int_{-\mu}^{\mu} k'(\mu^{-1}z) k'(\mu z) dz \\ + M^{-1} \frac{f(\omega)f'(\omega)}{\omega} \int_{-\mu}^{\mu} k'(\mu^{-1}z) k'(\mu z) \cos 2M\omega z dz \\ + 0(M^{-3}) + 0(M^{-p+1}) \quad (3.106)$$

(c) for $0 \leq \frac{\pi}{\Delta t} - \omega \leq 0 \left(\frac{1}{M}\right)$

$$\begin{aligned}
 I = & Mf^2(\omega) \int_{-\mu}^{\mu} k(\mu^{-1}z) k(\mu z) (1 + \cos 2M(\frac{\pi}{\Delta t} - \omega)z) dz \\
 & + M^{-1} [f(\omega)f''(\omega) + f'(\omega)f'(\omega)] \int_{-\mu}^{\mu} k'(\mu^{-1}z) k'(\mu z) dz \\
 & - \frac{M^{-1}f(\omega)f'(\omega)\Delta t}{\pi - \omega\Delta t} \int_{-\mu}^{\mu} k'(\mu^{-1}z) k'(\mu z) \cos 2M(\frac{\pi}{\Delta t} - \omega)z dz \\
 & + 0(M^{-3}) + 0(M^{-(p+1)})
 \end{aligned} \tag{3.107}$$

Note that for Parzen's kernel the remainder is of course $0(M^{-3})$ and for Tukey's it is $0(M^{-2})$. In case (b) if $f(\omega)$ does not vary much near the origin we can simplify (3.106) by expanding $f(\omega)$ about the origin to obtain the simpler result

$$\begin{aligned}
 I = & M [f^2(0) + \omega^2 f(0)f''(0)] \int_{-\mu}^{\mu} k(\mu^{-1}z) k(\mu z) (1 + \cos 2M\omega z) dz \\
 & + M^{-1} f(0)f''(0) \int_{-\mu}^{\mu} k'(\mu^{-1}z) k'(\mu z) (1 + \cos 2M\omega z) dz + 0(M^{-3}) + 0(M^{-(p+1)})
 \end{aligned} \tag{3.108}$$

In case (c) we expand about $\pi/\Delta t$ and in (3.108) we replace 0 by $\pi/\Delta t$ and ω by $\pi/\Delta t - \omega$.

3.11 Theorems on Estimates for Normal Time Series

The first two theorems are about the noise process only. We state first a theorem about the limiting value as $T \rightarrow \infty$ of the expectation of a truncated spectral estimate and of the covariance of two such estimates. Note that all the following theorems are true only if the noise process is a normal process.

Theorem 4. Suppose $Y(t)$, $t = \Delta t, \dots, N'\Delta t$ is a sample from a discrete parameter normal, zero-mean, stationary, ergodic time series with absolutely summable autocovariance function $R(v)$ and spectral density function $f(\omega)$ on Ω . Then for fixed v and w

$$\lim_{N \rightarrow \infty} E[R_N(v)] = R(v) \quad (3.109)$$

and

$$\begin{aligned} \lim_{N \rightarrow \infty} N \operatorname{cov} [R_N(v), R_N(w)] &= \sum_{s' = -\infty}^{\infty} [R(s+v) R(s+w) + R(s+v) R(s-w)] \\ &= 4\pi \int_{\Lambda} \cos v\lambda \cos w\lambda f^2(\lambda) d\lambda \end{aligned} \quad (3.110)$$

We have a similar theorem for the truncated spectral estimate rather than the estimate of the autocovariance function.

Theorem 5. Suppose $Y(t)$, $t = \Delta t, \dots, N'\Delta t$ is a sample from a discrete parameter, normal, zero-mean, stationary, ergodic time series with absolutely summable autocovariance function $R(v)$. If the spectral density function of this series defined on Ω is $f(\omega)$, then for every function and parameter fixed except N

$$\lim_{N \rightarrow \infty} E[f_N(\omega, K, M)] = \int_{\Lambda} f(\lambda) K(\lambda, \omega, M) d\lambda \quad (3.111)$$

and

$$\begin{aligned} \lim_{N \rightarrow \infty} N \operatorname{cov} [f_N(\omega_\alpha, K_1, M_i), f_N(\omega_\beta, K_2, M_j)] \\ = 4\pi \int_{\Lambda} f^2(\lambda) K_1(\lambda, \omega_\alpha, M_i) K_2(\lambda, \omega_\beta, M_j) d\lambda \end{aligned} \quad (3.112)$$

Combining (3.111) and (3.95) or (3.100) we have asymptotic estimates for the bias of the truncated spectral estimate.

Corollary 5. If in addition to the conditions of Theorem 5 we assume that
 $\sum_V |v R^2(v)| < \infty$, then as $N \rightarrow \infty$ we have

$$N \operatorname{cov} [R_N(v), R_N(w)] = 4\pi \int_{\Lambda} \cos v\lambda \cos w\lambda f^2(\lambda) d\lambda + o(N^{-1}) \quad (3.113)$$

We now state some theorems for processes with mixed spectra analogous to Theorems 4 and 5. The first two will be about processes with a signal having a single harmonic component, the following two will generalize these results to signals having a finite member of such terms.

Theorem 6. Suppose we are given a sample of N observations from the time series $X(t) = C \cos(t\omega_s + \phi) + Y(t)$ $t = \Delta t, \dots, N \cdot \Delta t$ where

- (i) C, ω_s and ϕ are fixed, $\omega_s \neq 0$ or $\pi/\Delta t$
- (ii) $Y(t)$ is a stationary, ergodic, normal, zero-mean time series with autocovariance function $R(v)$, such that $\sum_{v'=-\infty}^{\infty} |v' R(v')| < \infty$ and spectral density function $f(\omega)$ on Ω .

Then for fixed v and w , as $N \rightarrow \infty$

$$E[R_N(v)] = \frac{1}{2} C^2 \cos v\omega_s + R(v) + o(N^{-1}) \quad (3.114)$$

and

$$N \text{ cov} [R_N(v), R_N(w)] = 4\pi \cos v\omega_s \cos w\omega_s C^2 f(\omega_s) + 4\pi \int_{\Lambda} \cos v\lambda \cos w\lambda f^2(\lambda) d\lambda \\ + o(N^{-1}) \quad (3.115)$$

Theorem 7. If the conditions on $X(t)$ are the same as in Theorem 6, then as

$N \rightarrow \infty$

$$E[f_N(\omega, K, M)] = \frac{1}{2} C^2 K(\omega_s, \omega, M) + \int_{\Lambda} K(\lambda, \omega, M) f(\lambda) d\lambda + o(N^{-1}) \quad (3.116)$$

and

$$N \text{ cov} [f_N(\omega_\alpha, K_1, M_i), f_N(\omega_\beta, K_2, M_j)] = 4\pi K_1(\omega_s, \omega_\alpha, M_i) K_2(\omega_s, \omega_\beta, M_j) C^2 f(\omega_s) \\ + 4\pi \int_{\Lambda} K_1(\lambda, \omega_\alpha, M_i) K_2(\lambda, \omega_\beta, M_j) f^2(\lambda) d\lambda + o(N^{-1}) \quad (3.117)$$

We now extend Theorems 6 and 7 to the case of many sine waves in noise. We include in these results the special case of a constant (i. e., zero frequency) term, and an on-off (i. e., frequency $\frac{\pi}{\Delta t}$) term. The generalization of Theorem 6 is

Theorem 8. Suppose we are given a sample of N' observations from the time

series $X(t) = \sum_{j=0}^q C_j \cos(t\omega_j + \phi_j) + Y(t)$ $t = \Delta t, \dots, N' \Delta t$ where

- (i) C_j, ω_j and ϕ_j are fixed with $C_j \geq 0, 0 = \omega_0 < \omega_1 < \dots < \omega_{q-1} < \omega_q = \pi/\Delta t$ and
 $\phi_0 = 0, \phi_q = 0$ or π .

(ii) Y(t) is a stationary, ergodic, zero-mean, normal time series with auto-covariance function R(v), such that $\sum_{v'=-\infty}^{\infty} |vR(v)| < \infty$ and spectral density function f(ω) on Ω.

Then for fixed integers v and w, as N → ∞

$$E[R_N(v)] = C_0^2 + \frac{1}{2} \sum_{j=1}^{q-1} C_j^2 \cos v\omega_j + (-1)^{v'} C_q^2 + R(v) + o(N^{-1}) \quad (3.118)$$

and

$$\begin{aligned} N \operatorname{cov}[R_N(v), R_N(w)] &= 8\pi C_0^2 f(0) + 4\pi \sum_{j=1}^{q-1} \cos v\omega_j \cos w\omega_j C_j^2 f(\omega_j) \\ &+ (-1)^{v+w} 8\pi C_q^2 f\left(\frac{\pi}{\Delta t}\right) + 4\pi \int_{\Lambda} \cos v\lambda \cos w\lambda f^2(\lambda) d\lambda + o(N^{-1}) \end{aligned} \quad (3.119)$$

and the generalization of Theorem 7 is

Theorem 9. Suppose X(t) is as in Theorem 8. Then as N → ∞

$$\begin{aligned} E[f_N(\omega, K, M)] &= K(0, \omega, M) C_0^2 + \frac{1}{2} \sum_{j=1}^{q-1} K(\omega_j, \omega, M) C_j^2 \\ &+ K\left(\frac{\pi}{\Delta t}, \omega, M\right) C_q^2 + \int_{\Lambda} K(\lambda, \omega, M) f(\lambda) d\lambda + o(N^{-1}) \end{aligned} \quad (3.120)$$

and

$$\begin{aligned} N \operatorname{cov}[f_N(\omega_\alpha, K_1, M_i), f_N(\omega_\beta, K_2, M_j)] &= 8\pi K_1(0, \omega_\alpha, M_i) K_2(0, \omega_\beta, M_j) C_0^2 f(0) \\ &+ 4\pi \sum_{k=1}^{q-1} K_1(\omega_k, \omega_\alpha, M_i) K_2(\omega_k, \omega_\beta, M_j) C_k^2 f(\omega_k) \\ &+ 8\pi K_1\left(\frac{\pi}{\Delta t}, \omega_\alpha, M_i\right) K_2\left(\frac{\pi}{\Delta t}, \omega_\beta, M_j\right) C_q^2 f\left(\frac{\pi}{\Delta t}\right) \\ &+ 4\pi \int_{\Lambda} (K_1(\lambda, \omega_\alpha, M_i) K_2(\lambda, \omega_\beta, M_j)) f^2(\lambda) d\lambda + o(N^{-1}) \end{aligned}$$

4. COMPUTATIONAL PROCEDURES FOR SPECTRAL ESTIMATION

4.1 Computation of the Truncated Spectral Estimate

We are given a sample $\{X(t), t = \Delta t, \dots, N'\Delta t\}$. We compute the truncated spectral estimate as follows:

Step 1

Choose a truncation point M , where M is an integer-valued function of N , such that M/N is in the order of 0.1

Step 2

For each v in $\{0, \Delta t, 2\Delta t, \dots, M'\Delta t\}$ compute the sample auto-covariance function $R_N(v)$ where

$$R_N(v) = \frac{1}{N'} \sum_{t'=1}^{N'-v'} X(t) X(t+v) \tag{4.1}$$

Do this by the procedure given in Fig. 4 for computing inner products.

Step 3

Choose three numbers M_1, M_2, M_3 such that $0 < M_1 < M_2 < M_3 = M < N$ and carry out the remaining steps for each value $M_i, i = 1, 2, 3$.

Step 4

Choose a number Q , where Q is to be the number of subintervals into which we wish to divide the interval $[0, \pi/\Delta t]$ on which the truncated spectral estimate is defined.

Step 5

For $\omega = 0, \frac{\pi}{Q\Delta t}, \frac{2\pi}{Q\Delta t}, \dots, \frac{\pi}{\Delta t}$ compute the truncated spectral estimate

$$f_N(\omega, K, M_i) = \frac{\Delta t}{2\pi} \sum_{v'=-M_i'}^{M_i'} k\left(\frac{v}{M_i}\right) R_N(v) e^{-i v \omega} \tag{4.2}$$

```

2 PROCEDURE COVARIANCE(N,M,L1,L2,X() $ R1(),R2(),CI(),CT(),D1,D2,D3)$
2 COMMENT THIS PROCEDURE COMPUTES THE AUTO AND CROSS CORRELATION FUNC-
2 TIONS, R1(I),R2(I),CI(I) AND CT(I), FOR I=1,2,...,M+1. THE FUNCTION.
2 AT LAG ZERO IS STORED AT I=1, THE FUNCTION AT LAG M IS STORED AT
2 I=M+1. THE TIME SERIES ARE OF EQUAL LENGTH N AND BOTH ARE STORED IN
2 THE ARRAY Y(), ONE BEGINNING AT L1, THE OTHER AT L2. THE AUTO-CORR
2 FUNCTIONS ARE NORMALIZED TO HAVE A VALUE 1 AT THE ORIGIN AND THE
2 CROSS CORRELATIONS ARE ALSO CONSISTENTLY NORMALIZED. THE NORMAL-
2 IZING FACTORS ARE D1,D2 AND D3. THE FUNCTIONS ARE ADDED INTO THE
2 ARRAYS R1(),R2(),CI() AND CT() TO ALLOW POOLING OF COVARIANCES. SUM=
2 INPROD(K,L,N,A(),B()) IS AN EXTERNAL FUNCTION EQUIVALENT TO
2 'SUM=0.0, FOR I=(0,1,N-1), SUM=SUM+A(K+I).B(L+I)' $
2 BEGIN
2     INTEGER I...,J...,K...,L...,M...,N... $
2     D1 = INPROD(L1,L1,N,X(),X())$
2     D2 = INPROD(L2,L2,N,X(),X())$
2     D3 = SORT(D1,D2) $
2     FOR KK = (1,1,M+1) $
2 BEGIN
2     R1(KK)=R1(KK)+INPROD(L1,L1+KK-1,N-KK+1,X(),X())/D1$
2     R2(KK)=R2(KK)+INPROD(L2,L2+KK-1,N-KK+1,X(),X())/D2$
2     CI(KK)=CI(KK)+INPROD(L1,L2+KK-1,N-KK+1,X(),X())/D3$
2     CT(KK)=CT(KK)+INPROD(L2,L1+KK-1,N-KK+1,X(),X())/D3$
2 END $
2 RETURN END $

```

Fig. 4 Procedure Covariance (from Ref. 9).

For purposes of computation we rewrite (4.2) in the form

$$f_N(\omega, K, M_i) = \frac{\Delta t}{\pi} \left[\frac{1}{2} R_N(0) + \sum_{v'=-M_i'}^{M_i'} \cos v \omega k\left(\frac{v}{M_i}\right) R_N(v) \right] \quad (4.3)$$

The kernel $k(\cdot)$ will be Parzen's, Tukey's or Bartlett's kernel which are defined by Eqs. (3.77), (3.83) and (3.89) respectively of Sec. 3.9. The computation is carried out by means of the procedure given in Fig. 5 for computing finite Fourier transforms.

Step 6

Plot $\log_e f_N(\omega, K, M_i)$ against $\log_e \omega$ for $\omega=0, \frac{\pi}{Q\Delta t}, \frac{2\pi}{Q\Delta t}, \dots, \frac{\pi}{\Delta t}$ and interpolate linearly or otherwise between these points.

4.2 Discussion of the Computation

Step 1

Large sample statistical theory for normal noise processes implies that, for $0 < \omega < \frac{\pi}{\Delta t}$, Eq. (3.68) becomes

$$\text{var} \left[\log_e f_N(\omega, K, M_i) \right] \approx \frac{M_i}{N} \int_{-\infty}^{\infty} k^2(x) dx \quad (4.4)$$

with the added factor of 2 for $\omega = 0$ or $\frac{\pi}{\Delta t}$. From (4.4) we thus get

$$\left| \log_e f_N(\omega, K, M_i) - \log_e f(\omega) \right| \leq 2 \left(\frac{M_i}{N} \int_{-\infty}^{\infty} k^2(x) dx \right)^{1/2} = \Delta \quad (4.5)$$

and this gives us upper and lower bounds, that is a confidence band, on the percentage error of the truncated spectral estimate since (4.5) implies

$$e^{-\Delta} \leq \frac{f_N(\omega, K, M_i) - f(\omega)}{f(\omega)} \leq e^{\Delta} \quad (4.6)$$

The following table shows that only for $M/N < .1$ is this error of reasonable size:

| $\frac{M_i}{N}$ | $e^{-\Delta}-1$ | $e^{\Delta}-1$ |
|-----------------|-----------------|----------------|
| 0.05 | -0.3 | 0.4 |
| 0.10 | -0.4 | 0.6 |
| 0.20 | -0.5 | 0.9 |
| 0.40 | -0.6 | 1.5 |

therefore we should choose M_i no greater than 10% of N . We might now be tempted to choose M very much smaller than this to reduce the above variance and percentage error of the estimate, however, the smaller M_i becomes the larger is the bias of the estimate, which may be seen in the asymptotic case for normal processes by combining Eqs. (3.111) and (3.95) or (3.100) to show that the bias defined in (3.32) varies $1/M_i$. The best choice of M_i to balance the bias and variance contributions to the mean-square error (3.29) is a difficult problem. The result of this discussion then is that we must choose M_i to be of the order of 10% of N (up to 40%, say), since values greater (lower) than this would increase the variance (bias) by an unreasonable amount.

Step 2

The choice of M in Step 1 greatly reduces the amount of computation necessary at this step since we need to compute $R_N(v)$ at a maximum of $0.4N'$ instead of N' points. For each of these computations we call on an external procedure for computing inner products. A good example is the "procedure covariance" given in Fig. 4, and another efficient method is due to Stockham of MIT.

We now discuss some of the properties of $R_N(v)$ as opposed to other estimates of the autocovariance function. It is easily verified that

$$E[R_N(v)] = \left(1 - \frac{v}{N}\right)R(v) \tag{4.7}$$

so that its bias is given by

$$\text{bias } [R_N(v)] = \frac{v}{N} \tag{4.8}$$

which is nonzero. However it is obviously asymptotically unbiased since

$$\lim_{N \rightarrow \infty} \text{bias } [R_N(v)] = 0 \tag{4.9}$$

Also $R_N(v)$ is a positive definite function, meaning that for any k , any set of complete numbers c_i and any set of real numbers v_i in $\{0, \pm \Delta t, \pm 2\Delta t, \dots\}$ $i = 1, 2, \dots, k$ we have

$$\sum_{i=1}^k \sum_{j=1}^k c_i \overline{c_j} R_N(v_i - v_j) > 0 \tag{4.10}$$

This may be verified from the fact that

$$\begin{bmatrix} R_N(0) & R_N(\Delta t) & R_N(2\Delta t) & \dots & \dots & \dots \\ R_N(\Delta t) & R_N(0) & R_N(\Delta t) & \dots & \dots & \dots \\ R_N(2\Delta t) & R_N(\Delta t) & R_N(0) & \dots & \dots & \dots \\ \dots & \dots & \dots & \dots & \dots & \dots \\ \dots & \dots & \dots & \dots & \dots & \dots \end{bmatrix} = C^* C \tag{4.11}$$

where

$$C = \frac{1}{\sqrt{N}} \begin{bmatrix} X(\Delta t) & X(2\Delta t) & X(3\Delta t) & \dots & \dots & \dots \\ 0 & X(\Delta t) & X(2\Delta t) & \dots & \dots & \dots \\ 0 & 0 & X(\Delta t) & \dots & \dots & \dots \\ \dots & \dots & \dots & \dots & \dots & \dots \\ \dots & \dots & \dots & \dots & \dots & \dots \end{bmatrix} \tag{4.12}$$

The above matrices are of the singly infinite Toeplitz type. The true autocovariance function is a positive definite function as we remarked in (3.21) so that it seems a good idea to use estimates, like the sample autocovariance function, which have this property. We now show that the commonly used unbiased estimate

$$R_N^*(v) = \frac{1}{N^1 - v^1} \sum_{t^1=1}^{N^1 - v^1} X(t) X(t+v) \quad (4.13)$$

is not positive definite. This follows at once by taking $k=3$; $c_1=1$, $c_2=0$, $c_3=-1$; $v_1=\Delta t$, $v_2=2\Delta t$, $v_3=3\Delta t$ and $X(\Delta t)=1$, $X(2\Delta t)=0$, $X(3\Delta t)=1$. Then $R_N(0)=2/3$, $R_N(\Delta t)=0$, $R_N(2\Delta t)=1/3$ while $R_N^*(0)=2/3$, $R_N^*(\Delta t)=0$, $R_N^*(2\Delta t)=1$ so that

$$\sum_{i=1}^3 \sum_{j=1}^3 \bar{c}_i c_j R_N(v_i - v_j) = \frac{2}{3}, \quad \sum_{i=1}^3 \sum_{j=1}^3 \bar{c}_i c_j R_N^*(v_i - v_j) = -\frac{2}{3} \quad (4.14)$$

Parzen remarks, however, that even $R_N(v)$ does not give a good estimate of $R(v)$ since it does not damp out to zero for large v ($\leq N$). Nevertheless, its appropriately modified finite Fourier transform, in other words the truncated spectral estimate, does give a reasonable estimate of the spectral density function.

We remark that the computation time for the sample autocovariance function in Step 2 is proportional to $M^1 \times N^1$.

Step 3

Since we cannot specify the best value of M to minimize the sum of the errors due to bias and variance, and since later we wish to deal with cases where we have not only a continuous but also a discrete spectrum, we find it best in practice to compute the truncated spectral estimate for several values of the truncation point. Suitable values are obtained by taking M_1^1 to be an even integer between $0.05 N^1$ and $0.1 N^1$, $M_2^1 = 2M_1^1$ and $M_3^1 = 2M_2^1$. Then we have

$$\begin{aligned}
 0.05 &< \frac{M_1}{N} < 0.1 \\
 0.1 &< \frac{M_2}{N} < 0.2 \\
 0.2 &< \frac{M_3}{N} < 0.4
 \end{aligned} \tag{4.15}$$

In graphing $f_N(\omega, K, M_i)$ it is useful to note that

$$f_N(0, K, M_i) = \frac{\Delta t}{2\pi} \sum_{v' = -M_i}^{M_i} k\left(\frac{v}{M_i}\right) R_N(v) \tag{4.16}$$

which is a monotonic function of M_i , hence graphs for different values of M_i can easily be distinguished by observing their heights at the origin.

It may happen that our estimates contain spurious cycles. These can be identified by applying them to the constant time series $X(t) \equiv 1$ or more generally to other standard series with known spectral density function. If the estimate produces peaks other than the spike at the origin, we should be suspicious of such a peak if it occurs when our estimate is applied to a time series with unknown spectral density function.

Step 4

The choice of Q depends on the method of interpolation that we use to join up the computed points on the graph of $\log_e f_N(\omega, K, M_i)$. A sampling theorem tells us that if the truncation point is M_i then $f_N(\omega, K, M_i)$ can be recovered from its value at M_i equally spaced points. However, this cannot necessarily be accomplished by linear interpolation so that rather than taking $Q = M_i + 1$ points and using a more complicated interpolation procedure, we prefer to take $Q = 2M_i$ or $4M_i$. In practice with the three values of M_i chosen above, we take Q approximately equal to the greatest of these, and we make sure that if there are any physically distinguished frequencies present then Q is chosen so that these are multiples of the grid spacing $\frac{\pi}{Q\Delta t}$. The reason why Q is chosen no larger is given in the discussion of Step 6.

Step 5

The computation time for the truncated spectral estimate of Step 5 is found to be proportional to $Q \cdot M'$. The calculation is carried out by the procedure (see Fig. 5) for evaluating finite Fourier transforms due to Goertzel, which is quoted by Parzen under the name "procedure transform". Other efficient methods are due to Cooley and Tukey, and also to Stockham of MIT.

Since the spectral density function is always positive it is possibly desirable that we should try to choose a $k(\cdot)$ which gives rise always to positive estimates. It can be shown that Parzen's kernel has this property, whilst Tukey's does not. Note that in order for an estimate to be of positive type it is necessary and sufficient that the corresponding spectral window be positive, that is for all λ we have

$$K(\lambda, 0, M) \geq 0 \quad (4.17)$$

Another advantage of Parzen's kernel over that of Tukey's is that both its variance and bandwidth-variance factor are smaller. This may be seen by combining Eqs.(3.68), (3.82) and (3.88) for fixed M and N .

Step 6

Here we discuss questions about folding and resolution. A fundamental notion is that of the Nyquist or folding frequency which occurs if our sample series is really a sample from a continuous stochastic process. The truncated spectral estimate is a periodic function, with period $2\pi/\Delta t$, which, however, is an even function so that its value in $[0, \pi/\Delta t]$ will determine it completely. To get an estimate of the true spectral density function which of course is aperiodic we take the estimate to be equal to the truncated spectral estimate in $[0, \pi/\Delta t]$ and zero elsewhere. The effect of this periodicity is to make frequencies differing by multiples of $2\pi/\Delta t$ indistinguishable and the net result


```

2 PROCEDURE TRANSFORM(M,N,W(),R1(),RE(),RO(),R2())SF1(),F2(),CO(),QU())$
2 BEGIN
2 COMMENT THIS PROCEDURE COMPUTES N+1 POINTS OF TWO ESTIMATED SPECTRAL
2 DENSITY FUNCTIONS AND OF THE CO-SPECTRUM AND QUADRATURE-SPECTRUM
2 FROM R1() AND R2() WHICH ARE THE AUTO-CORRELATION FUNCTIONS AND RE()
2 AND RO() WHICH ARE THE EVEN AND ODD PARTS OF THE CROSS-CORRELATION
2 FUNCTION OF TWO TIME SERIES. THE TRUNCATION POINT IS M, THE WEIGHT
2 ING KERNAL USED IS W(). THE SINES AND COSINES NEEDED ARE COMPUTED
2 RECURSIVELY. REFERENCES 1. HAMMING, R.W., NUMERICAL METHODS FOR
2 SCIENTISTS AND ENGINEERS, MCGRAW-HILL 1962, PAGES 71-74 $
2 INTEGER I.... J.... K.... L.... M.... N.... $
2 PI = 3.1415927 $ PIV = 0.31830989 $
2 C = M $ C1 = C3 = D1 = COS(PI/C) $
2 D4 = C2 = SIN(PI/C) $ D6 = 2.C1 $
2 P1=0.5.R1(1) $ P2=0.5.RE(1) $ P4=0.5.R2(1) $
2 FOR I=(2,1,M+1) $
2 BEGIN
2 A = W(I) $
2 P1=P1+R1(I).A $ P2=P2+RE(I).A $ P4=P4+R2(I).A $
2 END $
2 F1(I) = P1.PIV $ F2(I) = P4.PIV $
2 CO(I) = P2.PIV $ QU(I) = 0.0 $
2 FOR J = (1,1,N)$
2 BEGIN
2 U11 = U12 = U13 = U14 = U21 = U22 = U23 = U24 = 0.0 $
2 FOR J = (M+1,-1,2)$
2 BEGIN
2 A = W(J) $
2 U31 = D6.U21-U11+R1(J).A $
2 U32 = D6.U22-U12+RE(J).A $
2 U33 = D6.U23-U13+RO(J).A $
2 U34 = D6.U24-U14+R2(J).A $
2 U11 = U21 $ U21 = U31 $ U12 = U22 $ U22 = U32 $
2 U13 = U23 $ U23 = U33 $ U14 = U24 $ U24 = U34 $
2 END $
2 F1(I+1) = (D1.U21 - U11 + R1(I).0.5).PIV $
2 CO(I+1) = (D1.U22 - U12 + RE(I).0.5).PIV $
2 QU(I+1) = D4.U23.PIV $
2 F2(I+1) = (D1.U24 - U14 + R2(I).0.5).PIV $
2 D1 = C1.C3-C2.D4 $ D4 = D4.C1+C3.C2 $
2 C3 = D1 $ D6 = 2.D1 $
2 END $
2 RETURN END $

```

Fig. 5 Procedure Transform (from Ref. 9)

is to fold over the true spectrum onto the interval $[0, \pi/\Delta t]$ in the way described in Sec.2. Thus we must either choose Δt so small that the true spectral density function is also zero outside this interval or prefilter the data, as we did in Sec.2, to remove these high frequency sections.

In Sec.2 it was also shown that the effect of finite data length is to blur the spectrum in an equivalent way to looking at it through a spectral window of bandwidth proportional to $1/N$ which for fixed ratio M/N is proportional to $1/M$. Hence it is pointless to look for resolution in an interval smaller than this, so that it would be pointless to choose Q larger than $O(M')$. Note that the bandwidth of the truncated spectral estimate is also proportional to $1/M$, so that it is automatically of the right order. The discussion of Step 4 gave a lower bound for the choice of Q .

The reason for preferring the scale $\log_e \omega$ instead of ω is because it magnifies the low frequency part which we are particularly interested in. Plotting $\log_e f_N(\omega, K, M)$ instead of $f_N(\omega, K, M)$ is advantageous because we have asymptotic confidence bands for this estimate in the case of normal noise as was noted in (4.6) in the discussion of Step 1.

4.3 Correlation Analysis

It may be preferred to compute estimates of the correlation function and its Fourier transform rather than the covariance function and the spectral density function. In this case the procedure is as follows.

Step 1

Choose a truncation point M which is an integer-valued function of N such that M/N is in the order of 0.1.

Step 2

For each v in $\{0, \Delta t, \dots, M' \Delta t\}$ compute $N' \times R(v)$ where $R_N(v)$ is the sample autocovariance function

$$R_N(v) = \frac{1}{N'} \sum_{t'=1}^{N'-v'} X(t) X(t+v) \quad (4.18)$$

Do this by the subroutine given in Fig. 4 for computing inner products.

Step 3

For v in $\{0, \Delta t, \dots, M' \Delta t\}$ compute the sample autocorrelation function $\rho_N(v)$ where

$$\rho_N(v) = \frac{R_N(v)}{R_N(0)} \quad (4.19)$$

Step 4

Choose three numbers $0 < M_1 < M_2 < M_3 = M < N$ and carry out the remaining steps for each M_i , $i=1, 2, 3$.

Step 5

Choose a number Q , where Q is the number of subintervals into which we divide the interval $[0, \pi/\Delta t]$.

Step 6

For $\omega = 0, \pi/Q\Delta t, 2\pi/Q\Delta t, \dots, \pi/\Delta t$ compute the truncated normalized spectral estimate $\phi_N(\omega, K, M_i)$ where

$$\phi_N(\omega, K, M_i) = \frac{\Delta t}{2\pi} \sum_{v'=-M_i'}^{M_i'} k\left(\frac{v}{M_i}\right) \rho_N(v) e^{-i\omega v} \quad (4.20)$$

which can also be written in the form

$$\phi_N(\omega, K, M_i) = \frac{\Delta t}{\pi} \left[\frac{1}{2} + \sum_{v'=-M_i'}^{M_i'} \cos v\omega k\left(\frac{v}{M_i}\right) \rho_N(v) \right] \quad (4.21)$$

Step 7

Plot $\log_e \phi_N(\omega, K, M_i)$ against $\log_e \omega$ for $\omega=0, \pi/Q\Delta t, \dots, \pi/\Delta t$ and interpolate linearly or otherwise between these points.

Discussion: the same considerations apply to the above computation as did to the autocovariance approach. The autocorrelation approach may be viewed as a normalized version of the autocovariance approach. It is equivalent to replacing the sample series $\{X(t), t = \Delta t, \dots, N'\Delta t\}$ by the sample series

$$\left\{ \frac{X(t)}{\sqrt{\sum_{t=1}^{N'} |X(t)|^2}}, t = \Delta t, \dots, N'\Delta t \right\}$$

and then carrying out the calculations for the autocovariance approach on this normalized series. In a sense the vector which represents this realization of the process has unit length.

4.4 Finding the Noise and Signal Components from the Truncated Spectral Estimate

We must first assume that we know the frequencies of the signal components. In another paragraph we shall show how to estimate these from our estimate if we do not know them a priori.

We concentrate now on the case of a single sine wave of frequency ω_s in noise with the additional assumption that ω_s is no nearer to 0 or $\pi/\Delta t$ than the bandwidth of the widest spectral window in use. In other words

$$\omega_s \gg \frac{1}{M}, \quad \frac{\pi}{\Delta t} - \omega_s \gg \frac{1}{M} \quad (4.22)$$

The subsequent theory will as before deal only with normal processes.

Under these conditions we look at the truncated spectral estimate at the signal frequency ω_s . From Theorem 7 using Theorems 1 and 2 we easily obtain

$$E \left[f_N(\omega_s, K, M) \right] = \frac{1}{4} K C^2 M + f(\omega_s) + O(M^{-2}) \quad (4.23)$$

and similarly from Theorem 7 and Theorem 3(a) we obtain

$$N \text{ cov} \left[f_N(\omega_s, K, M_i), f_N(\omega_s, K, M_j) \right] = \pi M_{ij}^2 K^2 C^2 f(\omega_s) + M_{ij} I_{ij} f^2(\omega_s) + O(M_{ij}^{-1}) \quad (4.24)$$

We now use (4.23) to separate the signal and noise components. We look on this as an equation in which the estimates are a linear function of the truncation point with an error term. Thus the estimates will lie about a regression line with slope $\frac{1}{4} K C^2$ and intercept on the f_N - axis given by $f(\omega_s)$, where $K = \frac{3}{8\pi}$ for Parzen's kernel and $K = \frac{1}{2\pi}$ for Tukey's kernel. Hence by finding this regression line we can determine C^2 and $f(\omega_s)$ at once. The problem of fitting a regression line with correlated variables is well known and we merely outline its solution here. Suppose we have m spectral estimates corresponding to the truncation points $M_1 < M_2 \dots < M_m$. Write

$$f_N = \begin{pmatrix} f_N(\omega_s, K, M_1) \\ \vdots \\ f_N(\omega_s, K, M_m) \end{pmatrix} \quad (4.25)$$

$$M_{1,0} = \begin{pmatrix} M_1 & 1 \\ \vdots & \vdots \\ M_m & 1 \end{pmatrix} \quad (4.26)$$

From (4.24) we obtain the approximate covariance matrix \sum of the estimates f_N which has (i, j) th element approximately given by

$$\sum_{ij} = \frac{\pi}{\Delta t} N^{-1} M_{ij}^2 K^2 C^2 f(\omega_s) + N^{-1} M_{ij} I_{ij} f^2(\omega_s) \quad (4.27)$$

Then from (4.23) we have approximately

$$E \begin{bmatrix} f_N \\ f(\omega_s) \end{bmatrix} = M_{1,0} \begin{bmatrix} \frac{1}{4} K C^2 \\ f(\omega_s) \end{bmatrix} \quad (4.28)$$

from which it follows that the best linear unbiased estimates for C^2 and $f(\omega_s)$ are given by

$$\begin{bmatrix} \frac{1}{4} K C_N^2 \\ f_N(\omega_s) \end{bmatrix} = \left[M'_{1,0} \sum^{-1} M_{1,0} \right]^{-1} M'_{1,0} \sum^{-1} f_N \quad (4.29)$$

with covariance matrix

$$\left[M'_{1,0} \sum^{-1} M_{1,0} \right]^{-1} \quad (4.30)$$

A nasty complication is that through \sum the expression (4.29) for the estimates C_N^2 and $f_N(\omega_s)$ depend on the true values C^2 and $f(\omega_s)$ of these quantities. This means that (4.29) must be solved iteratively. Suitable starting values for the iteration are $C_N^2=0$ and $f_N(\omega_s) = 1$ in \sum , the latest estimates of these quantities are then used at each subsequent step.

We remark that even if we use a kernel which will produce a non-negative estimate $f_N(\omega_s, K, N)$, there is no guarantee that the estimates C_N and $f_N(\omega_s)$ will be non-negative. We should note that we might also consider a direct least squares or Gauss Markov estimate of the signal. However, the method proposed above, even though it requires considerably more computation, is applicable even if the signal frequency is not precisely known or if it is a spectral peak of very narrow bandwidth rather than a spectral line. In addition the variance of our method is asymptotically equal to that of these alternative estimates.

If there is no signal present our regression line should have zero slope as is seen from (4.23), and this test may be used in deciding if we have chosen suitable truncation points for our estimates. If there is more than one sine wave in the signal, and these have frequencies between 0 and $\pi/\Delta t$ separated according to the conditions

$$\omega_s - \omega_{s-1} \gg \frac{1}{M}, \quad \omega_{s+1} - \omega_s \gg \frac{1}{M} \quad (4.31)$$

then exactly the same equations apply for the determination of ω_s as in the single sine wave case, in other words the signals at frequencies other than ω_s have a negligible effect on the estimates at ω_s . Of course, we can always choose an estimate with a sufficiently narrow bandwidth to satisfy (4.31), but only at the expense of increased variance or length of sample.

For the constant term at zero frequency with

$$\omega_1 \gg \frac{1}{M} \quad (4.32)$$

we obtain

$$E \left[f_N(0, K, M) \right] = KC_o^2 M + f(0) + O(M^{-2}) \quad (4.33)$$

instead of (4.23), and in place of (4.24) we have

$$N \text{ cov} \left[f_N(0, K, M_i), f_N(0, K, M_j) \right] = \frac{8\pi}{\Delta t} M_{ij}^2 K^2 C_o^2 f(0) + 2M_{ij} I_{ij} f^2(0) + O(M_{ij}^{-1}) \quad (4.34)$$

Similarly for the on-off term of frequency $\pi/\Delta t$ with

$$\frac{\pi}{\Delta t} - \omega_{q-1} \gg \frac{1}{M} \quad (4.35)$$

we obtain

$$E \left[f_N\left(\frac{\pi}{\Delta t}, K, M\right) \right] = KC_q^2 M + f\left(\frac{\pi}{\Delta t}\right) + O(M^{-2}) \quad (4.36)$$

$$N \text{ cov} \left[f_N\left(\frac{\pi}{\Delta t}, K, M_i\right), f_N\left(\frac{\pi}{\Delta t}, K, M_j\right) \right] = \frac{8\pi}{\Delta t} M_{ij}^2 K^2 C_q^2 f\left(\frac{\pi}{\Delta t}\right) + 2M_{ij} I_{ij} f^2\left(\frac{\pi}{\Delta t}\right) + O(M_{ij}^{-1}) \quad (4.37)$$

which are of the same form as (4.23) and (4.24). Of course, the regression procedure is the same in all these cases as in the case of a single sine wave with the change of a few constants in the equations. The simplicity of the method rests on the fact that the part of the spectral estimate due to the signal increases linearly with M , while the noise component is independent of M .

When a component due to a signal is very strong or very close in frequency to another component, the approximations in the proof of Theorem 9 will not be valid. In these instances we may either look more carefully at the arguments leading to (4.23) and (4.24), in which case we can develop regression methods depending simultaneously on the quantities of interest at both frequencies, or we can use the techniques of super-resolution in Hext¹⁰.

4.5 Estimates of the Derivatives of the Noise Spectral Density Function

When the frequencies of the signal components are unknown it is necessary for us to estimate the derivatives of the quantities we have been considering. We assume we are dealing with a discrete parameter stationary time series whose autocovariance function satisfies

$$\sum_{v'=-\infty}^{\infty} |v^p R(v)| < \infty \quad (4.38)$$

for some positive integer p . For all integers q , $0 < q \leq p$, the q^{th} spectral derivative is

$$f^{(q)}(\omega) = \frac{(-i)^q \Delta t}{2\pi} \sum_{v'=-\infty}^{\infty} v^q R(v) e^{-iv\omega} \quad (4.39)$$

and the q^{th} generalized spectral derivative is defined to be

$$f^{[q]}(\omega) = \frac{1 \Delta t}{2\pi} \sum_{v'=-\infty}^{\infty} |v|^q R(v) e^{-iv\omega} \quad (4.40)$$

Similarly the q^{th} generalized spectral derivatives of the truncated spectral estimate and of the spectral window are defined as

$$f_N^{[q]}(\omega, K, M) = \frac{\Delta t}{2\pi} \sum_{v'=-M'}^{M'} |v|^q k\left(\frac{v}{M}\right) R_N(v) e^{-iv\omega} \quad (4.41)$$

and

$$K^{[q]}(\lambda, \omega, M) = \frac{\Delta t}{2\pi} \sum_{v'=-M'}^{M'} |v|^q k\left(\frac{v}{M}\right) \cos v\omega e^{-iv\lambda} \quad (4.42)$$

We quote theorems for these derivatives which are analogous to Theorems 7 and 9.

Theorem 10 Given N^1 observations of the time series

$X(t) = C \cos(\omega_s t + \phi) + Y(t)$, $t = \Delta t, \dots, N^1 \Delta t$, where (i) C , ω_s , and ϕ are fixed with $\omega_s \neq 0$ or $\pi/\Delta t$. (ii) $Y(t)$ is a stationary and ergodic normal time series having zero mean, autocovariance function $R(v)$, $v = 0, \Delta t, 2\Delta t, \dots$ for which $\sum_V |vR(v)| < \infty$ and spectral density function $f(\omega)$ on $\left[-\frac{\pi}{\Delta t}, \frac{\pi}{\Delta t}\right]$. Then for fixed nonnegative integers r and s , as $N \rightarrow \infty$

$$E \left[f_N^{(r)}(\omega, K, M) \right] = \frac{1}{2} C^2 K^{(r)}(\omega, \omega_s, M) + \int_{\Lambda} K^{(r)}(\omega, \lambda, M) f(\lambda) d\lambda + o(N^{-1}) \quad (4.43)$$

and

$$N \text{ cov} \left[f_N^{(r)}(\omega_\alpha, K, M_i), f_N^{(s)}(\omega_\beta, K, M_j) \right] = \frac{4\pi}{\Delta t} K^{(r)}(\omega_\alpha, \omega_s, M_i) K^{(s)}(\omega_\beta, \omega_s, M_j) C^2 f(\omega_s) + \frac{4\pi}{\Delta t} \int_{\Lambda} K^{(r)}(\omega_\alpha, \lambda, M_i) K^{(s)}(\omega_\beta, \lambda, M_j) f^2(\lambda) d\lambda + o(N^{-1}) \quad (4.44)$$

and similar results hold for generalized spectral derivatives on both sides of these equations.

If instead of a single sine wave the signal has q components, we have as we should expect

Theorem 11 Given N^1 observations of the time series

$X(t) = \sum_{j=0}^q C_j \cos(\omega_j t + \phi_j) + Y(t)$, $t = \Delta t, 2\Delta t, \dots, N^1 \Delta t$, where (i) the C_j , ω_j and ϕ_j are fixed with $C_j \geq 0$ and $0 = \omega_0 < \omega_1 < \dots < \omega_{q-1} < \omega_q = \pi/\Delta t$, $\phi_0 = 0$, $\phi_q = 0$ or π . (ii) $Y(t)$ is a stationary, ergodic, normal time series having zero mean, autocovariance function $R(v)$, $v = 0, \Delta t, 2\Delta t, \dots$ such that $\sum_{v=-\infty}^{\infty} |vR(v)| < \infty$ and spectral density function $f(\omega)$ on $\left[-\frac{\pi}{\Delta t}, \frac{\pi}{\Delta t}\right]$. Then for fixed nonnegative integers r and s , as $N \rightarrow \infty$

$$\begin{aligned}
 N \operatorname{cov} \left[f_N^{(r)}(\omega_\alpha, K, M_i), f_N^{(s)}(\omega_\beta, K, M_j) \right] &= \frac{8\pi}{\Delta t} K^{(r)}(\omega_\alpha, 0, M_i) K^{(s)}(\omega_\beta, 0, M_j) C_o^2 f(0) \\
 &+ \frac{4\pi}{\Delta t} \sum_{k=1}^{q-1} K^{(r)}(\omega_\alpha, \omega_k, M_i) K^{(s)}(\omega_\beta, \omega_k, M_j) C_k^2 f(\omega_k) \\
 &+ \frac{8\pi}{\Delta t} K^{(r)}(\omega_\alpha, \frac{\pi}{\Delta t}, M_i) K^{(s)}(\omega_\beta, \frac{\pi}{\Delta t}, M_j) C_q^2 f(\frac{\pi}{\Delta t}) \\
 &+ \frac{4\pi}{\Delta t} \int_{\Lambda} K^{(r)}(\omega_\alpha, \lambda, M_i) K^{(s)}(\omega_\beta, \lambda, M_j) f^2(\lambda) d\lambda + o(N^{-1})
 \end{aligned} \tag{4.46}$$

and similar results hold for generalized spectral derivatives on both sides of these equations. Using these results we may derive the following analogues of Eqs. (4.23) and (4.24): provided $p \geq 2$ ($p = 2$ for Parzen, $p = 1$ for Tukey!)

$$E \left[f_N^{(2)}(\omega_s, K, M) \right] = -\frac{1}{4} C^2 K^{(2)} M^3 + k''(0) f''(\omega_s) + O(M^{-(p-1)} \log_e M) \tag{4.47}$$

and provided $p \geq 1$

$$\begin{aligned}
 N \operatorname{cov} \left[f_N^{(2)}(\omega_s, K, M_i), f_N^{(2)}(\omega_s, K, M_j) \right] &= \frac{\pi}{\Delta t} M_{ij}^6 K^{(2)} K^{(2)} C^2 f(\omega_s) \\
 &+ M_{ij}^5 I_{ij}^{(2)} f^2(\omega_s) + O(M_{ij}^{-3})
 \end{aligned} \tag{4.48}$$

where in each case we have assumed that

$$\omega_s \gg \frac{1}{M} \quad \text{and} \quad \frac{\pi}{\Delta t} - \omega_s \gg \frac{1}{M}$$

and where $K^{(2)}$ is the peak curvature factor of the window defined as

$$K^{(2)} = \frac{1}{2\pi} \int_{-1}^1 x^2 k(x) dx \tag{4.49}$$

and

$$I^{(2)}(\mu, K) = \int_{-\mu}^{\mu} x^4 k(\mu^{-1}x) k(\mu x) dx \tag{4.50}$$

and

$$I^{(2)}(M_i, M_j, K) = I^{(2)}(\mu_{ij}, K) \tag{4.51}$$

$K^{(2)} = \frac{1}{32\pi}$ for Parzen's kernel and $(\frac{1}{6\pi} - \frac{1}{\pi 3})$ for Tukey's.

We can now estimate C^2 and $f''(\omega_s)$ by regression techniques similar to those of Sec. 4.4. The resulting best linear unbiased estimates for C^2 and $f''(\omega_s)$ are given by

$$\begin{bmatrix} -\frac{1}{4} K^{(2)} C^2 \\ f''_N(\omega_s) \end{bmatrix} = \left[M'_{3,0} \left(\sum^{(2,2)} \right)^{-1} M_{3,0} \right]^{-1} M'_{3,0} \left(\sum^{(2,2)} \right)^{-1} f^{(2)}_N \tag{4.52}$$

with covariance matrix

$$\left[M'_{3,0} \left(\sum^{(2,2)} \right)^{-1} M_{3,0} \right]^{-1} \tag{4.53}$$

where

$$M_{3,0} = \left\{ \begin{array}{cc} M_1^3 & 1 \\ \cdot & \cdot \\ \cdot & \cdot \\ \cdot & \cdot \\ M_m^3 & 1 \end{array} \right\} \tag{4.54}$$

and we have the approximate covariance matrix $\sum^{(2,2)}$ with

$$\sum_{ij}^{(2,2)} = \frac{\pi}{\Delta t} N^{-1} M_{ij}^6 K^{(2)} K^{(2)} C^2 f(\omega_s) + N^{-1} M_{ij}^5 I_{ij}^{(2)} f^2(\omega_s) \tag{4.55}$$

Through $\sum^{(2,2)}$ the estimates $f''_N(\omega_s)$ and C^2_N are functions of the true values of C^2 and $f(\omega_s)$, which may be supplied approximately from the regression in

Sec. 4.4. We see then that we have two estimates for C^2 and we should test whether the difference between them is statistically significant taking into account the correlation between them. If the difference is significant we must reexamine the model we have taken for the time series and also the various approximations we have made. If the difference is not significant we can combine the regressions of (4.23) and (4.47) and solve them simultaneously thus obtaining an estimate of the signal component, the noise component and the second derivative of the noise component. To do this we need an expression for the covariance of a spectral estimate and a second derivative estimate. This is obtained easily from Theorem 10 and we do not go into details.

To obtain a result of the same kind as (4.47) for the first derivative in the case of the simple mixed spectrum model we again use Theorem 10 to obtain the expression

$$E\left[f_N^{(1)}(\omega_s, K, M)\right] = f^{(1)}(\omega_s) + \frac{1}{2} C^2 O(M^{-p}) + O(M^{-2}) \quad (4.56)$$

hence we have that approximately the first derivative of the noise spectral density is equal to the expected value of the first derivative of the truncated spectral estimate. The covariance of two estimates is given by

$$N \text{cov}\left[f_N^{(1)}(\omega_s, K, M_i), f_N^{(1)}(\omega_s, K, M_j)\right] = M_{ij}^3 I^{(1)}(\mu_{ij}, K) f^2(\omega_s) + O(M_{ij}) \quad (4.57)$$

By the usual regression analysis on (4.56) and (4.57) we obtain the best linear unbiased estimate for $f'(\omega_s)$ as

$$f'_N(\omega_s) = \left[M'_o \left(\sum^{(1,1)} \right)^{-1} M_o \right]^{-1} M'_o \left(\sum^{(1,1)} \right)^{-1} f'_N(\omega_s) \quad (4.58)$$

with variance

$$\left[M'_o \left(\sum^{(1,1)} \right)^{-1} M_o \right]^{-1} \quad (4.59)$$

where M_o is a column vector of ones. For the full mixed spectrum model the results are the same provided ω_s is not too near ω_{s-1} or ω_{s+1} . For the special frequencies $\omega_o = 0$ and $\omega_q = \pi/\Delta t$ (4.47) becomes

$$E \left[f_N^{(2)}(0, K, M) \right] = -\frac{1}{2} C_o^2 K^{(2)} M^3 + k''(o) f''(o) + O(M^{-(p-1)} \log_e M) \quad (4.60)$$

(4.55) becomes

$$\sum_{ij}^{(2,2)} = \frac{8\pi}{\Delta t} N^{-1} M_{ij}^6 K^{(2)} K^{(2)} C_o^2 f(o) + 2N^{-1} M_{ij}^5 I_{ij}^{(2)} f^2(o) \quad (4.61)$$

(4.56) is unaltered. For $\omega_q = \pi/\Delta t$ the results are the same with C_o replaced by C_q and the frequency o by $\pi/\Delta t$.

4.6 Estimates of the Signal Frequency

Consider the simple mixed spectrum model

$$X(t) = C \cos(\omega_s t + \phi) + Y(t) \quad t = \Delta t, 2\Delta t, \dots, N\Delta t \quad (4.62)$$

The expected spectral estimate is

$$f(\omega, K, M) = \frac{\Delta t}{2\pi} \sum_{v'=-M'}^{M'} \cos v\omega k\left(\frac{v}{M}\right) R(v) \quad (4.63)$$

Suppose that the derivative of the noise spectral density function at a signal frequency ω_p is known to have value D (for example $D=0$), then because of (4.56) this will be approximately equal to the derivative of (4.63). Thus our estimate ω_p^* of ω_p will be the solution of

$$D = -\frac{\Delta t}{2\pi} \sum_{v'=-M'}^{M'} v \sin v\omega_p^* k\left(\frac{v}{M}\right) R(v) \quad (4.64)$$

the variance of which is given by

$$\text{var} [\omega_p^*] = O(N^{-1} M^{-3}) \quad (4.65)$$

which decreases rapidly as the bandwidth of the spectral window decreases. This suggests we should use an estimate with the least bandwidth of any, namely the periodogram. We solve (4.64) as before and instead of (4.65) we obtain

$$\text{var}[\omega_p^*] \approx \frac{8}{3} C^{-4} f^2(\omega_p^*) N^{-4} \quad (4.66)$$

If the derivative of the noise spectral density is not known at the signal frequency, there are methods for estimating both of these quantities simultaneously, however, we do not go into the matter here. It depends essentially on (4.56) which shows that if we graph $f_N^{(1)}(\omega, K, M_i)$ $i = 1, 2, \dots, m$ against ω , then all the curves should intersect in the point $(\omega_s, f^{(1)}(\omega_s))$.

4.7 Narrowband Signals in Noise

We shall now consider time series satisfying the following model

$$X(t) = \sum_{j=1}^q Z_j(t) + Y(t) \quad (4.67)$$

where $Y(t)$ is a noise process of the type considered above and the $Z_j(\cdot)$ are mutually independent processes, which are also independent of the $Y(\cdot)$ series. Then

$$R(v) = \sum_{j=1}^q R_j(v) + R_o(v) \quad v = 0, \Delta t, \dots \quad (4.68)$$

and provided $R_o(\cdot)$ and the $R_j(\cdot)$ are all absolutely summable, we have

$$f(\omega) = \sum_{j=1}^q f_j(\omega) + f_o(\omega) \quad (4.69)$$

The $Z_j(\cdot)$ series replace the pure sine wave signals and are considered to be slightly distorted (in amplitude and phase) sine wave signals whose spectra have pronounced peaks at the central frequencies ω_j .

For simplicity we carry out our analysis for the simple narrowband signal model

$$X(t) = Z(t) + Y(t) \quad (4.70)$$

where $Z(\cdot)$ has central frequency ω_s . We shall assume further that

$$R_s(v) = \frac{1}{2} C^2 h(v) \cos v \omega_s \quad (4.71)$$

where $h(0) = 1$ and $h(v)$ is an even, slowly varying, integrable, nonnegative definite function. Note: $h(v) \equiv 1$ corresponds to a pure sine wave signal. The more slowly $h(v) \rightarrow 0$ as $v \rightarrow \infty$, the narrower will be the bandwidth of the narrowband signal. Since $h(v)$ is a weight factor for the autocovariance (4.71) we can define the bandwidth of the signal by analogy with the bandwidth of a spectral window by making $h(v)$ correspond to $k(\frac{v}{M})$. Thus

$$\beta_s = \frac{1}{\frac{\Delta t}{2\pi} \sum_{v'=-\infty}^{\infty} h(v)} \quad (4.72)$$

Using the truncated spectral estimate $f_N(\omega_s, K, M)$ we wish to find estimates of $f_o(\omega_s)$, $\frac{1}{2}C^2$ and β_s . By analysis of the type we have so often used before, we arrive at the expression

$$E\left[f_N(\omega_s, K, M)\right] \approx \frac{\Delta t}{8\pi} C^2 \sum_{v'=-M'}^{M'} h(v) k\left(\frac{v}{M}\right) + f_o(\omega_s) \quad (4.73)$$

provided $\frac{1}{M} \ll \omega_s \ll \frac{\pi}{\Delta t} - \frac{1}{M}$. When M is sufficiently small $h(M)$ is almost unity so that (4.73) is approximately

$$E\left[f_N(\omega_s, K, M)\right] \approx \frac{\Delta t}{8\pi} C^2 \sum_{v'=-M'}^{M'} k\left(\frac{v}{M}\right) + f_o(\omega_s) \quad (4.74)$$

$$\approx \frac{1}{4} K C^2 M + f_o(\omega_s) \quad (4.75)$$

from which estimates of $\frac{1}{2} C^2$ and $f_o(\omega_s)$ by the regression methods of previous paragraphs. Here β_s is much smaller than β so that the narrowband signal looks like a pure sine wave. On the other hand, if there are sufficiently large values of M so that $k(\frac{v}{M})$ is almost unity while $h(v)$ is small (4.73) becomes approximately

$$E \left[f_N(\omega_s, K, M) \right] \approx \frac{\Delta t}{8\pi} C^2 \sum_{v'=-\infty}^{\infty} h(v) + f_o(\omega_s) \approx \frac{1}{4} \frac{C^2}{\beta_s} + f_o(\omega_s) \quad (4.76)$$

from which we may estimate β_s since we already have estimates of $\frac{1}{2} C^2$ and $f_o(\omega_s)$. However, as M increases so does the variance of the estimates $f_N(\omega_s, K, M)$ so that these estimates of β_s must be regarded with caution. This occurs because in this case β is much smaller than β_s so that we are essentially estimating the spectral density function at the signal frequency.

4.8 Stagewise Autoregressive Estimation

The idea behind this is to attempt to find constants a_1, \dots, a_p , for some integer p , such that Eq. (3.25) holds. That is

$$X(t) = \sum_{s'=1}^p a_{s'} X(t - s) + \epsilon(t) \quad (4.77)$$

where $\epsilon(t)$ is a white noise process. We do this by a stagewise procedure, picking the constant at each step which reduces the variance of the estimate by the greatest amount. The time series need not satisfy an expression of the form (4.77) and we may find in that case that our procedure does not terminate. However, if it does terminate, from Eq. (3.26) we obtain at once an analytic formula for the spectral density function $f(\omega)$, and thus an approximation to the spectral density function of the process $X(\cdot)$. Having determined the coefficients a_1, \dots, a_p we must check to see if the residual series

$$X(t) - \sum_{s'=1}^p a_{s'} X(t - s) \quad (4.78)$$

is in fact approximately a white noise process. To do this we must carry out a spectral analysis of it.

Our stagewise procedure will be given below. It is based on the fact that if $X(\cdot)$ satisfies (4.77) for each t in $\{\Delta t, \dots, N\Delta t\}$ then the a_1, \dots, a_p satisfy the normal equations

$$\sum_{s'=1}^p R(v - s) a_{s'} = R(v), \quad v' = 1, \dots, p \quad (4.79)$$

In practice we cannot find $R(v)$ but only the consistent estimate $R_N(v)$. However, the solutions a_1, \dots, a_p of the estimated normal equations

$$\sum_{s'=1}^p R_N(v - s) a_{s'} = R_N(v), \quad v' = 1, \dots, p \quad (4.80)$$

are consistent estimates of the solutions of (4.79). In order to keep the computations within practical bounds we shall assume that we do not seek models with p greater than 50.

The steps of our computation are as follows. First we compute the estimated autocorrelation function

$$\rho_N(v) = \frac{R_N(v)}{R_N(0)} \quad (4.81)$$

for $v = \Delta t, \dots, p\Delta t$ and we form the statistic

$$\rho_1^2 = \sum_{v'=1}^p \rho_N^2(v) \quad (4.82)$$

If ρ_1^2 is essentially zero we go no farther since this means $X(t)$ is approximately independent of $X(t - s)$, $s' = 1, \dots, p$. On the other hand, if ρ_1^2 is different from zero, we choose s_1 such that

$$\rho_{N_1}^2(s_1) = \max \{ \rho_{N_1}^2(v), 1 \leq v' \leq p \} \quad (4.83)$$

and we form

$$X_{s_1}(t) = a_{s_1} X(t - s_1) \quad (4.84)$$

for all t in $\{(s_1' + 1)\Delta t, \dots, N\Delta t\}$, where a_{s_1} is the solution of the estimated normal equation

$$R(o) a_{s_1} = R(s_1) \quad (4.85)$$

Next we calculate the estimated autocorrelation function $\rho_{N_1}(v)$ of $X_{s_1}(t)$ for $v' = \Delta t, \dots, p\Delta t$, and we form the statistic

$$\rho_2^2 = \sum_{\substack{v'=1 \\ v' \neq s_1'}}^p \rho_{N_1}^2(v) \quad (4.86)$$

If ρ_2^2 is not significantly different from zero we halt. At this point we have the approximate representation

$$X(t) = a_{s_1} X(t - s_1) + \epsilon(t) \quad (4.87)$$

where $\epsilon(t)$ has to be analyzed to see if it is approximately a white noise process. However, if ρ_2^2 is significant, proceed to the second step. We choose s_2 such that

$$\rho_{N_1}^2(s_2) = \max \{ \rho_{N_1}^2(v), 1 \leq v' \leq p, v' \neq s_1' \} \quad (4.88)$$

and we form

$$X_{s_1 s_2}(t) = a_{s_1'} X(t - s_1) + a_{s_2'} X(t - s_2) \quad (4.89)$$

where $a_{s_1'}$, $a_{s_2'}$ are solutions of the normal equations

$$R(0) a_{s_1'} + R(s_1 - s_2) a_{s_2'} = R(s_1) \quad (4.90)$$

$$R(s_2 - s_1) a_{s_1'} + R(0) a_{s_2'} = R(s_2)$$

Note that the $a_{s_1'}$ in (4.89) is not the same as in (4.84). This gives us the approximate representation

$$X(t) = a_{s_1'} X(t - s_1) + a_{s_2'} X(t - s_2) + \epsilon(t) \quad (4.91)$$

and so on. A program which carries out this procedure is given in Fig. 6.

```

2 PROCEDURE SELECT( R(), K, L $COF(),IN(), NC )$ BEGIN
2 COMMENT THIS PROCEDURE COMPUTES THE BEST FITTING AUTO-REGRESSIVE
2 COEFFICIENTS FOR A TIME SERIES WITH SAMPLE CORRELATION FUNCTION R()
2 OF TRUNCATION POINT K. L IS THE LENGTH OF THE TIME SERIES, USED FOR
2 COMPUTING DEGREES OF FREEDOM. THE NC SIGNIFICANT COEFFICIENTS
2 ARE RETURNED IN COF() WITH THEIR INDICES IN IN(). REFERENCES 1.)
2 EFROYMSON, M.A., 'MULTIPLE REGRESSION ANALYSIS', IN 'MATHEMATICAL
2 METHODS FOR DIGITAL COMPUTERS', EDITED BY RALSTON, A. AND WILF, H.S.,
2 WILEY, 1962 $
2 GLOBAL A(,) $
2 INTEGER I, J, K, L, M, N $
2 ARRAY CB(72) $
2 ARRAY CHI2(52) = (6.63, 9.21, 11.3, 13.3, 15.1, 16.8, 18.5, 20.1, 21.7,
2 23.2, 24.7, 26.2, 27.7, 29.1, 30.6, 32.0, 33.4, 34.8, 36.2, 37.6,
2 38.9, 40.3, 41.6, 43.0, 44.3, 45.6, 47.0, 48.3, 49.6, 50.9, 52.2,
2 53.5, 54.8, 56.1, 57.3, 58.6, 59.9, 61.2, 62.4, 63.7, 65.0, 66.2,
2 67.5, 68.7, 70.0, 71.2, 72.4, 73.7, 74.9, 76.2, 77.4, 78.6 ) $
2 TOL = 0.001 $ N = K+1 $ F2 = 6.635 $ KP = 0 $
2 COMMENT PLACING THE COVARIANCE FUNCTION IN THE MATRIX $
2 FOR I=(1,1,N) $
2 BEGIN
2 A(I,I) = 1.0 $
2 FOR J=(1,1,I-1) $ A(I,J) = A(J,I) = R(I-J+1)$
2 END $
2 FIVE..
2 F1 = CHI2(K - KP ) $ PHI = L - KP - 1 $ RTOT = 0.0 $
2 VMIN = 2*F0 $ VMAX = 0.0 $ NMIN = NMAX = 0 $
2 FOR I=(1,1,K) $ IF (A(I,I) GTR TOL )$
2 BEGIN
2 V = (A(I,N).A(N,I))/A(I,I) $
2 IF V GTR 0.0 $ RTOT=RTOT+V $ COMMENT I NOT IN MODEL $
2 EITHER IF (V LSS 0.0) $ COMMENT I IS IN MODEL $
2 BEGIN
2 CB(I)=A(I,N) $
2 IF (ABS(V) LSS ABS(VMIN) )$ (VMIN= V$ NMIN= I) $
2 END $
2 OR IF (V GTR VMAX)$ (VMAX= V$ NMAX=I$ CB(I)= 0.05)$
2 OTHERWISE $ CB(I) = 0.0 $
2 END$
2 EITHER IF ABS(VMIN) LSS F2.A(N,N)/PHI $ (K1=NMIN $ KP=KP-1) $
2 OR IF RTOT GTR F1.(A(N,N)/PHI)$ (K1 = NMAX $ KP=KP+1) $
2 OTHERWISE$ GO TO ALM $
2 COMMENT WE COMPUTE THE NEW MATRIX. IF K1 = NMIN THEN WE ARE DELETING A
2 VARIABLE. IF K1 = NMAX WE ARE ADDING A VARIABLE. IN EITHER CASE THE
2 COMPUTATIONS ARE THE SAME $
2 PIVOT = 1.0/ A(K1,K1) $
2 FOR J=(1,1,N)$ A(K1,J) = A(K1,J).PIVOT $ COMMENT CHANGE PIVOTROWS
2 FOR I=(1,1,N)$ IF I NEQ K1 $
2 BEGIN
2 TEMP = A(I,K1)$
2 FOR J=(1,1,N)$ A(I,J) = A(I,J) - TEMP.A(K1,J)$
2 A(I,K1)=-TEMP.PIVOT $
2 END$
2 A(K1,K1) = PIVOT $
2 GO TO FIVE $
2 ALM..
2 NC = 0 $
2 FOR I=(K,-1,1)$
2 IF (CB(I) NEQ 0.0)$ (NC=NC+1$ COF(NC)=CB(I)$ IN(NC)=K-I+1)$
2 IF NC GTR 20 $ NC = 20 $
2 RETURN END $

```

Fig. 6 Procedure Select for Stagewise Autoregression (from Ref. 9).

5. CONCLUSIONS AND RECOMMENDATIONS

We have presented in detail various techniques for the extraction of oscillator fluctuations, and for the estimation of the fluctuation spectra from the extracted fluctuations. The choice of techniques to be used for the study of a particular oscillator depends on the properties of the fluctuation spectrum and the limitations of the various extraction techniques. Adequate information on these two factors is not available at this time, hence it is not possible to recommend a single complete procedure that would reduce the problem of spectral measurement of oscillator fluctuations to routine operations.

It is clear that the next logical step in a continuing effort in this area would be to judiciously utilize some of the techniques presented here to determine the limitations of the extraction techniques and the properties of some fluctuation spectra, and then modify the procedures to utilize the new information. It is possible to recommend a complete test program to achieve this purpose, as follows. Use the phase-locked loop technique (Fig. 2c) with an automatic spectrum analyzer to obtain the fluctuation spectrum of the oscillator under test down to about 10 Hz. Also, measure the residual fluctuation spectrum with the loop in common mode, as explained in Sec. 2.1 above to ensure that the internal VCO fluctuations are sufficiently small. Then, use the phase-detector technique (Fig. 2b) to extract the phase fluctuations for the high and medium regions.

For the high region, use an analog filter on the output with a cutoff frequency at about 50 Hz and a roll-off in excess of 12 dB/octave. Sample and quantize the output every 5 ms, and record the samples on punched-paper tape (if the recorder is fast enough) or on magnetic tape. Take several records,

each 10,000 samples or 50 seconds long. For the medium region, use an analog filter on the phase-detector output with a cutoff frequency at about 0.5 Hz and roll-off in excess of 12 dB/octave. Sample and quantize the output every 0.5 second, and record the samples on punched-paper tape. Take several records, each 10,000 samples or 5,000 seconds long. In the initial experiments, it is best to postpone taking data for the low region in order to avoid the added complexity of digital filtering. Also, take similar data for the residual fluctuations with phase detector operating in common mode, to ensure that the internal fluctuations are sufficiently small.

Next, use the computational procedure given in Sec. 4.1 to estimate the spectra in each region for each record. Use the Parzen Kernel (Eq. (3.77)) in the computations of Step 5. The Cooley-Tukey method for implementing Eq. (4.2) on the computer should be considered, since this method is presently available in the form of standard subroutines for some computers. Experiment with the computational parameters M , N , Q and observe the choice yielding most consistent estimates. In particular, choose $M/N = 0.1, 0.2, 0.3$ and 0.4 , and $Q/N = 0.4$. Similar records should yield close estimates. Furthermore, the estimates in the overlapping decade between two adjacent regions should agree closely. Look for hidden periodicities (i. e., "signals," in the language of Secs. 3 and 4). If any are suspected, then the more elaborate techniques of Secs. 4.4-4.7 may be used to estimate their frequencies and magnitudes.

NOTATION FOR PART II

| | |
|-------------------------|------------------------------------------------------------------------------|
| $X(\cdot)$ | |
| s, t | time variables |
| Δt | time between samples |
| s', t' | integers $s' = \frac{s}{\Delta t}$, $t' = \frac{t}{\Delta t}$ |
| N | duration of sample |
| N' | integer $N' = N/\Delta t$ |
| T | domain of $X(\cdot)$ |
| $m(\cdot)$ | trend or signal |
| $Y(\cdot)$ | noise time series with zero mean |
| $g_k(\cdot)$ | components in $m(\cdot)$ |
| q | number of components in $m(\cdot)$ |
| C_k, ω_k, ϕ_k | amplitude, frequency, phase of $f_k(\cdot)$ |
| $R(\cdot)$ | autocovariance function of $X(\cdot)$ (and $Y(\cdot)$) |
| $\rho(\cdot)$ | autocorrelation function of $X(\cdot)$ (and $Y(\cdot)$) |
| v | variable in domain of $R(\cdot)$ and $\rho(\cdot)$ |
| v' | integers $v' = v/\Delta t$ |
| V | domain of $R(\cdot)$ and $\rho(\cdot)$ |
| $F(\cdot)$ | spectral distribution function of $X(\cdot)$ (and $Y(\cdot)$) |
| $f(\cdot)$ | spectral density function of $X(\cdot)$ (and $Y(\cdot)$) |
| $\phi(\cdot)$ | normalized spectral density function of $X(\cdot)$ (and $Y(\cdot)$) |
| $J(\cdot)$ | spectral jump function of $X(\cdot)$ |
| ω | variable in domain of $F(\cdot)$, $f(\cdot)$, $\phi(\cdot)$ and $J(\cdot)$ |
| $a_{s'}$ | autoregressive coefficient |
| p | order of autoregressive scheme |
| $\epsilon(\cdot)$ | white noise process |

| | |
|------------------|----------------------------------------------------------------------|
| M_i | truncation point in domain of $R(\cdot)$ and $\rho(\cdot)$ |
| M_i' | integer $M_i' = M_i/\Delta t$ |
| E or $E[\cdot]$ | expectation operator |
| var [] | variance operator |
| cov [] | covariance operator |
| $m_N(\cdot)$ | estimate of $m(\cdot)$ based on sample of duration N |
| $f_N(\cdot)$ | estimate of $f(\cdot)$ based on sample of duration N |
| $\phi_N(\cdot)$ | estimate of $\phi(\cdot)$ based on sample of duration N |
| $f_N(\dots)$ | truncated spectral estimate based on sample of duration N |
| $\phi_N(\dots)$ | normalized truncated spectral estimate based on sample of duration N |
| $R_N(\cdot)$ | estimate of $R(\cdot)$ based on sample of duration N |
| $R_N^*(\cdot)$ | unbiased estimate of $R(\cdot)$ based on sample of duration N |
| $\rho_N(\cdot)$ | unbiased estimate of $\rho(\cdot)$ based on sample of duration N |
| Q | number of subdivisions of Ω |
| $A(\cdot)$ | spectral window |
| $a(\cdot)$ | covariance window |
| T_f | generalized function corresponding to f |
| $\beta(\cdot)$ | bandwidth |
| $k(\cdot)$ | window generating function |
| $K(\dots)$ | spectral window |
| λ | variable in domain of $K(\dots)$ |
| Λ | domain of $K(\dots)$ |
| K | peak height factor |
| VBW(\cdot) | variance-bandwidth factor |
| r | characteristic exponent |
| $k^{[r]}(\cdot)$ | characteristic coefficient |
| $f^{[q]}(\cdot)$ | generalized spectral q^{th} derivative |

| | |
|------------------------------------------------|----------------------------------------------------------------------------------|
| μ_{ij} | truncation ratio |
| M_{ij} | mean truncation point |
| $f(\dots)$ | expected spectral estimate |
| Σ | approximate covariance matrix, Σ_{ij} element of Σ |
| $\Sigma^{(1,1)}$ | approximate covariance matrix, $\Sigma_{ij}^{(1,1)}$ element of $\Sigma^{(1,1)}$ |
| $\Sigma^{(2,2)}$ | approximate covariance matrix, $\Sigma_{ij}^{(2,2)}$ element of $\Sigma^{(2,2)}$ |
| $f_N^{[q]}(\dots)$ | generalized spectral q^{th} derivative of truncated spectral estimate |
| $K^{[q]}(\dots)$ | generalized spectral q^{th} derivative of spectral window |
| $f_N^{(r)}(\dots)$ | r^{th} derivative of truncated spectral estimate |
| $K^{(r)}(\dots)$ | r^{th} derivative of spectral window |
| m | number of spectral estimates |
| $K^{(2)}$ | peak curvature factor |
| I_{ij} | } integrals |
| $I_{ij}^{(1)}, I^{(1)}(\dots)$ | |
| $I_{ij}^{(2)}, I^{(2)}(\dots), I^{(2)}(\dots)$ | |
| M_o | $m \times 1$ vector of ones |
| $M_{1,0}$ | $m \times 2$ matrix |
| D | value of derivative of noise spectral density |
| $Z_j(\cdot), Z(\cdot)$ | narrowband signals |
| $R_j(\cdot)$ | autocovariance of $Z_j(\cdot)$ |
| $R_o(\cdot)$ | autocovariance of $Y(\cdot)$ in presence of narrowband signal |
| $f_j(\cdot)$ | spectral density function of $Z_j(\cdot)$ |

$f_o(\cdot)$ spectral density function of $Y(\cdot)$ in presence of narrowband signal
 β_s bandwidth of narrowband signal
 ρ_1^2, ρ_2^2 autoregressive statistics
 $X_{s_1}(\cdot),$
 $X_{s_1 s_2}(\cdot)$ { first- or second-order autoregressive models

REFERENCES FOR PART II

1. ADCOM, Inc., "Theory, Characterization, and Measurement of Short-Term Frequency Stability with Application to Frequency Synthesis," Final Report, Task No. ASTR-AD-2, Contract No. NAS8-11228, NASA report for George C. Marshall Space Flight Center, Huntsville, Alabama, 31 December 1964.
2. Baghdady, E. J., Lincoln, R. N. and Nelin, B. D., "Short-Term Frequency Stability: Characterization, Theory, and Measurement," Paper presented at the Symposium on the Definition and Measurement of Short-Term Frequency Stability, held at Goddard Space Flight Center, 23-24 November 1964.
3. Baghdady, E. J., Lincoln, R. N. and Nelin, B. D., "Short-Term Frequency Stability: Characterization, Theory and Measurement," Proc. IEEE, Vol. 53, No. 7, pp. 704-722, July 1965.
4. Baghdady, E. J., Lincoln, R. N., Mullen, J. A. and Nelin, B. D., "Short-Term Frequency Stability," Proc. IEEE, Vol. 53, No. 12, p. 2110, December 1965.
5. ADCOM, Inc., "Oscillator Stability in a Tracking System," Final Report, Task III, Contract No. NAS5-9742, report to Goddard Space Flight Center, Greenbelt, Maryland, 26 August 1965.
6. ADCOM, Inc., "System for the Measurement of Oscillator Instability," Final Report, Task Orders Nos. ASTR-AD-12 and ASTR-AD-13, Contract No. NAS8-11228, report to George C. Marshall Space Flight Center, Huntsville, Alabama, 31 October 1965.
7. Blackman, R. B. and Tukey, J. W., The Measurement of Power Spectra, Dover Publications, Inc., 1959.
8. Parzen, E., "An Approach to Time Series Analysis," Ann. Math. Stat., 32, pp. 951-989, 1961.
9. Parzen, E., "An Approach to Empirical Time Series Analysis," Radio Science, Vol. 68D, No. 9, pp. 937-951, September 1964.
10. Hext, G. R., "A New Approach to Time Series with Mixed Spectra," Technical Report No. 17, prepared under grant DA-ARO(D)-31-124-G726, for U. S. Army Research Office, by Department of Statistics, Stanford University, May 16, 1966.

REFERENCES FOR PART II (Cont'd)

11. Schaerf, M.C., "Estimation of the Covariance and Autoregressive Structure of a Stationary Time Series," Ph. D. Dissertation, Department of Statistics, Stanford University, October 1963.
12. Langill, A.W., Jr., "Digital Filters," Frequency, Vol. 2, No. 6, pp. 26-31, November - December 1964.